Different adipose tissue development in mice pair fed fish oil and different carbohydrates

Ragnhild Helene Jarlsby

Master Thesis in Human Nutrition

Institute of Medicine, University of Bergen (UoB)

National Institute of Nutrition and Seafood Research (NIFES)

May 2011

Different adipose tissue development in mice pair fed fish oil and different carbohydrates

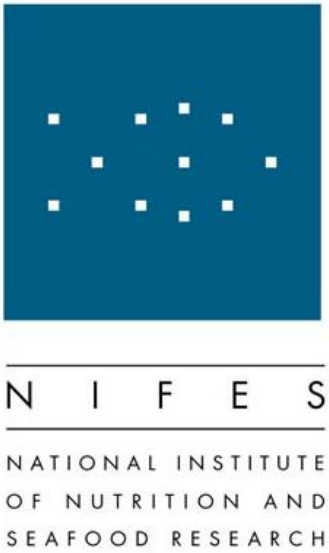

Master Thesis in Human Nutrition

Ragnhild Helene Jarlsby

May 2011

Cover illustrations:

C57BL6/J Mouse: http://www.harlan.com/image.axd/153ca96e0f44403a9d81492ecd05a8f6.jpg

Fish oil-fish: http://3.bp.blogspot.com/_81Muh4Wz7oU/TIFPwS2yg9I/AAAAAAAABOs/LgjCrvCKfF0/s1600/fish-oil-456.jpg

ACKNOWLEDGEMENTS

The work presented in this thesis was performed at the National Institute of Nutrition and Seafood Research (NIFES) at Nordnes, Bergen. The work started autumn 2008, was postponed due to maternity leave, and ended spring 2011.

I want to express my gratitude to my main supervisor Dr. philos. Lise Madsen for all her guidance, support, help and good sense of humor. Her experience and insight in the field has been invaluable to me. I would also like to extent my gratitude towards my co-supervisor Dr. philos. Livar Frøyland and everyone at the Seafood and Health group for providing a good working atmosphere.

Further, I especially want to thank Aase Heltveit at the animal facility for her excellent guidance through the animal experiment. I would also like to thank everyone at the molecular and microbiological laboratories for all help, training and patience. My thanks to all those who taught me the experimental methods and statistical analysis, especially Haldis Haukås Lillefosse, Hui-Shan Tung, Eva Mykkeltvedt, Leikny Fjeldstad, Pål Olsvik, Pedro Araujo and my fellow co-students Ha Thi Ngo and Even Fjære. Thanks to Jaboc Wessels and Jan Idar Hjelle for performing the maxmat- and lipid class-analysis.

I would also like to thank my fellow students for creating a good college environment and providing support and encouragement. Thank you for all good discussions, both school-related and not school-related.

Finally, I would like to thank my father for his constant complaining, my sister and brother for their curious questions, my husband for his invaluable support and my daughter for being my inspiration. I would also like to thank my mother, whom I know would have been very proud of me.

Bergen, May 2011

Ragnhild Helene Jarlsby

TABLE OF CONTENTS

TABLE OF CONTENTS

LIST OF FIGURES

LIST OF TABLES

LIST OF ABBREVATIONS

ACC – Acetyl Coenzyme A carboxylase (enzyme)

ACO – Acetyl Coenzyme A oxidase (enzyme)

AGXT – Alanine glyoxylate transaminase (enzyme)

ALT – Alanine aminotransferase (enzyme)

ANOVA – Analysis of variance (statistics)

ATP – Adenine triphosphate (molecule)

AUC – Area under the curve (statistics)

BAT – Brown adipose tissue

BMI – Body mass index

cAMP – Cyclic adenine monophosphate (molecule)

CCL2 - CC-chemokine ligand 2 (enzyme)

Ccr2 - CC-chemokine receptor 2 (enzyme)

cDNA – Complementary deoxyribonucleic acid (molecule)

CD68 – Cluster of differentiation 68 (enzyme)

C/EBP – CCAAT/enhancer-binding protein (enzyme)

COX – Cyclooxygenase (enzyme)

CPS1 – Carbamoyl-phosphate synthase-1 (enzyme)

CPT – Carnitine-palmitoyl transferase (enzyme)

CREM – Cyclic-adenine monophosphate-responsive element modulator (enzyme)

DHA – Docosahexaenoic acid (molecule)

dsDNA – Double-stranded deoxyribonucleic acid (molecule)

ELISA – Enzyme-linked immunosorbent assay (method)

EPA – Eicosapentaenoic acid (molecule)

eWAT – Epididymal white adipose tissue (visceral)

FA – Fatty acid (molecule)

FAS – Fatty acid synthase (enzyme)

FFA – Free fatty acid (molecule)

GI – Glycemic index

GIP - Glucose-dependent insulinotropic polypeptid (hormone)

GLUT – Glucose transporter (enzyme)

GOT – Glutamate oxaloacetate transaminase (enzyme)

GPT – Glutamic pyruvic transaminase (enzyme)

HMGCS2 – 3-hydroxy-3-methylglutaryl-Coenzyme A synthase 2 (enzyme)

HMG-CoA-cycle - Hydroxymethylglutaryl Coenzyme A-cycle

HFCS – High fructose corn syrup

iBAT – Intrascapular brown adipose tissue

IL – Interleukin (molecule)

iWAT – Inguinal white adipose tissue (subcutaneous)

LCFA – Long-chained fatty acid (molecule)

LCPUFA – Long-chained polyunsaturated fatty acid (molecule)

LDH – Lactate dehydrogenase (enzyme)

LDL – Low density lipoprotein (molecule)

MCP1 – Monocyte chemotactic protein-1 (enzyme)

MUFA – Monounsaturated fatty acid (molecule)

mRNA – Messenger ribonucleic acid (molecule)

n-3 – Omega 3 fatty acid (molecule)

n-3 LCPUFA – Omega-3 long-chained polyunsaturated fatty acid (molecule)

n-6 – Omega 6 fatty acid (molecule)

NCD – Noncommunicable disease

NEFA – Non-esterified fatty acid (molecule)

NIFES – National Institute of Nutrition and Seafood Research

NO – Nitric oxide (molecule)

PAI – Plasminogen activator inhibitor (enzyme)

PCK1 – Phosphoenolpyruvate carboxykinase (PEPCK) (enzyme)

PCR – Polymerase chain reaction (method)

PDE4c – Cyclic-adenine monophosphate-specific phosphodiesterace 4c (enzyme)

PGC-1α – Peroxisome proliferator-activated receptor-γ coactivator 1α (enzyme)

PPAR – Peroxisome proliferator-activated receptor (enzyme)

PUFA – Polyunsaturated fatty acid (molecule)

qPCR – Quantitative real-time polymerase chain reaction (method)

RIα – Protein kinase A regulatory subunit 1α (enzyme)

RIIβ– Protein kinase A regulatory subunit 2β (enzyme)

RIN – RNA integrity number (method)

RNA – Ribonucleic acid (molecule)

rWAT – Retroperoniteal white adipose tissue (visceral)

RT – Reverse transcriptase (enzyme)

Rt –Reaction – RealTime reaction (method)

SCD1 – Stearoyl-Coenzyme A desaturase 1 (enzyme)

SD – Standard deviation (statistics)

SEM – Standard error of the mean (statistics)

SFA – Saturated fatty acid (molecule)

SIRT3 - NAD-dependent deacetylase sirtuin-3 (enzyme)

SREBP – Sterol regulatory element binding protein (enzyme)

ssDNA –Single-stranded deoxyribonucleic acid (molecule)

TBP - TATA box binding protein (enzyme)

TCA – Tricarboxylic acid cycle

TNFα – Tumor necrosis factor α (enzyme)

WAT – White adipose tissue

TAG – Triacylglycerol (molecule)

TCA – tricarboxylic acid cycle

TG – Triglycerid (molecule)

TLR-4 – Macrophage toll-like receptor-4

TNFα – Tumor necrosis factor α

UCP – Uncoupling protein (enzyme)

WAT – White adipose tissue

ABSTRACT

Obesity causes several health problems, including insulin resistance, Type 2 diabetes, heart diseases, disrupted energy metabolism and low-grade inflammation. Being obese increases the risk of getting metabolic syndrome.

A high intake of certain carbohydrates is known to cause rapid rise in blood glucose, which increases insulin secretion and over time causes insulin resistance and hyperglycemia. A high consumption of sucrose and glucose is considered harmful beyond being a source of energy due to their ability to disturb energy metabolism. On the other hand, fish oil, enriched in the polyunsaturated fatty acids eicosapentaenoic acid (EPA; 20:5n-3) and docosahexaenoic acid (DHA; 22:6n-3), can protect against the development of obesity, improve insulin sensitivity, reduce visceral fat, reduce inflammation of adipose tissue and reduce metabolic efficiency. This study seeks to elucidate the potential ameliorating effect of fish oil on the negative effects of high carbohydrate consumption.

Two trials using C57BL/6J mice were performed simultaneously. One of the trials investigated the effect of different sugars, namely the disaccharide sucrose and the monosaccharides glucose and fructose. Three groups of mice received either high sucrose, high glucose or high fructose diet in combination with fish oil. The other trial investigated the effects of different starches, namely amylose and amylopectin, in combination with fish oil. One group was given amylose (low GI carbohydrate) and the other group was given amylopectin (high GI). All the five experimental diets were high in fat, primarily fish oil. All groups, except the chow diet controlgroup, were *pair-fed*. Feed intake was recorded daily and body weight was recorded twice a week. After 9 weeks of experimental feeding, the mice were terminated and tissues and blood samples were collected. Gene expression analysis of the different tissues was performed by quantitative real-time PCR. Blood plasma was analyzed for plasma parameters. Paraffin-embedded, stained sections of adipose tissue were examined in a microscope. Fatty acid compositions were determined in liver and muscle.

The results show that fish oil protected the mice given fructose and low GI carbohydrates from developing obesity. These groups had smaller adipose tissues and less inflammation compared to other groups. The primary cause of this seems to be that the PUFAs in fish oil decrease hepatic and adipose tissue lipogenesis.

1. INTRODUCTION

1.1 OBESITY

Overweight and obesity are defined as the excessive accumulation of fat to the point where it presents a risk to the individual's health (WHO 2011). Obesity can be measured by the body mass index (BMI). An individual's BMI is calculated by his or her weight in kilograms, divided by the square of his or her height in meters:

$$\text{BMI} = \frac{\text{weight (kg)}}{\text{height} * \text{height (m} * \text{m)}}$$

The optimum BMI range is between 18.5 and 25. A person with BMI equal to or above 25 is considered as overweight, whereas a person with BMI of 30 or more is considered as obese. It is natural for a woman to have lower BMI compared to a man of same height, due to less muscle mass in the average female body. The optimum BMI range of 18.5 to 25 does not apply to lean people of heavy muscular build, children or elderly. Also, due to the nature of the BMI formula, it has limited use for people who are relatively short or tall of stature. For people of short stature (150≤ cm for women and 160 cm≤ for men), obesity-related problems increase when the BMI exceeds 23 (Lara-Esqueda et al 2004). Inversely, tall people can have higher BMI without being overweight. There are several other ways of measuring obesity, e.g. the waist-hip ratio or body fat percentage.

Obesity is caused by a positive energy balance, which is energy intake that exceeds energy expenditure. In some countries the average energy intake is decreasing, but the prevalence of obesity is still increasing (Elmadfa et al 2009). This may primarily be caused by a more sedentary lifestyle which decreases energy expenditure, but it is our hypothesis that the development of obesity may be influenced by the diet.

Obesity and overweight the rank among the highest risk factors for premature death. Every year, at least 2.8 million adults die prematurely as a result of being overweight or obese (WHO 2011). Obesity increases the risk of chronic diseases like diabetes Type 2, cardiovascular diseases, hypertension, cancer, stroke, gallstone formation, musculoskeletal disorders, sleep apnea and back pain (Helsedirektoratet 2008). The risk of developing these diseases increase with increasing BMI (WHO 2011). In addition to being a problem for the individual's health, welfare and life expectancy, it is also a major expenditure for the society in the form of increased health care costs and decreased tax revenues (Finkelstein et al 2003).

In 2008, 1.5 billion adults at the age of 20 and older were overweight. 500 millions of these were obese. In 2010, nearly 43 million children under the age of 5 were overweight. Obesity was once considered a problem in developed countries, but in recent years it has been on the rise in developing countries as well (WHO 2011). In developing countries, poverty can cause both undernutrition and overnutrition, even within the same household, partly due to the high cost of healthy foods. The prevalence of obesity worldwide is higher in cities compared to rural areas and higher in female population compared to males (Usfar et al 2010). In EU countries, obesity is more widespread among men compared to females. Norway has one of the lowest prevalence of obesity in Europe (Elmadfa et al 2009), even though 13-22% of 40-45 year olds are reported to be obese (FHI 2011).

Childhood obesity is associated with a higher risk of obesity and obesity-related diseases in adulthood. It is also difficult to maintain long lasting weigh reduction for people who have previously suffered from overweight or obesity. Prevention of obesity development, especially in children, is therefore of critical importance. Among the advice given from World Health Organization (WHO) to prevent obesity are limiting the energy intake from total fats and sugar, increasing consumption of fruit, vegetables, whole grains and nuts, and engaging in regular physical activity (WHO 2011). These vague advices are supported by the WHO "2008-2013 Action Plan for the Global Strategy for the Prevention and Control of Noncommunicable Diseases" (NCDs). This Action Plan mentions obesity only once and states that one should promote interventions aimed to reduce unhealthy diets in e.g. schools, workplaces, households and local communities. The plan was developed to "help the millions who are already affected cope with these lifelong illnesses and prevent secondary complications. (...) The action plan provides a roadmap to establish and strengthen initiatives for the surveillance, prevention and management of NCDs." (WHO 2008). Good intentions seem to be of abundance in the area of politics, whereas measurable results are scarce.

1.2 MACRONUTRIENTS IN RELATION TO OBESITY

The three macronutrient classes are carbohydrates, fats and proteins. Carbohydrates include starches, sugars and fiber. Fat is broadly divided into saturated, monounsaturated and polyunsaturated fats, all of which have different effect on human health in addition to being a source of energy. Examples of omega-3 polyunsaturated fatty acids include alpha-linolenic acid (ALA), eicosapentaenoic acid (EPA) and docosahexaenoic acid (DHA), where EPA and

DHA are found in marine foods. EPA and DHA are essential to human health, but ingested ALA can to some extent be converted into EPA and DHA. Proteins consist of 20 different amino acids, where 8 are essential to human health.

Dietary carbohydrates

Dietary carbohydrates account for 45-70% of energy intake in developed countries. Carbohydrates are divided into starches, sugars and fiber. Sugars refer to monosaccharides, like glucose and fructose, and disaccharides, like sucrose. Sucrose consists of one glucose and one fructose molecule (Fig 1.1). Sucrose is broken down into glucose and fructose upon digestion (Schaefer et al 2009).

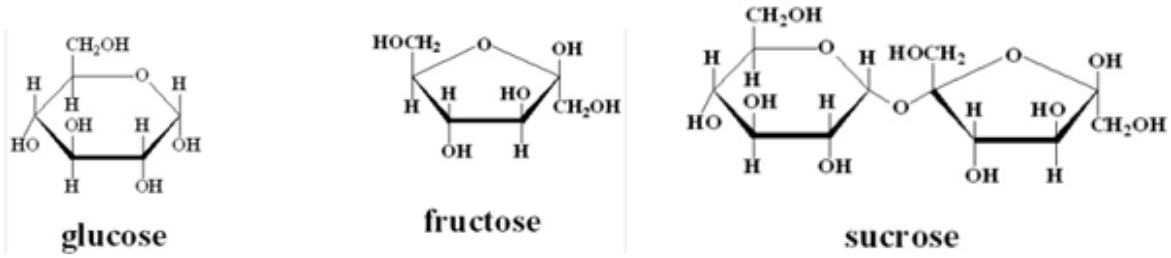

Figure 1.1: *Glucose, fructose and sucrose molecules. (Adapted from http://drpinna.com/fructose-is-a-cause-of-cancer-18119/glucose-fructose-and-sucrose-3)*

Sugar is added to food because of its sweet taste and inexpensive cost. Since the advent of modern food-processing methods, sugar consumption has risen steadily. Whereas sucrose is the main sweetener in most countries, high fructose corn syrup (HFCS) made from corn starch is an even cheaper, widely used sweetener in USA. HFCS consists of approximately 45% glucose and 55% fructose and has a slightly sweeter taste compared to sucrose (Bray et al 2004).

The body uses glucose as its primary source of energy and transports it around by the blood stream. The brain and red blood cells are dependent on glucose and ketones as fuel, therefore blood glucose levels are tightly regulated. Glucose is broken down to carbon dioxide and water through the tricarboxylic acid cycle (TCA). Glucose is also stored as glycogen in liver and muscles, as a source of rapidly available energy. Excess glucose ingested is converted to fatty acids for storage in adipose tissues (Schaefer et al 2009).

Blood glucose levels are tightly regulated, primarily by the hormone insulin. Insulin is released by β-cells in the pancreas as a response to postprandial high glucose levels. It has several effects, the most important being that it binds to target organ cells and promote

glucose transport into the cell. Thus, it reduces blood glucose to normal levels. Insulin resistance is the state where the cells no longer respond to normal levels of insulin and blood glucose levels remain high. This increases the insulin production in the pancreas, putting strain on the β-cells. Insulin resistance is an early sign of Type 2 diabetes (Petersen and Shulman 2002). Fructose does not raise blood glucose or insulin levels. These may seem beneficial, but fructose is converted into glucose or fat in the liver. High fructose diets are a common way of inducing insulin resistance, obesity and metabolic syndrome in rat models (Hwang et al 1987, Tran et al 2009) . High fructose intake has been associated with lipid abnormalities, visceral adiposity and nonalcoholic liver steatosis (Schaefer et al 2009, Tappy and Le 2010).

Starches are polymers of glucose molecules which are either linear or branched. Amylose and amylopectin are both starches found in plants (Fig 1.2). Amylose molecules only have α-1,4 linkages between the glucose molecules, making them linear. Amylopectin molecules are large, made up by over 10 000 glucose molecules, and have α-1,6 linkages between the glucose molecules, in addition to the α-1,4 linkages. This gives amylopectin a branched, tree-like structure. Total ingested starch usually consists of 20-30% amylose and 70-80% amylopectin (Cummings and Englyst 1995).

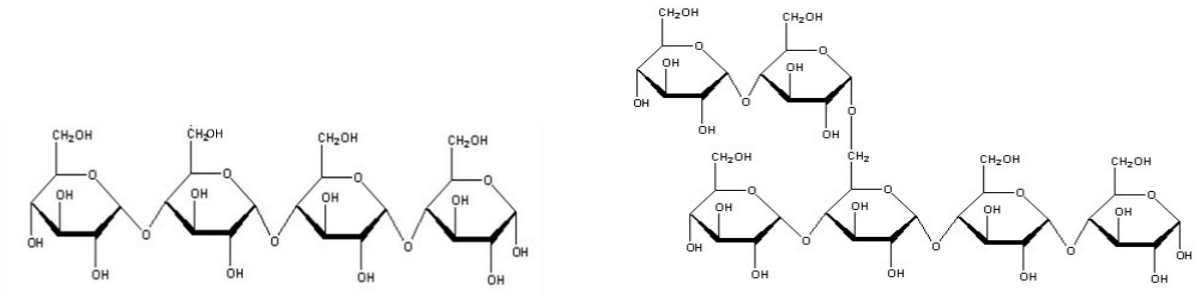

***Figure 1.2**: Amylose (left) and amylopectin (right). (Adapted from http://www.cbu.edu/~seisen/OrganicChemistry.htm)*

Before absorption from the gut into the body, the starches must be cleaved into monosaccharides. The digestion enzymes in the gut can only cleave glucose molecules off the end of the polysaccharides. Since the branched amylopectin molecule have many ends for the digestion enzymes to work on, glucose molecules are rapidly released from amylopectin compared to amylose (Cummings and Englyst 1995).

Glycemic index

The term glycemic index (GI) refers to how a food, meal or diet can raise blood glucose after consumption. The GI of a food is defined as the two-hour area under the blood glucose response curve (AUC) after eating a portion of that food which contains 50 g of carbohydrates. This number is then divided by the AUC number of a standard, which is 50 g glucose or white bread consumed by the same person that same day, and then multiplied by 100 (van Baak and Astrup 2009). The GI values of different foods have been published (Atkinson et al 2008), but it is reported that the same food can give varying GI results (Wolever et al 2008). The glycemic response is affected by the nature of the carbohydrate (e.g. mono-, di- or polysaccharide), food processing (e.g. cooking and churning) and the presence of other macronutrients in the food (e.g. fat, protein and dietary fiber). Glucose has a high GI whereas fructose has a low GI (van Baak and Astrup 2009), this is because fructose is absorbed further down in the small intestine and it has to be converted into glucose before it can affect the insulin-secreting pancreas. The pancreas does not respond well to the fructose molecule because it lacks the glucose transporter 5 (GLUT5), which is the most effective transporter of fructose into cells (Sato et al 1996, Wood and Trayhurn 2003). Insulin secretion is also influenced by other hormones. Endocrine cells in the gastrointestinal tract secret glucose-dependent insulinotropic peptide (GIP) in response to glucose ingestion. This hormone increases the secretion of insulin at an early point, reducing the risk of high blood glucose level immediately after a meal (Song and Wolfe 2007). Fructose does not stimulate the release of GIP, and thus does not have the same insulin-increasing effect as glucose does.

Amylose has low GI due to its linear chains of glucose molecules. The digestive enzymes can only release glucose molecules from the polysaccharide at the end of the chains, meaning that the linear amylose polysaccharide have only one site for the digestive enzymes to work on. Amylopectin has high GI due to its branched composition of glucose molecules, which provides the digestive enzymes with multiple sites from which to release glucose molecules from the polymer and finally into the blood stream (Wheeler and Pi-Sunyer 2008).

The glycemic index of food may be a risk factor for developing metabolic syndrome. A low GI diet has been reported to reduce risk of developing metabolic disease, Type 2 diabetes, insulin resistance and coronary heart disease, and improved lipid status and inflammatory status, although not all studies have come to this conclusion. The different effects of high and low GI foods are proposed to be caused by the different rates of glucose uptake from the gut to the blood. The sharp increase in blood glucose after eating a high GI food triggers a large

insulin response from the pancreas and strongly inhibits the release of glucagon. This high insulin: glucagon ratio causes glucose uptake in liver and muscle to increase, as well as lipogenesis in adipose tissue. Release of glucose from the liver is inhibited, as well as release of free fatty acids (FFA) from adipose tissue. The high GI food is rapidly absorbed, putting an end to the release of nutrients into blood, but the effect of the high insulin: glucagon ratio persists. This causes blood levels to fall, often dropping below fasting levels (Fig 1.3). The resulting hypoglycemia triggers the release of glucagon, adrenaline and growth hormone. These hormones increase blood glucose levels by increasing gluconeogenesis and glycogen breakdown in the liver and decreasing glucose uptake in skeletal muscles. They also affect the adipose tissues by increasing lipolysis and the release of FFA, thus increasing the FFA in blood above normal levels. High FFA levels cause lipid accumulation in liver and skeletal muscles, which results in insulin resistance in these organs. Hyperglycemia, hyperinsulinemia, hypertriglyceridemia and insulin resistance are factors that contribute to the development of metabolic syndrome. Low GI foods are digested slower in the gut, and thus produce a less dramatic increase in blood glucose levels (Fig 1.3). They do not result in the hypoglycemic undershoot produced by the ingestion of high GI foods and the blood glucose level remains above fasted level for a longer period of time. This slower release of nutrients and more gradual drop in blood glucose levels allows the body to properly adjust insulin: glucagon hormone levels. Glucose and FFA in blood are maintained within normal range and thus do not disrupt insulin sensitivity. More stable hormone and nutrient levels are factors which can protect against the development of metabolic syndrome. Also, low GI diets puts less strain on the insulin-secreting β-cells in the pancreas compared to high GI diets. This may improve insulin secretion (Aston 2006). Still, many studies see no correlation between low GI diet and decreased body weight (Aston 2006, Aston et al 2008).

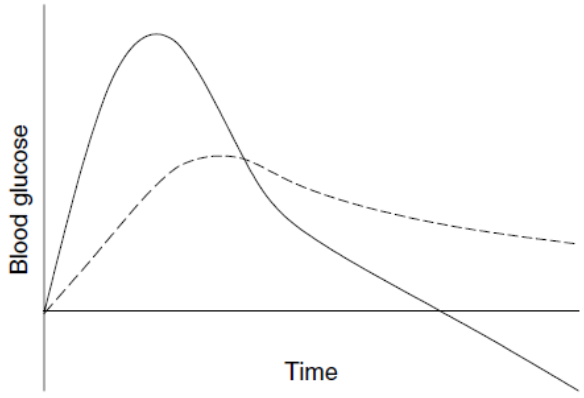

Figure 1.3: *The glycemic response curve to high glycemic index food (solid line) and low glycemic index food (dotted line). The line at the x-axis is the fasting blood glucose level. (Aston 2006)*

Dietary fat

Fat in the diet is either saturated (SFA), monounsaturated (MUFA) or polyunsaturated (PUFA). Saturated fatty acids (FA) have no double bonds in their carbon chain, monounsaturated FAs have one and polyunsaturated FAs have two or more double bonds. In addition to differing in the number of double bonds, FAs have different chain-length. The different types of FAs ingested in the diet are reflected in the plasma and tissue lipids and elicit different responses in the body. All cell membranes are composed of phospholipids with two FA tails, and the FA structure affects the flexibility and function of the cell. FA composition also affects gene expression and enzyme activities. SFAs are associated with increased risk of cardiovascular disease, reduced insulin resistance and increased visceral adiposity. Replacing SFAs with MUFAs or PUFAs is demonstrated to increase insulin sensitivity (Jucker et al 1999, Storlien et al 1987) and reduce risk of cardiovascular disease (Harris 1997, Marik and Varon 2009, Riserus et al 2009). PUFAs are e.g. omega-3 (n-3) or omega-6 (n-6) fatty acids, depending on where the last double bond occurs on the carbon chain. n-3 FAs have their last double bond on the third carbon atom from the methyl end of the carbon chain (omega = end), whereas n-6 FAs have their last double bond on carbon atom number six. The number and placements of the other double bonds varies between different PUFAs. Fish oil is rich in the long-chained n-3 FAs eicosapentaenoic acid (EPA) and docosahexaenoic acid (DHA) (Fig 1.4). These are collectively called omega-3 long-chained polyunsaturated fatty acids, or n-3 LCPUFAs (Buckley and Howe 2009, Schmitz and Ecker 2008).

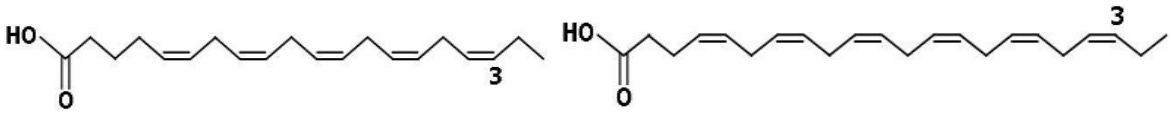

Fig 1.4: *Eicosapentaenoic acid (left) and docosahexaenoic acid (right). (Adapted from http://www.eufic.org/article/en/artid/The-importance-of-omega-3-and-omega-6-fatty-acids/)*

n-3 LCPUFAs are known to reduce the risk of cardiovascular disease. An increasing number of animal studies have also demonstrated that n-3 LCPUFAs reduce obesity when incorporated into high-fat diets, but few human studies are available (Buckley and Howe 2009). n-3 LCPUFAs have also been demonstrated to be essential for normal growth and development, regulate lipid levels and immune system functions and have anti-inflammatory, antithrombotic, antiarrhytmic and vasodilatory properties. They are therefore proposed to have play a role in the prevention and management of dyslipidemia, insulin resistance,

metabolic syndrome and Type 2 diabetes (Lombardo and Chicco 2006). The main mechanisms of the anti-obesogenic effect of fish oil are summed up in figure 1.5.

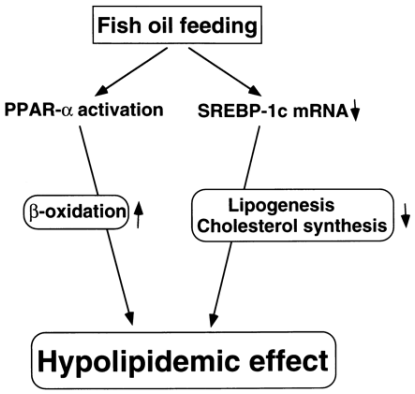

Figure 1.5*: Fish oil increases fatty acid breakdown through PPARα-activation and SREBP-1c-inactivation.The transcription factors PPARα and SREBP-1c are described below. (Kim et al 1999)*

Dietary protein

There is a link between dietary protein and the development of obesity (Abete et al 2010), but the theme is too big to be discussed in this thesis. It is to be noted that in the absence of glucose in the diet, amino acids from both diet and muscle can be turned into glucose and ketone bodies to be used as fuel for the brain and red blood cells (Noguchi et al 1978). Also, exchanging dietary carbohydrates with protein is demonstrated to reduce feed efficiency in mice given n-6 PUFAs (Madsen et al 2008).

1.3 ADIPOSE TISSUE

Excess nutrients from the diet are converted into triglycerides (TGs) and stored in adipose tissue depots around the body. The adipose tissue functions as the body's energy reserve, it also cushions the body and protects the internal organs. Adipose tissues can be either white or brown. Brown adipose tissue (BAT) gets its name from the increased number of mitochondria present in the adipocytes, giving the cells a brown color. BAT has the capacity of turning fat into heat, and thus increasing the body temperature. This is especially valuable for animals with high surface area and low body weight, including human babies. As babies grow beyond approximately 10 kg, the brown adipose tissue mass is reduced and mostly white adipose tissue (WAT) is left. Some remaining clusters of brown adipocytes are found along the spine (paravertebral), neck (cervical) and shoulder blades (supraclavicular) in the adult human (Gesta et al 2007).

There are two main types of white adipose tissue depots; subcutaneous and visceral. The subcutaneous adipose tissue is located under the skin, distributed all over the body. The visceral fat depot is located around internal organs, which contains it to the stomach area. In obese humans, as well as other animals, adipose tissues expand in both these depots as well as in other adipose tissue depots around the body (Fig 1.6). It accumulates around the heart, kidneys and the connective tissue around blood vessels (Ouchi et al 2011). Visceral fat promotes a higher risk of developing metabolic syndrome compared to fat depots on hips and thighs (Gesta et al 2007).

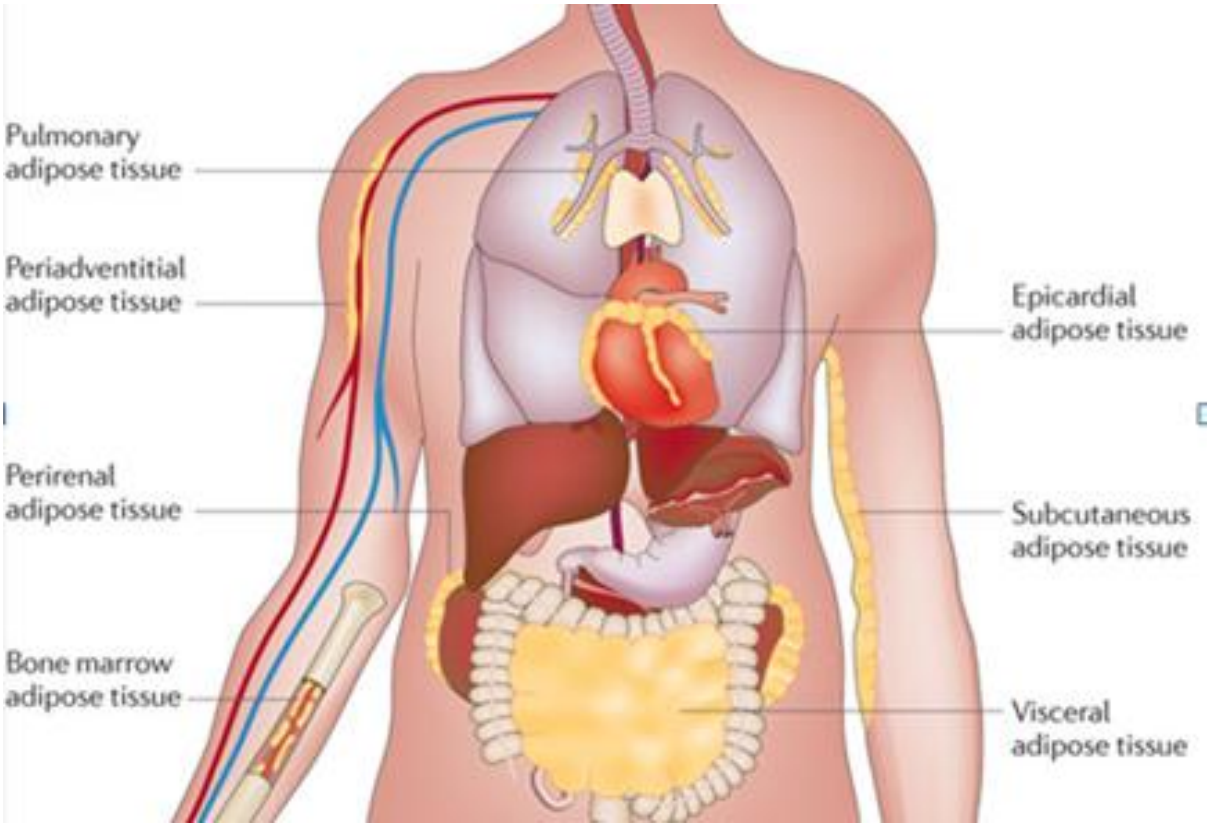

Figure 1.6*: Different adipose tissues around the body. Pulmonary adipose tissue, periadventitial adipose tissue, perirenal adipose tissue, bone marrow adipose tissue, epicardial adipose tissue, subcutaneous adipose tissue and visceral adipose tissue. (Ouchi et al 2011)*

The main components of the adipose tissue are the adipocytes. They store energy in the form of TGs and exert endocrine activity. Other cell types present in adipose tissue include adipocyte precursor cells, fibroblasts, vascular cells and immune cells (Fig 1.7). These cells constitute the connective tissue of the adipose tissue. Blood vessels are required for the flow of nutrients and oxygen to the adipose tissues, they also distribute hormones and adipokines to and from adipocytes. Macrophage cells and T-cells determine the inflammatory and immune status of the adipose tissue (Ouchi et al 2011).

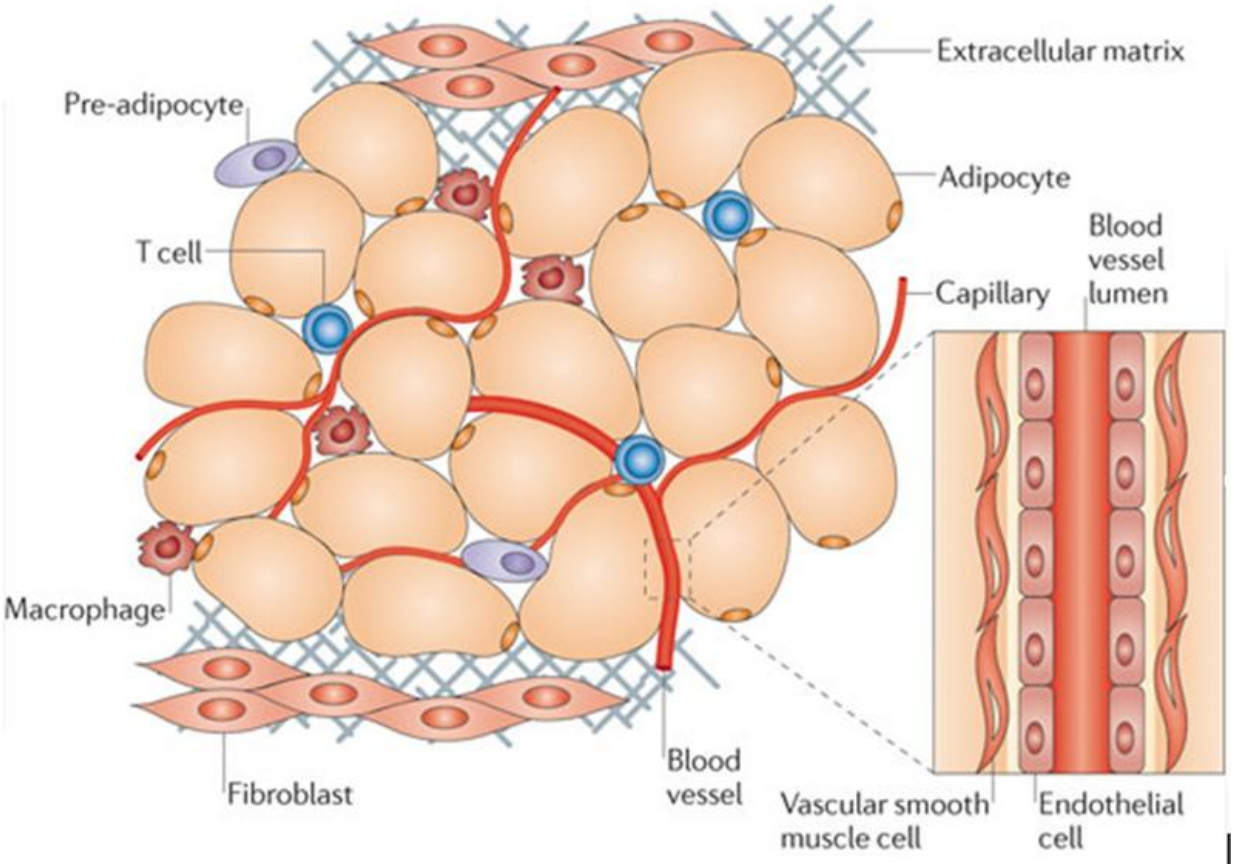

Figure 1.7: *Simplified illustration of adipose tissue containing adipocytes, pre-adipocytes, T-cells, macrophages, fibroblasts, blood vessels and capillaries. (Ouchi et al 2011)*

1.4 ENZYMES INCREASING LIPOGENESIS

There are many enzymes linked to adipogenesis, not all will be discussed here. In this study we measured the mRNA levels of SREBP-1c, ACC1, ACC2, FAS, SCD1, DGAT and PPARγ, so these enzymes will be the main focus of this section.

SREBP-1C: The gene *Srebp1c* codes for the Sterol regulatory element-binding protein-1c (SREBP-1c). This is a transcription factor which regulates the mRNA expression levels of lipogenic enzymes, such as fatty acid synthase (FAS), Acetyl-CoA carboxylases (ACCs) and Stearoyl-CoA Desaturase 1 (SCD1) (Horton et al 1998, Jump et al 2005).

SREBPs are located in the endoplasmatic reticulum as inactive precursors. After transport to the Golgi apparatus they are cleaved into active forms and subsequently translocated into the nucleus. Here, they activate the transcription of lipogenic genes. This means that the level of *Srebp1c* mRNA is not necessary a true measurement of the amounts of active SREBP-1c

enzyme present in the cell. SREBP-1c is the predominant type of SREBP-1 in both human and rodent liver and plays an important role in the metabolism of fatty acids and cholesterol.

Levels of SREBP-1c are influenced by diet and hormones. Food intake, especially sucrose, and insulin increases the expression of SREBP-1c. Insulin resistance in patients with Type 2 diabetes leads to increased levels of insulin in the blood. This leads to elevated levels of hepatic SREBP-1c, which again increases the expression of lipogenic genes and causes fat to accumulate in the liver. Fatty liver can result in the development fibrosis, cirrhosis and liver failure (Horton et al 2002). The glucagon hormone is shown to decrease the levels of SREBP-1c, but it can also be done by diet. PUFAs reduce the levels of *Srebp1c* mRNA (Xu et al 2001) and they are shown to disrupt the inactive precursors of SREBP-1c before they reach the nucleus (Yahagi et al 1999). This down-regulates the levels of mature SREBP-1c and thus reduces the levels of lipogenic enzymes in the liver (Osborne 2000). SREBP-1c is not the sole regulator of the expression of lipogenic enzymes, studies have shown that SREBP-1c deficient mice have reduced, but not eliminated expressions of lipogenic genes, e.g. ACCs and FAS (Liang et al 2002).

ACC1 and ACC2: Acetyl-CoA carboxylases 1 and 2 (ACC1 and ACC2) are lipogenic enzymes. They catalyze the synthesis of malonyl-CoA, which is a substrate for fatty acid synthesis and also a regulator of fatty acid breakdown. The *Acc1* and *Acc2* genes are generally expressed in all tissues (Abu-Elheiga et al 1997, Castle et al 2009). Both genes are regulated by multiple promoters, which are influenced by both hormones and diet. A low-fat diet rich in carbohydrates induces the synthesis of ACC1 and ACC2. Insulin up-regulates the expression of *Acc1* through the transcription factor SREBP-1c, while glucagon down-regulates it. ACC activity is also affected by glucose levels. High glucose levels activate carbohydrate response element binding protein (ChREBP), which is a transcription factor for both *Acc* and *Fas* (Ishii et al 2004, Kim 1997). Low glucose levels leads to the activation of AMP-activated protein kinase (AMPK), which inactivates the ACC enzyme by phosphorylation (Park et al 2002).

The malonyl-CoA molecules formed by the different ACC enzymes are segregated within the cell. The malonyl-CoA generated from the ACC1 enzyme is utilized by FAS for *de novo* synthesis of fatty acids in the cytosol. The ACC2-generated malonyl-CoA is an inhibitor of the carnitine palmitoyltransferase 1 (CPT1, described below) mitochondrial enzyme. This inhibits the breakdown of fatty acids by preventing the transfer of acyl-CoA groups from the cytosol into the mitochondria for β-oxidation (Wakil and Abu-Elheiga 2009).

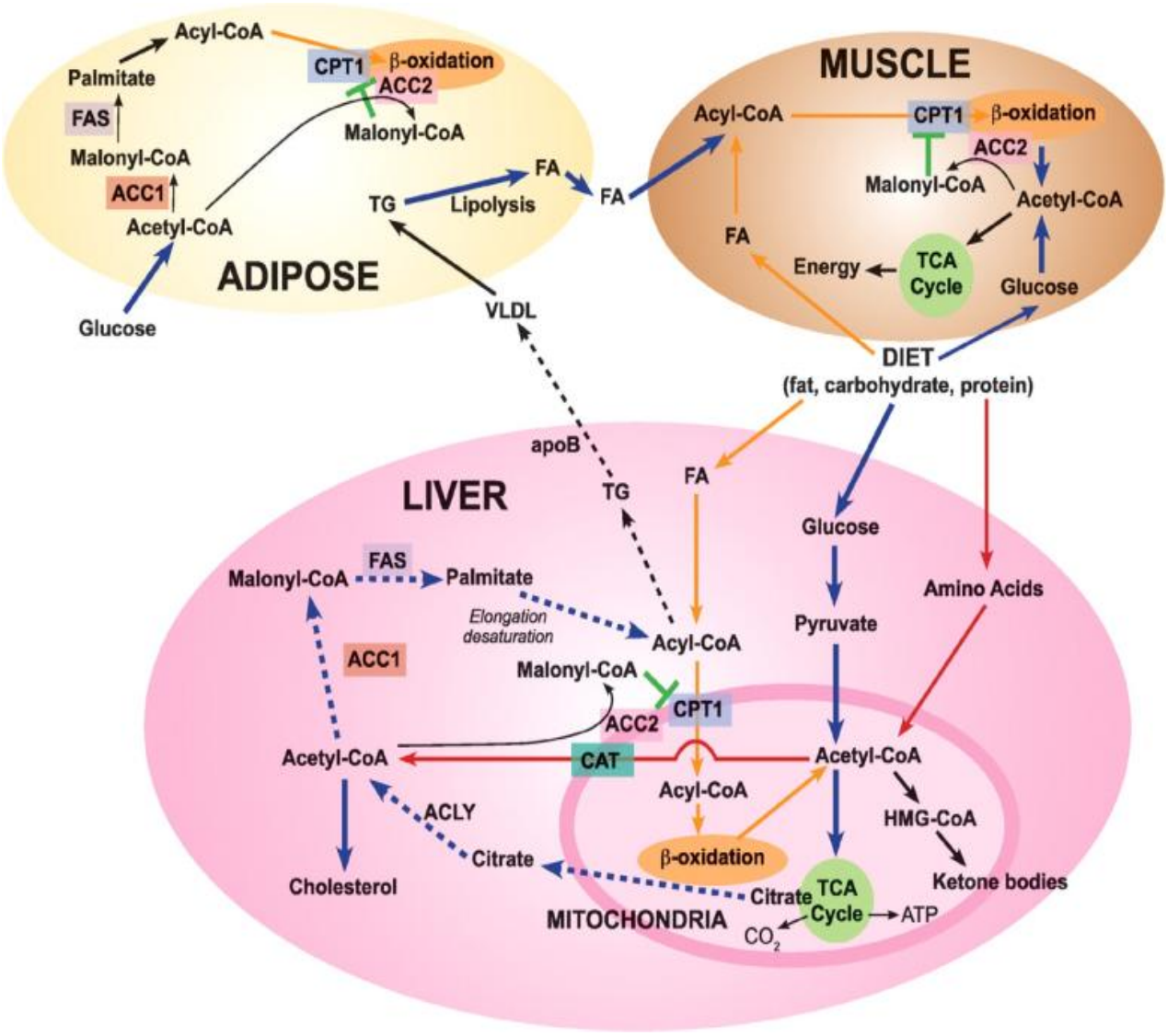

Figure 1.8: *Interplay between the enzymes ACC1, FAS, CPT1 and ACC2 in fatty acid synthesis, β-oxidation and tricarboxylic acid cycle, as well as the metabolites glucose, acetyl-CoA, malonyl-CoA, palmitate, acyl-CoA, fatty acids and ketone bodies. (Wakil and Abu-Elheiga 2009)*

FAS: Fatty acids are built from two-carbon building blocks, assembled by the fatty acids synthase (FAS) enzyme. The synthesis of fatty acids requires acetyl-CoA, malonyl-CoA and NADPH. Malonyl-CoA provided by the ACC1 enzyme is the C_2 donor in the de novo synthesis of fatty acids and it also inhibits fatty acid oxidation (Kim 1997, McGarry et al 1977). As previously mentioned, FAS is under control of the SREBP-1c transcription factor, it is thus under indirect influence of both hormonal and dietary factors (Xu et al 1999, Xu et al 2001). The interplay between ACC1, ACC2, CPT1 and FAS is shown in figure 1.8.

SCD1: Stearoyl-CoA Desaturase 1 (SCD1) is the rate-limiting enzyme catalyzing monounsaturated fatty acids. It uses palmitoyl-CoA and stearoyl-CoA as substrates to form

palmitoleyl-CoA and oleyl-CoA, respectively. These fatty acids are subsequently used to form triglycerides for storage of fat or phospholipids for constructing cell membranes. Obese mice with high levels of *Scd1* are reported to suffer from insulin resistance and fatty liver. Mice deficient in SCD1 are on the other resistant to obesity (Miyazaki et al 2009). The SCD1 gene is expressed in various tissues, including liver and adipose tissues in both mice and humans. SREBP-1c is identified as one of many promoters of SCD1, which means it is under the influence of insulin and also diet (Mauvoisin and Mounier 2011). Polyunsaturated fatty acids are known to be inhibitors of SCD1 gene expression (Ntambi 1999).

DGAT: Acyl Coa: diacylglycerol acyltransferase (DGAT) is an enzyme with a central role in the metabolism of glycerolipids. DGAT synthesizes triacylglycerol by using diacylglycerol and fatty acyl-CoA as substrates (Lehner and Kuksis 1996). Regulation of DGAT enzymes is complex and not fully understood. It is not reported to be under control of the SREBP-1c transcription factor, but it may be influenced by CCAAT enhancer-binding protein α (C/EBPα) or peroxisome proliferator-activated receptor γ (PPARγ), which are transcription factors which controls several other lipogenic genes (Yen et al 2008).

PPARγ: The peroxisome proliferator-activated receptor γ (PPARγ) transcription factor is necessary for adipocyte differentiation from fibroblasts, and also for maintaining the mature adipocyte. Expression of the PPARγ gene is promoted by C/EBPα. It is also regulated by several other pro- and anti-adipogenic factors, including SREBP-1c, as illustrated in figure 1.9. There are two isoforms of the PPARγ enzyme, PPARγ1 and PPARγ2. The *Pparγ1* and *Pparγ2* mRNAs are transcribed from the same DNA sequence, the different isoforms are generated through different promoter usage and alternative splicing of the pre-mRNA. Both are induced during adipogenesis, but PPARγ2 is found to be somewhat more efficient at promoting adipogenesis. PPARγ1 is also found in other cell types, for example macrophages. The PPARγ enzymes have to be activated by ligand to be transferred into the nucleus and induce adipogenesis (Rosen and MacDougald 2006). This means, like in the case of SREBP-1c, that the levels of *Pparγ* mRNA present in the tissue is not necessarily a good measurement of the amount of active PPARγ. Medicines that bind to PPARγ, e.g. rosiglitazone, and activate them have been used to treat Type 2 diabetes. Activated PPARγ increase insulin-stimulated glucose transport into the cells, which decrease hyperglycemia in diabetic patients. Activation of PPAR γ also leads to stimulation of adipogenesis, so even if PPARγ activating treats a symptom of Type 2 diabetes, it may aggravate obesity which is often one of the underlying factors for Type 2 diabetes development. It also may have adverse effects on skeletal

metabolism. As illustrated in figure 1.14, adipocytes and osteoblasts are derived from the same precursor cells. PPARγ activation leads to the formation of adipocytes in the skeleton, long-term use of rosiglitazone may thus lead to bone loss (Kawai and Rosen 2010, Wei et al 2010). Considering the risk of adverse effects when taking any form of drug, dietary strategies aimed to prevent and treat Type 2 diabetes is highly recommendable.

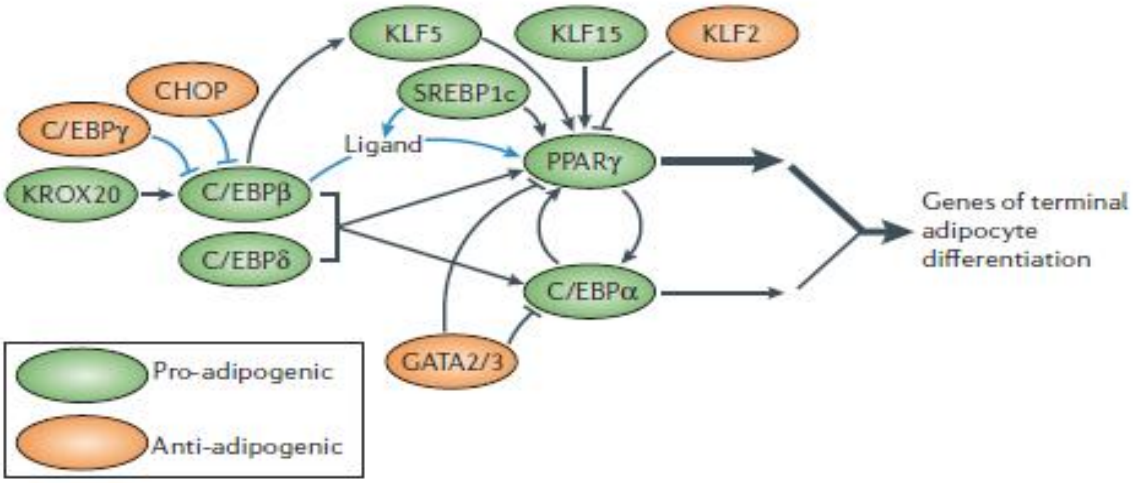

***Figure 1.9**: PPARγ is central in the regulation of adipogenesis. Black lines indicate effects on gene expression, blue lines are effects on protein activity. (Rosen and MacDougald 2006)*

1.5 ENZYMES INCREASING FATTY ACID BREAKDOWN

Fatty acid breakdown occurs through lipolysis and β-oxidation. Lipolysis is the hydrolyzation of triacylglycerol (TAG) into free fatty acids (FFAs). These free fatty acids are attached to coenzyme A, forming the acyl-CoA molecule. Acyl-CoA is broken down into acetyl units by β-oxidation in the cells mitochondria. This yields energy in the form of ATP-molecules. The metabolism of a FFA is illustrated in figure 1.10 (note that the FFA is labeled NEFA, which is the same thing). The oxidation of fat is highly regulated by diet, hormones and energy demands (Eaton 2002). Only the enzymes which mRNA levels were measured in this study will be described in this section. That includes PPARα, PPARδ, CPT-1A, CPT-2, HMGCS2 and ACO.

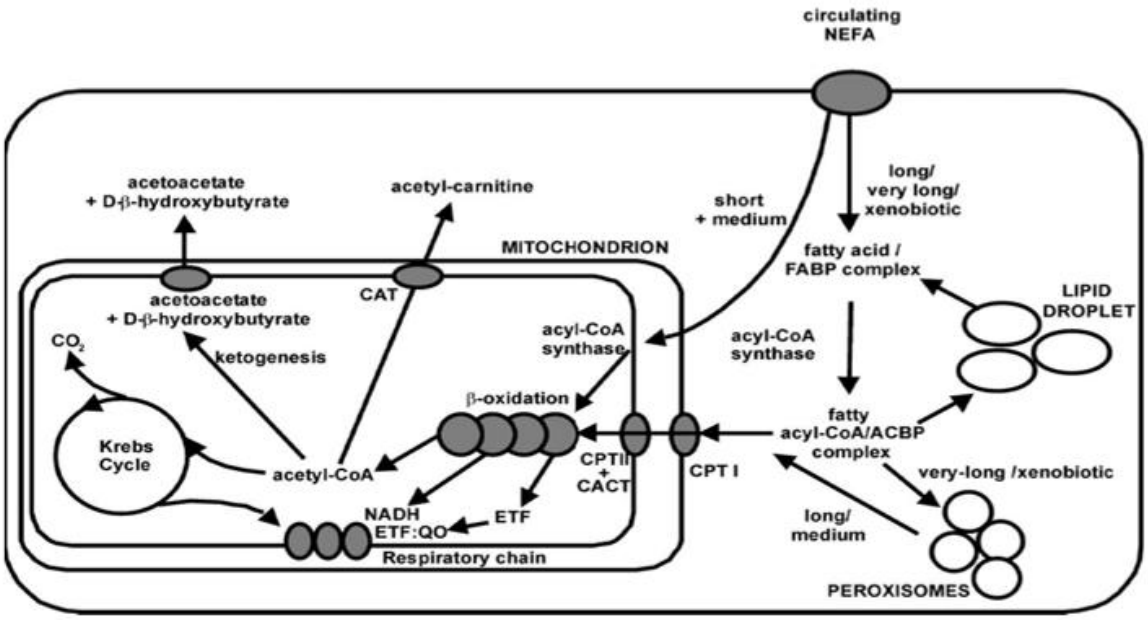

Figure 1.10: *Metabolism of non-esterified fatty acid (NEFA or FFA) in a generic cell. Fuel is generated in the mitochondria by the tricarboxylic acid cycle (also known as the citric acid cycle and Krebs cycle) of carbohydrates and β-oxidation of fatty acids. (Eaton 2002)*

PPARα and PPARδ: Peroxisome proliferator-activated receptors (PPARs) are a superfamily of transcription factors that coordinate lipid metabolism. Like in the case of SREBP-1c and PPARγ, these transcription factors have to be activated by ligand prior to transport into the nucleus to exert their effect on gene transcription. PPARs are in several studies shown to be activated by unsaturated fatty acids, such as PUFAs (Chawla et al 2001, Hostetler et al 2005). *Pparα* is highly expressed in liver, kidney, heart and brown adipose tissue. In the liver, PPARα affect the uptake of fatty acids through membranes, fatty acid activation, intracellular trafficking, oxidation and ketogenesis as well as triglyceride storage and lipolysis. Among the many target genes for PPARα is the Acyl-CoA oxidase (*Aco*) gene, which is the rate-limiting enzyme in peroxisomal long-chain fatty acid oxidation (Rakhshandehroo et al 2010). *Ppar*δ is equally expressed in all tissues and was until recently regarded as a housekeeping gene. The role of PPARδ is not fully described, but *Ppar*δ-knockout mice have reduced adipose tissue mass, implying its involvement in adipogenesis (Barak et al 2002). More recent studies have proposed that PPARδ favors the oxidation of fat. Activation of PPARδ led to reduced adipose tissue mass and improved adiposity, whereas PPARδ-deficient mice were prone to obesity on a high-fat diet (Wang et al 2003). PPARδ is also shown to activate target genes associated with oxidation of fat in cell cultures, including *Cpt1* (Alaynick 2008).

CPT: Carnitine palmitoyltransferase 1A (CPT1A) is found in liver cells, whereas the isoform CPT1B is found in muscle tissue. The enzyme is located on the mitochondrial membrane, with its active site facing the cytosol (van der Leij et al 1999). Here the CPT1A controls much of the hepatic β-oxidation as the rate-controlling enzyme, transferring long-chain acyl-moieties of acyl-CoA from coenzyme A to carnitine. The acyl-carnitine is then transferred from the cytosol to inside the mitochondria by the carnitine-acylcarnitine transporter. Inside the mitochondria, the action of CPT1 is reversed by CPT2, which exchanges the carnitine for CoA, regenerating acyl-CoA. The acyl-CoA released from CPT2 is broken down into acetyl-CoA by β-oxidation (Rufer et al 2009). The actions of CPT1 and CPT2 are illustrated in figure 1.11.

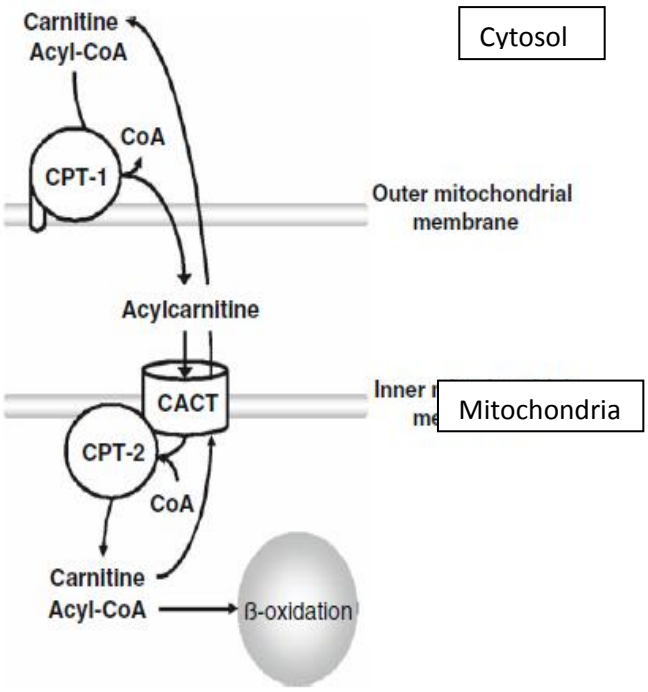

Figure 1.11: *Transfer of acyl-CoA from cytosol into mitochondria. (Rufer et al 2009)*

CPT1 is inhibited by malonyl-CoA, the product of ACC2, as described above (Eaton 2002). Transcription of the *Cpt1a* gene is reduced by insulin (Park et al 1995). *Cpt1a* is up-regulated by the presence of LCFA, such as PUFAs. This up-regulation can be done by the transcription factors PPARα and peroxisomal proliferator-activated receptor gamma coactivator-1 (PGC-1α) (Napal et al 2005). CPT2 is an enzyme with good substrate capacity and is not considered to be a rate-limiting enzyme (Eaton 2002).

HMGCS2: The Hydroxymethylglutaryl CoA synthase 2 (*Hmgcs2*) gene codes for a mitochondrial enzyme that controls the hydroxymethylglutaryl CoA-cycle (HMG-CoA cycle).

This gene is also induced by PPARα (Vila-Brau et al 2011). The HMG-CoA cycle converts acetyl-CoA from the β-oxidation into the ketone bodies acetoacetate, β-hydroxybutyrate and acetone. This is known as ketogenesis. Ketogenesis occurs in the liver and the ketone bodies can be used as substitutes for glucose (Hegardt 1999).

ACO: Acyl-CoA oxidase (ACO) is located in the peroxisome and is highly expressed in liver. It specifically oxidizes long-chain fatty acids, including PUFAs. PPARα is an inducer of *Aco*, demonstrated by the fact that PPARα-knockout mice do not have raised levels of *Aco* in the presence of PUFAs (Duplus and Forest 2002). The rare disorder of Acyl-CoA oxidase deficiency causes the hepatic peroxisomes to increase in size. It also causes very long chain fatty acids (VLCFA) to accumulate in serum and tissues (Poll-The et al 1988).

1.6 GLUCONEOGENESIS IN LIVER

This section will focus on the enzymes PCK1 and PGC-1α, which were measured in the liver of our animals. PGC-1α was also measured in adipose tissues, but its function in adipose tissues is quite different. This is described in section 1.10.

PCK1: During fasting, glucose levels are maintained through gluconeogenesis. In Type 2 diabetic patients, gluconeogenesis is consistently upregulated, contributing to high blood glucose levels. Phosphoenolpyruvate carboxykinase (PCK1, also known as PEPCK) is the rate-limiting enzyme in gluconeogenesis. *Pck1* is upregulated by the hormones glucagon and glucocorticoids (Herzig et al 2001) and is thus under dietary influence.

PGC-1α: PPAR*γ* coactivator 1 (PGC-1) is a gene coactivator. Whereas transcription factors bind to DNA and thereby control the transcription of a gene, coactivators can modify chromatin, unwind DNA and recruit RNA polymerase II. PGC-1α interacts with and coactivates a number of transcription factors and nuclear receptors, influencing energy metabolism and thermogenesis. *Pgc1α* expression is regulated by PGC-1α itself, via interaction with myocyte enhancer factor-2 (MEF2). PGC-1α activity is regulated by posttranslational modifications, including phosphorylation and deacetylation (Lin et al 2005). Active PGC-1 potentiates glucocorticoid induction of *Pck1* transcription. Obese mice have elevated blood glucose during fasting and are also shown to have elevated levels of *Pgc1α* and *Pck1*. Hyperglycemia is also seen in patients with Type 2 diabetes, and it is suggested that PGC-1α and PCK1 contributes to the pathogenesis of this disease (Yoon et al 2001).

1.7 HEPATIC AMINO ACID DEGRADATION

Many amino acids can be converted into alanine and alanine can be converted into glucose. In obese, insulin-resistant patients, amino acid degradation is upregulated to increase gluconeogenesis. This results in hyperglycemia seen in Type 2 diabetic patients. This section will focus on the enzymes AGXT, GOT, GPT1 and CPS1.

AGXT: The *Agxt* gene codes for the peroxisomal enzyme alanine-glyoxylate aminotransferase (AGXT) in the liver. It is induced by glucagon and cyclic AMP. In mice, it breaks down L-amino acids and glyoxylate into pyruvate and glycine. The pyruvate can be used for gluconeogenesis (Noguchi et al 1978).

GOT: The glutamate oxaloacetate transaminase (GOT) enzyme exists as two similar enzymes, GOT1 is located in the cytosol while GOT2 is in the mitochondria. The genes coding for the different enzymes are quite homologous. The mitochondrial GOT2 is predominant in liver. This enzyme catalyzes the formation of oxaloacetate from glutamate. Oxaloacetate is an intermediate in the tricarboxylic acid cycle, but can also be used in gluconeogenesis.

GPT: The glutamate pyruvate transaminase (*Gpt1*) gene codes for the enzyme alanine aminotransferase 1 (ALT1). *Gpt1* is mainly expressed in liver, bowel and white adipose tissue (Jadhao et al 2004). The ALT enzymes transfer the α-amino group from the glutamate amino acid to a pyruvate molecule. This forms the amino acid alanine, which can be transformed into glucose. This is useful during fasting, when blood glucose is low (Felig 1973), but for obese patients with insulin resistance it leads to hyperglycemia.

CPS1: The gene *Cps1* codes for the mitochondrial enzyme Carbamoyl-phosphate synthase 1 (CPS1). This enzyme catalyzes the first committed step of the urea cycle, which removes excess nitrogen in the form of urea from the cells. It uses ammonia and bicarbonate to synthesize carbamoyl phosphate, which is subsequently transformed into urea (Shambaugh 1978). Upregulation of this gene is a sign of increased amino acid breakdown.

1.8 CYCLIC AMP SIGNALING

Cyclic adenosine monophosphate (cAMP) is a signal of starvation. It is generated by adenylate cyclases from ATP at the cytosolic side of the cells plasma membrane (Houslay and Adams 2003). Elevated cAMP levels induces gluconeogenesis in liver and lipolysis in adipose tissue (Madsen and Kristiansen 2010). cAMP levels could not be measured in this experiment due to the fast degradation of the molecule in dead tissue, so we measured the expression levels of *Crem, RIα, RIIβ* and *Pde4c*. Their function will be briefly described in this section.

PKA isoforms - RIα and RIIβ: It is suggested that cAMP-dependent protein kinase A (PKA) is required for cAMP-induced gene transcription (Montminy 1997). The PKA is assembled from two regulatory (R, α and β) and two catalytic units. The holoenzyme PKA is activated by cAMP, which releases the two catalytic units from the regulatory units. The catalytic units exert several effects on metabolism, mainly increasing lipolysis and inducing gluconeogenesis. In mice, there are two isoforms of the regulatory subunits, RI and RII. The RIIβ isoform is expressed in both white and brown adipose tissues in mice. Mice with disrupted RIIβ isoform are protected against diet-induced obesity. The loss of the RIIβ isoform in these mice leads to a compensatory increase in the RIα-isoform of PKA. The RIα-isoform eagerly binds to cAMP, so this form of PKA is more easily activated by cAMP compared to the wild-type enzyme. Active PKA catalytic units phosphorylate and thus activate enzymes involved in metabolism. They increase the activity of uncoupling protein (UCP), which increases the metabolic rate and elevates body temperature. The higher ratio of RIα compared to RIIβ leads to healthy, lean mice which are protected from diet-induced obesity and hepatic steatosis (Cummings et al 1996).

CREM: cAMP-responsive element modulator (*Crem*) is an enhancer of genes that are transcribed in response to increased cAMP-levels. It is induced by several transcription factors, including cAMP-responsive element binding protein (CREB) (Montminy 1997). Both CREM and CREB bind to a DNA sequence known as the cAMP responsive element (CRE), which is present in the regulatory region of target genes. CREM is activated by PKA by phosphorylation and is thus regulated by cAMP (de Groot et al 1994, Montminy 1997). The *Crem* mRNA can be alternatively spliced into both transcriptional activators and repressors (Inada et al 1999).

PDE: cAMP phosphodiesterases (PDEs) have a regulatory role in the sense that it is the only enzyme capable of degrading cAMP. PDEs are thus located at multiple sites in the cell,

including the cytosol, nucleus, various membranes and in the cytoskeleton. In the PDE families, there are over 30 isoforms capable of degrading cAMP. The PDE4 family consists of four subfamilies, the PDE4a-d. These generate over 16 isoforms. Mice with inactive PDE4s exhibits decreased inflammation (Houslay and Adams 2003).

1.9 INFLAMMATION MARKERS IN ADIPOSE TISSUE

Inflammation of the adipose tissue is a chronic, low inflammatory state that occurs when adipocytes enlarge in size and recruit macrophages. Enlargement of adipocyte size is a result of accumulation of excess triglycerides. Large adipocytes release more free fatty acids (FFAs), especially saturated fatty acids, which bind to macrophages at the macrophage toll-like receptor-4 (TLR-4). Saturated fatty acids from diet activate the TLR-4, while polyunsaturated fatty acids block it. Activated TLR-4 causes the macrophages to change their phenotype from M2, which is a partially activated state, to M1, which is a constant activated state. M1 macrophages secret higher levels of tumor necrosis factor α (TNFα). The TNFα binds to adipocytes, causing them to increase lipolysis and express various pro-inflammatory genes, e.g. CC-chemokine ligand 2 (CCL2, also known as monocyte chemotactic protein-1, MCP-1) (Ouchi et al 2011). The development from normal adipose tissue to inflamed adipose tissue is illustrated in figure 1.13. Inflammation of adipose tissue is worse in visceral fat compared to the subcutaneous fat depots (Gesta et al 2007).

The vicious cycle of enlargement of adipose tissue and activation of macrophages also leads to reduced expression of adiponectin, a hormone excreted from adipose tissue with regulatory effects on glucose and fatty acid metabolism. Adiponectin has positive effects on the development of obesity, Type 2 diabetes and metabolic syndrome. Dietary fish-oil, rich in long-chain polyunsaturated fatty acids, is associated with increased levels of adiponectin in mice (Hajer et al 2008). The n-3 fatty acids EPA and DHA are also associated with reduced levels of inflammatory macrophages. This occurs through activation of the G protein-coupled receptor 120 (GPR120), which increases the gene expression of the anti-inflammatory M2 macrophage phenotype and reduces the gene expression of the proinflammatory M1 phenotype (Oh et al 2010).

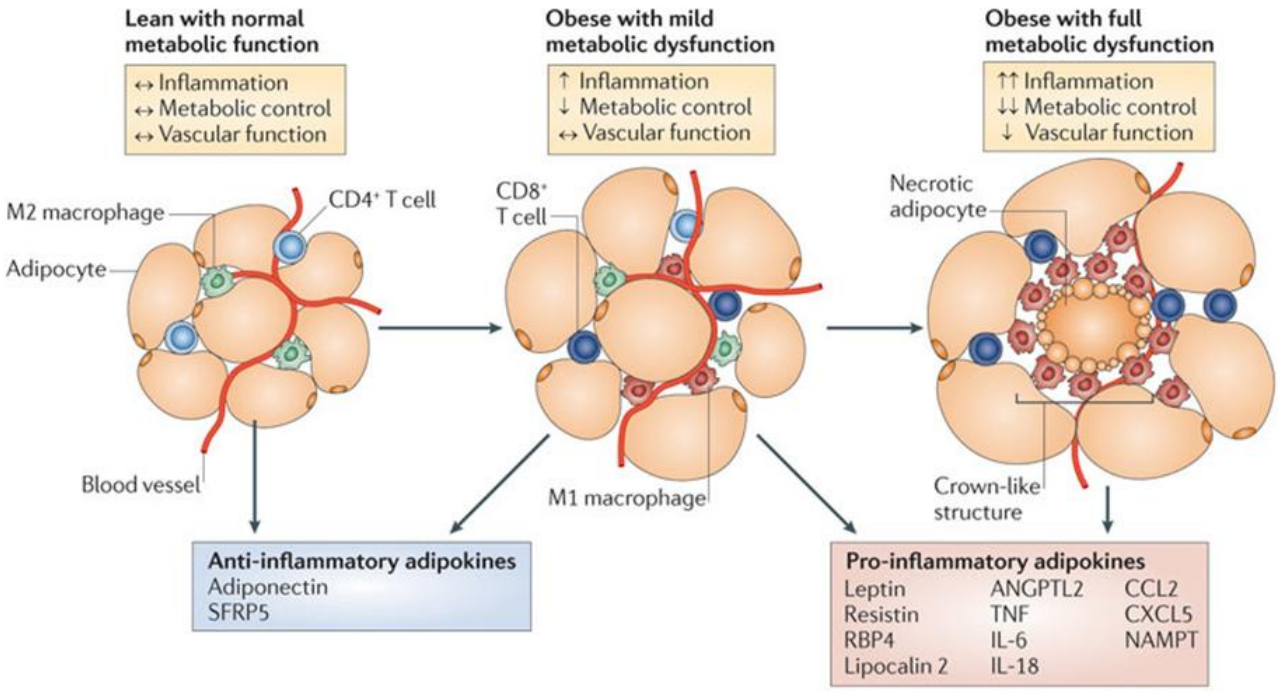

***Figure 1.12**: M1 macrophages generate large amounts of pro-inflammatory factors. This leads to a dysfunctional adipose tissue and the evolvement of crown-like structures, which is dead adipocytes with M1-type macrophages assembled around them. (Ouchi et al 2011)*

The adipocyte dysfunction illustrated in figure 1.12 can lead to Type 2 diabetes. High levels of FFAs secreted from adipocytes in obese patients inhibit insulin secretion from the pancreas. This is done in several ways; FFAs can open β-cell potassium channels, which reduce insulin secretion. FFAs also enhance the expression of uncoupling protein 2 (*Ucp2*), which diminishes ATP-production required for insulin secretion. FFAs are also shown to induce apoptosis of β-cells through endoplasmic stress response and by inhibiting the expression of anti-apoptopic factor Bcl-2. Also, tumor necrosis factor α (TNFα) secreted from inflamed adipose tissue induces pro-apoptopic NO production and inhibits insulin signaling in the β-cell. Obese patients may be leptin resistant, which also aggravate the insulin signaling. Leptin is able to reduce apoptosis through inhibition of nitric oxide (NO) production. Patients with leptin resistance do not gain from the anti-apoptopic effect of the leptin hormone.

FFAs, TNFα and leptin resistance together reduces insulin secretion from the pancreas, which contributes to the development of Type 2 diabetes, as illustrated in figure 1.13 (Hajer et al 2008).

In this study, we measured the inflammation markers *Ccl2*, *Serpine1*, *Cd68* and *Emr1* in epididymal and inguinal white adipose tissues.

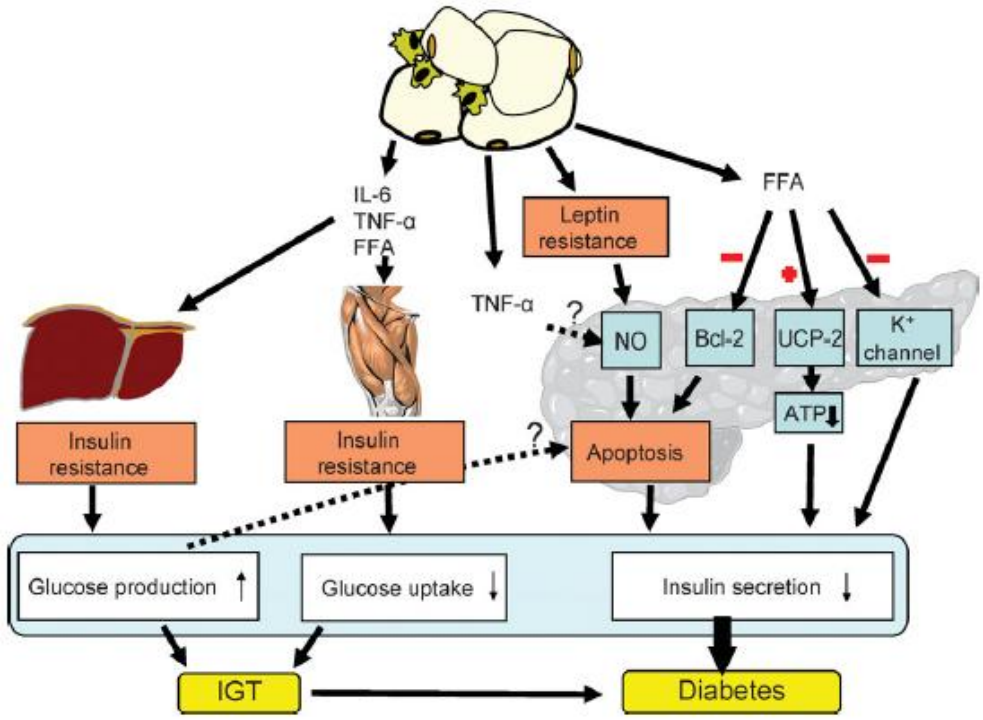

***Figure 1.13**: Adipocyte dysfunction leads to Type 2 diabetes. (Hajer et al 2008)*

CCL2: Obese mice as well as humans have elevated levels of *Ccl2* in adipose tissue. This leads to macrophage recruitment to adipose tissue and increased inflammation. It also promotes glucose intolerance and insulin resistance, as seen in Type 2 diabetes. CC-chemokine receptor 2 (Ccr2) is the receptor for CCL2. Mice with Ccr2 deletion gain as much weight as wild-type mice on a high-fat diet, but do not have adipose tissue inflammation and maintain insulin sensitivity (Ouchi et al 2011).

Serpine1 (also known as PAI-1): PAI-1 is the human homologue to serine peptidase inhibitor (Serpine1) in mice. Serpine1/PAI-1 is a regulator of fibrinolysis, the breaking down of blood clots. It is produced by visceral adipocytes and is shown to be regulated by TNFα, insulin, FFAs and glucocorticoids in vitro. Elevated levels of circulating PAI-1 are associated with increased risk of damage to the blood vessels. This is caused by the forming of small blood clots and plaque, resulting in narrowing of the blood vessels and small ruptures which attracts macrophages. *Pai1* is shown to be elevated in obese patients suffering from metabolic disease (Hajer et al 2008).

CD68: Macrosialin is the mouse analog to human Cluster of Differentiation (CD68). They are 80% similar and are both expressed by macrophages (Holness et al 1993). Its function is still uncertain, but it is found almost exclusively on macrophages (Kurushima et al 2000).

EMR1 (also known as F4/80): EGF-like module-containing, mucin-like hormone, receptor-like sequence 1 (EMR1) is the human analog to the F4/80 found in mice. It is a monoclonal antibody that recognizes cell surface glycoprotein on macrophages. The macrophages regulate their immune responses through these cell surface receptors (McKnight et al 1996).

1.10 GENES EXPRESSED IN BROWN AND WHITE, BROWN-LIKE ADIPOCYTES

Adipocytes evolve from stem cells. The stem cells develops into mesenchymal stem cells which then commits into becoming osteocytes (bone), adipocytes (fat) or myocytes (muscle). The undifferentiated adipoblast precursor cell is influenced by different transcription factors and subsequently differentiates into a white or brown adipocyte, as illustrated in figure 1.14.

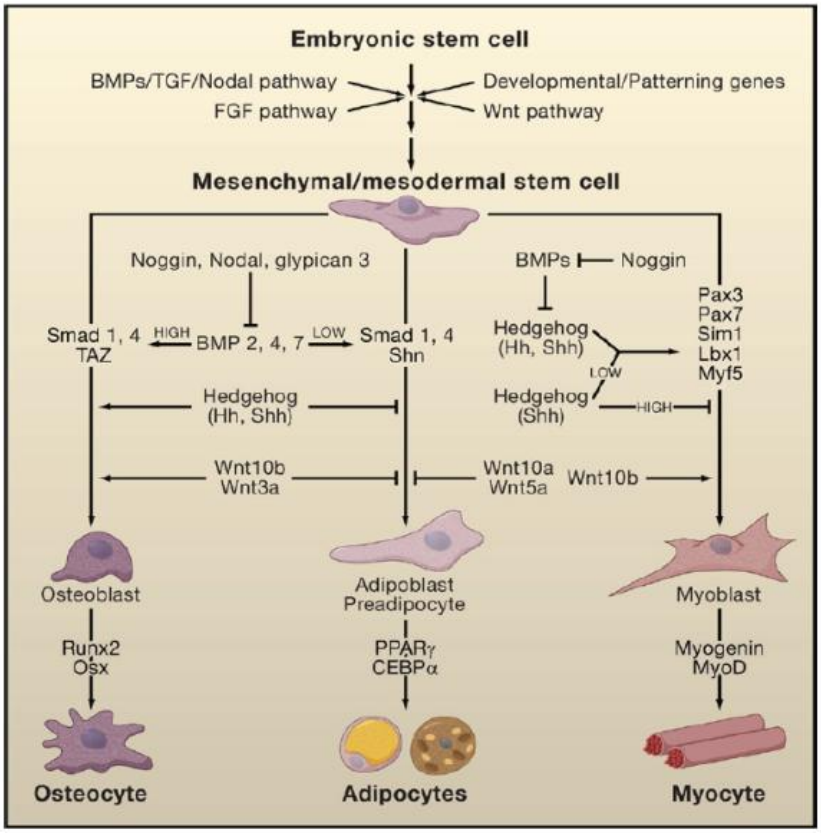

***Figure 1.14**: The evolvement of adipocytes from mesenchymal stem cells. (Gesta et al 2007)*

White adipocytes accumulate large amounts of fat, they have very little cytoplasm because the lipid droplet containing triglycerides occupies up to 95% of the cell volume. Brown adipocytes have small lipid droplets distributed around their considerable cytoplasm. The brown color of these cells is caused by the large amount of mitochondria present in the cell. Brown adipocytes have the capacity to burn fat and thus turning it into heat due to the

increased number of mitochondria (Gesta et al 2007). Studies have stated that brown and white adipocytes can change phenotypes. White and brown adipocytes accumulate in different tissues, but the white adipose tissue contains some brown adipocytes and vice versa. The phenotype of an adipocyte is able to change, a white adipocyte can acquire a brown-like phenotype through the increase of PGC-1α (Tiraby et al 2003) .

In this study, we measured the expression levels of *Pgc1α* and *Ucp1* in both brown and white adipose tissues. *Dio2*, *Cox2*, and *Rip140* were measured only in brown adipose tissues.

PGC-1α: Whereas elevated levels of *Pgc1α* in liver and blood is not a good thing, *Pgc1α* expression in white and brown adipose tissue is. PGC-1α in adipocytes is a transcriptional coactivator for uncoupling protein-1 (UCP1), which stimulates lipid oxidation, mitochondrial β-oxidation and heat production (Lin et al 2005). This increases energy expenditure and can protect against obesity. PGC-1α is also a coactivator for the NAD-dependent deacetylase sirtuin-3 (SIRT3), which activates the expression of UCP1 and other thermogenetic genes (Giralt et al 2011). *Pgc1α* is rapidly expressed in adipocytes by exposure to cold environment, resulting in maintenance of body temperature. Mice deficient in PGC-1α are extremely cold sensitive. PGC-1α is primarily found in brown adipocytes, where it may have a role in the development of brown adipocytes (Lin et al 2005).

Dio2: In brown adipose tissue, Type II iodothyronine deiodinase (Dio2) converts the inactive thyroid hormone prohormone thyroxin (T_4) into the active form triiodothyronine (T_3). T_3 reduces the half-life of UCP1 in the brown adipocyte, thereby increasing the cells capacity to turn fat into heat. *Dio2* is expressed in brown adipose tissue and is induced by cold exposure. It is also induced by both insulin and glucagon, as well as norepinephrine. The activity of Dio2 is increased by cAMP-dependent protein kinase (PKA) (Bianco et al 2002).

RIP140: Receptor-interacting protein 140 (RIP140) is a nuclear receptor corepressor with control over lipid metabolism. It represses the expression of *Ucp1*, leading to reduced oxidation of fat in brown adipocytes and increased accumulation of fat. RIP140-null mice are lean and resistant to diet-induced obesity (Christian et al 2005).

CytCox: Cytochrome c oxidase (CytCox) is an enzyme complex located at the inner mitochondrial membrane. It is derived from both nuclear and mitochondrial DNA, see figure 1.15. Cox2 is among the mitochondrial derived subunits. ATP production in mitochondria is driven by a proton gradient across the inner mitochondrial membrane. This proton gradient is

generated from electrons from NADH or $FADH_2$. These electrons are passed through redox systems and finally transferred to molecular oxygen by CytCox. CytCox is therefore vital for the mitochondrial function (Mick et al 2011).

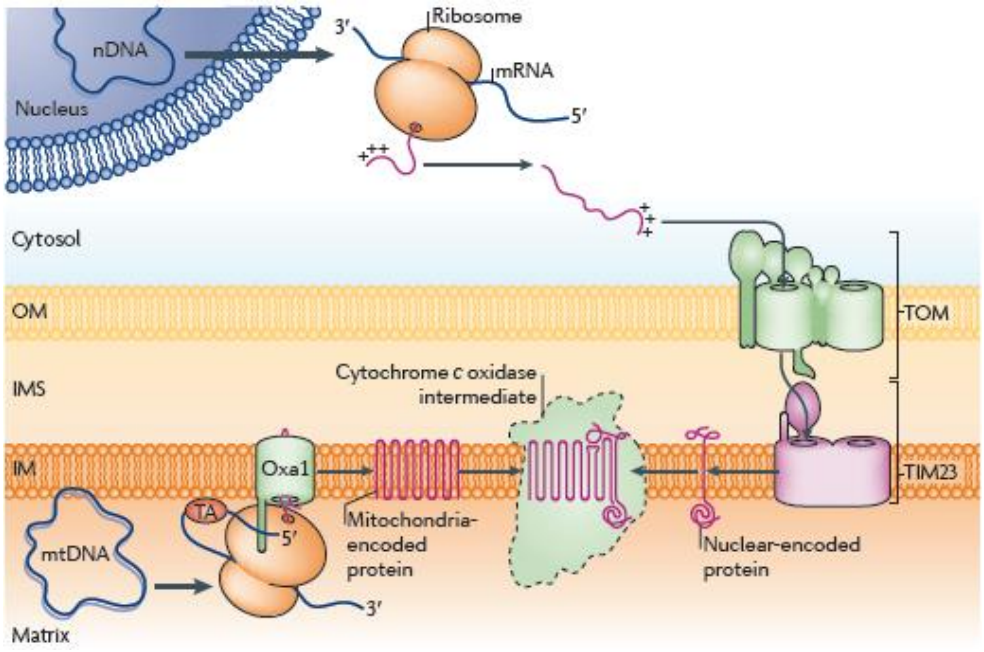

***Figure 1.15**: CytCox is assembled from subunits derived from both nuclear and mitochondrial DNA. Nuclear DNA is transcribed into mRNA and translated into precursor proteins in the cytosol. These precursor proteins are translocated to the inner mitochondrial membrane. Mitochondrial DNA is transcribed into mrRNA and subsequently translated into proteins at the inner mitochondrial membrane. After insertion of both nuclear- and mitochondria-derived protein into the membrane, these subunits are assembled into the functional CytCox complex. (Mick et al 2011)*

1.9 ACCUMULATION OF TRIGLYCERIDES IN LIVER, MUSCLE AND PLASMA

Accumulation of triglycerides in the liver leads to hepatic steatosis, or fatty liver disease. Non-alcoholic fatty liver disease is a common liver disease found in obese patients with Type 2 diabetes. It is primarily caused by the release of triglycerides from adipose tissue into the blood stream, which causes it to accumulate in liver and muscle (Fig 1.16). Steatosis can evolve into serious liver damage, also TG accumulation in liver and muscle is associated with reduced insulin sensitivity. It is still unclear whether TG accumulation causes insulin resistance or the other way around. Currently, there is no treatment for steatosis, apart from the life style modifications recommended to obese patients (Ferre and Foufelle 2010).

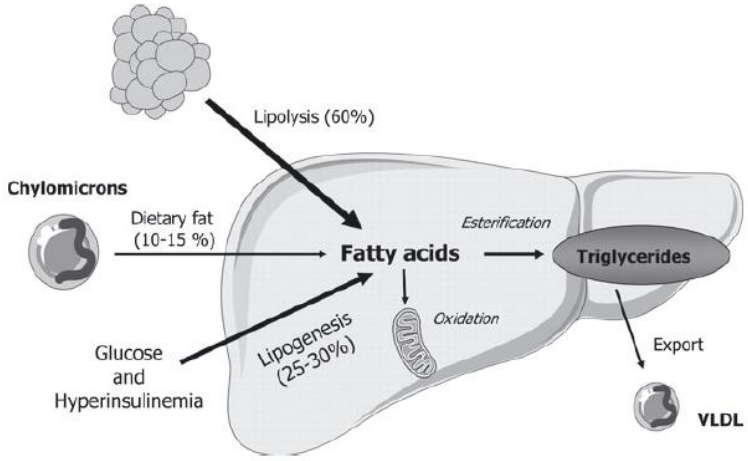

***Figure 1.16**: Contributions of various metabolic pathways to hepatic steatosis in obese humans. The major contributor to triglyceride accumulation in the liver is the increased release of FFA from adipose tissue. (Ferre and Foufelle 2010)*

1.10 SUMMARY AND AIM OF THE STUDIES

Obesity is caused by excess nutrients. Type of nutrients can influence how much fat is stored and where the body stores it. Visceral adipose tissue is more prone to inflammation compared to subcutaneous fat depots. White adipocytes stores fat, whereas brown adipocytes can turn fat into heat.

Carbohydrates exist in several forms. Fructose does not instantly raise insulin levels, in contrast to glucose. Glucose exists as monosaccharides, polysaccharides and as a part of disaccharides, e.g. sucrose.

Fatty acids are more than mere energy. They influence our health by incorporation into cellular membranes and can act as ligands for transcriptional factors and thus influence the expression of lipogenic, lipolytic, gluconeogenetic and inflammatory genes.

PUFAs are demonstrated in several studies to attenuate diet-induced obesity. On the other hand, sucrose and high GI diets are demonstrated to be obesogenic. The aim of this study is to investigate whether the obesogenic effects of sucrose and high GI diet, which we know are major components of most people's diet, can be attenuated by fish oil. We also want to investigate whether the fructose moiety of the sucrose molecule is obesogenic, antiobesogenic or neither. Finally, we want to see which diet, if any, is most likely to be healthy for humans.

2. MATERIALS AND METHODS

2.1 ANIMAL MODEL

Our choice of animal model fell on the C57BL/6J mouse, also called black-six mouse. This mouse has proved itself as a good model for human metabolic syndrome because it easily develops diet-induced obesity, along with hyperinsulinemia, hyperglycemia and hypertension. Black-six mice develop central obesity, which is also common in obese humans with Type 2 diabetes (Collins et al 2004). Male mice were chosen over female because males have an extra visceral fat depot, the epididymal fat, around their testes. It is also prohibited to keep female mice in separate cages, whereas males are best kept in single cages. In this experiment it was vital to keep the animals in separate cages to record each animals feed intake.

The mice were kept in accordance with guidelines provided by The Norwegian Animal Research Authority. The experiment was approved by the Norwegian State board of biological experiments.

Figure 2.1 *C57BL/6J mouse. From http://www.taconic.com/wmspage.cfm?parm1=760*

2.2 EXPERIMENTAL SETUP

46 male mice were purchased from Scanbur AS (Nittedal, Norway). On the 17th of September, they were weighed and separated into single cages. The mice then had three weeks to settle into their new environment, partly due to a delay in the arrival of the experimental feed. On October the 2nd, the mice were weighed again and five mice at the bottom and top of the weight scale were removed from the experiment, leaving 36 mice weighing from 26.32 and 30.90 gram. The mice were then between 13 and 14 weeks old. The mice were fed chow-diet during their acclimatization period and they had free access to tap water at all times. The mice were kept in a 12h light/dark cycle at 22-25 °C and 40-50% humidity. The bedding was wooden chip bedding (Scanbur Bedding Aspen, Norway). They were fed almost exclusively by me, at the same time, every single day. The animals were

observed for health problems and abnormal behavior every day. Water was changed every other day and their cages cleaned every 14th day. Body weight was recorded twice a week, Mondays and Thursdays. At the beginning of the trial, the 36 mice were divided into 6 groups, with 6 animals in each group. They were divided based on starting weight to achieve the same mean weight in each group.

2.3 DIETS

The 6 groups were given different diets. Diets were purchased from Ssniff (Spezialdiäten GmbH, Soest, Germany) and stored at -20 °C. All diets contained the same amount and type of protein, ash, fiber, vitamins and trace elements.

Group 1 was given low energy standard chow diet, containing low amounts of fat and high amounts of carbohydrates. Group 2-6 were all given high amounts of fish oil in combination with different types of carbohydrates. The fish oil diets contained 62 g/kg n-3 PUFAs, thereof 27 g/kg EPA and 18 g/kg DHA. Group 2 was given high amounts of sucrose, group 3 received glucose, group 4 fructose, group 5 amylose and group 6 amylopectin. Group 5 had to be given some amounts of amylopectin due to the welfare of the animals. Diets given to group 2-6 contained the same amount of metabolizable energy (ME). The amount of ingredients in each diet is listed in table 2.1.

Food intake was recorded every day and their bedding checked thoroughly for leftovers. Groups 2-6 were pair-fed, meaning that they all received the same amount of food every day. Group 1 had free access to food, but their food intake was also recorded.

2.4 DATA COLLECTION

The mice were euthanized after 9 weeks of experimental feeding. The mice were weighed before being gassed with the anesthetic Isofluran (Isoba-vet., Schering-Plogh, Denmark). The mice were anaesthetized using the apparatus Univentor 400 Anaesthesia Unit (Univentor Limited, Sweden), and killed by cardiac puncture.

Table 2.1 *Ingredients in the different diets, listed as percent of weight, not percent of metabolizable energy (ME).*

	Low energy	Sucrose	Fructose	Glucose	Low GI	High GI
Protein	**20 %**	**20 %**	**20 %**	**20 %**	**20 %**	**20 %**
Casein	20 %	20 %	20 %	20 %	20 %	20 %
L-Cysteine	0,3 %	0,3 %	0,3 %	0,3 %	0,3 %	0,3 %
Carbohydrate	**67 %**	**49 %**	**49 %**	**49 %**	**49 %**	**49 %**
Corn starch	53 %	1 %	1 %	1 %	1 %	1 %
Cellulose	5 %	5 %	5 %	5 %	5 %	5 %
Amylose					20 %	
Amylopectin					14 %	34 %
Sucrose	9 %	43 %	9 %	9 %	9 %	9 %
Fructose			34 %			
Glucose				34 %		
Fat	**7 %**	**25 %**	**25 %**	**25 %**	**25 %**	**25 %**
Soybean oil	7 %	7 %	7 %	7 %	7 %	7 %
Fish oil		18 %	18 %	18 %	18 %	18 %
MJ ME/kg	**16,2**	**20,1**	**20,1**	**20,1**	**20,1**	**20,1**
Vit A (IU/kg)	4 000	4 000	4 000	4 000	4 000	4 000
Vit D3 (IU/kg)	1 000	1 000	1 000	1 000	1 000	1 000
Vit E (mg/kg)	75	75	75	75	75	75
Vit K (mg/kg)	6	6	6	6	6	6
Cu (mg/kg)	11	11	11	11	11	11

2.4.1 Blood samples

The chest of the mice was cut open and a syringe placed directly into the heart to collect blood. Blood samples were stored in tubes containing EDTA as anticoagulant and immediately centrifuged at 2500 x g and 4 °C for 5 minutes. Plasma and red blood cells were stored at -80 °C for subsequent analysis.

2.4.2 Liver-, muscle- and adipose tissue

All tissues were weighed before further treatments. Tissue samples were put in small plastic bags and quickly frozen, using a freeze clamp and liquid nitrogen. A small piece of the liver was cut off and stored for lipid analysis, the rest was to be used for RNA analysis. The tibialis anterior muscle was cut off from each leg. One piece was frozen as described above, the other was stored for lipid analysis. Three white adipose tissue depots were collected; epididymal (eWAT), retroperitoneal (rWAT) and inguinal (iWAT). Epididymal adipose tissue is located around the ureters, bladder and epididymis. The retroperitoneal fat is located around each

kidney. Epididymal and retroperitoneal adipose tissue are regarded as visceral fat, whereas inguinal fat is subcutaneous fat. Brown adipose tissue depot was also excised and weighed; the intrascapular brown adipose tissue (iBAT). This is located at the back of the mouse, on top of the shoulder blades. Fat depots were frozen as described above and stored at -80 °C for RNA analysis. Additionally, tissue samples from two mice in each group were collected and stored in 70% ethanol for histology analysis. Only eWAT was used for histology analysis.

2.5 CHEMICALS AND REAGENTS

All chemicals and reagents were purchased from commercial sources. See Appendix I for details.

2.6 GENE EXPRESSION LEVELS

The gene expression levels gives information on what genes are being transcribed into proteins. Total RNA was extracted from liver, muscle, eWAT, rWAT, iWAT and iBAT from each mouse. Purity and quantity of extracted RNA was measured by using Nanodrop (Saveen Werner, Sweden). Integrity of the RNA was measured by using Bioanalyzer (Agilent Technologies, USA). The RNA was then transcribed into complementary DNA (cDNA) by the enzyme reverse transcriptase (RT-reaction). The gene expression levels were finally quantified by measuring the cDNA levels by the real-time polymerase chain reaction (rt-PCR).

2.6.1 Extraction of total RNA from tissue

Principle: Tissue samples are individually homogenized with Trizol. Chloroform is added to the homogenized tissue and the mix is centrifuged. The RNA is now located in the transparent water phase, which is transferred to another tube. Isopropanol is added to extract the RNA from the water phase. The enzyme DNase is used to eliminate remaining DNA.

Procedure: 1 ml of Trizol reagent and zirconium beads were added to each tube. 50-100 mg frozen tissue was added to the mix and homogenized using Precellys 24 lysis & homogenization instrument (Bertin Technologies), at full speed for 4-6 minutes. Samples

were centrifuged at 12000 x g for 10 minutes at 4 °C (Eppendorf Centrifuge 5415 R), the supernatant extracted into new tubes and incubated at room temperature for 5 minutes. Each sample was added 200 µl chloroform and shaken rigorously by hand for 15 seconds. Samples were again incubated for 2-3 minutes at room temperature, after that they were centrifuged at 12000 x g for 15 minutes at 4 °C. The upper layer water phase was extracted and transferred to new tubes. 500-750 µl isopropanol was added to each sample and mixed by turning the tubes upside down a few times. Samples were then incubated at room temperature for 10 minutes, then at 4 °C for another 10 minutes. Again, they were centrifuged at 12000 x g for 10 minutes at 4 °C. Now, the RNA was located in a pellet at the bottom of the tube. The supernatant was discarded using a vacuum apparatus (IBS Integra Biosciences, Vacuboy, Switzerland). The RNA pellet was washed with 1000-1500 µl cold 75% ethanol and vortexed into suspension. Samples were centrifuged at 7500 x g for 5 minutes at 4 °C. Supernatant was again removed by vacuum suction. The tubes with RNA pellet were incubated for 2-3 minutes on ice to vaporize any remaining liquid, then they were added 50-300 µl ddH_2O to dissolve the RNA. The RNA samples were subsequently purified for any DNA residues by using the "DNA free kit", according to the vendor's description. (NIFES 2005, 281 - RNA RENSING OG RNA KVANTITET)

2.6.2 RNA quality and quantity on the NanoDrop

Principle: The NanoDrop ND-1000 spectrophotometer (Saveen Werner, Sweden) makes an accurate analysis of RNA purity and quantity, using only 1.5-2 µl of the sample. Surface tension is used to hold a drop of the liquid RNA in place while a measurement is made at 230 nm, 260 nm and 280 nm.

Procedure: A drop of RNA dissolved in ddH_2O was placed on the apparatus. The 260nm/280nm ratio and 260nm/230nm ratio were calculated. A 260nm/280nm ratio lower than 1.6 indicated that there were protein residues or that the RNA had not dissolved properly in the liquid. Protein residues may degrade the RNA. A 260nm/280nm ratio above 2.2 indicated that there were phenol remnants in the sample. A 260nm/230nm ratio lower than 1.7 indicates organic contaminations. Samples with nonsatisfactory ratios were precipitated with 3M NaAc pH 5,2 and ethanol and incubated overnight at -80 °C. The samples were then centrifuged at 12000 x g for 10 minutes and the supernatant discarded with vacuum suction. The RNA was then washed with ethanol as described above, before a new measurement was

made on the NanoDrop. RNA concentration between 100-3000 ng/µl is preferable. The NanoDrop can detect concentrations as low as 1.5 ng/µl, but the concentration has to be higher than 30-50 ng/µl to run qPCR. Liver has the highest concentrations of RNA, while adipose tissues are on the lower end of the scale. After use, the droplet of RNA was simply wiped off with a soft paper tissue. (NIFES 2009, NanoDrop ND-1000)

2.6.3 RNA integrity on the BioAnalyzer

Principle: RNA integrity is checked on the BioAnalyzer RNA 6000 Nano (Agilent Technologies) before further analysis. RNA 6000 Nano LabChip Kit (Agilent Technologies) contains a chip and reagents designed to determine the size of RNA fragments. Every chip contains microchannels which separates nucleic acid fragments by electrophoresis, based on the size of the fragments. The results are displayed on the program Bioanalyzer software as a gel-like image, electropherogram, RNA Integrity Number (RIN) and ribosomal RNA (rRNA) ratio (28S/18S). The peaks on the electropherogram give a visual assessment of the RNA quality. The RIN gives information on the degradation of RNA. A RIN-number of 1 equals totally degraded RNA, while a RIN-number of 10 means that the RNA is fully intact. RNA needs to be as intact as possible to perform qPCR, but RIN as low as 7 were accepted. The BioAnalyzer also calculates RNA concentration, but it is less accurate than the NanoDrop.

Procedure: 12 samples of RNA with a concentration of 25-500 ng/µl were analyzed on the BioAnalyzer. A new RNA Nano chip was put in the Chip Priming station. 9 µl of gel-dye mixture was added to the bottom of the well in column 4, row 1, 2 and 3. 5 µl RNA 6000 Nano Marker was added to the well with a ladder symbol and in the 12 sample wells. 1 µl RNA was put into the well marked with the ladder and into each of the sample wells. The chip was now put on the IKA vortex mixer and vortexed for 1 minute at 2400 rpm. The chip was now run on the BioAnalyzer. (NIFES 2006, 278 - RNA kvalitet på BioAnalyzer (RNA 6000 Nano))

2.6.4 RT- Reaction

Principle: Total RNA is transcribed into complementary DNA (cDNA) by the enzyme reverse transcriptase with access to the four deoxyNTPs. This cDNA is used to determine gene expression levels in subsequent qPCR analysis. One RT-plate consists of 96 wells,

where 18 wells must be used to calculate a standard curve and two wells must be used for negative controls.

Procedure: Complementary DNA was made in duplicates from each tissue sample. A standard curve with the concentrations 1000 ng/µl, 500 ng/µl, 250 ng/µl, 125 ng/µl, 63 ng/µl and 31 ng/µl RNA was made from a pool of RNA from all samples. This standard curve was included on each RT-plate in a triplicate. Due to the number of animals, 36, and the limited number of wells on the RT plate, 96, one RT-plate had to be made for each tissue (liver, muscle, eWAT, rWAT, iWAT and iBAT). Two negative controls were included into each RT-plate, one "non amplification control" and one "non template control". 50 µl cDNA was made from the liver-RNA due to the high number of hepatic genes we wanted to run, while it was sufficient to make 30 µl cDNA for the other 5 tissues. The reagents used for both volumes are listed in table 2.2. 20 or 40 µl of this mix was added to each of the 96 wells on the RT-plate. 40 µl of the mixture was used for liver RNA and 20 µl mixture for all other tissues. 10 µl RNA was added to each well, except for the non template control. All RNA, except for RNA used for the standard curve, had a concentration of 50 (liver RNA) or 30 ng/µl (other tissues).

Table 2.2 *Reagents for 30 µl and 50 µl RT-reaction.*

	Reagents	30µl	50µl	Final concentration
Non enzymatic reagents	H_2O free from RNase	1,3	8,9	
	10X TaqMan RT buffer	3	5	1X
	25 mM $MgCl_2$	6,6	11	5.5 mM
	10mM deoxyNTPs Mixture (2.5 mM of each dNTP)	6	10	500 µM per dNTP
	50 µM Random hexamers/oligo d(T)16	1,5	2,5	2.5 µM
Enzymes	RNase Inhibitor (20U/µl)	0,6	1	0.4 U/µl
	Multiscribe Reverse Transcriptase (50U/µl)	1	1,67	1.67 U/µl

A cover was put on the RT plate before centrifugation at 50 x g for 1 minute (Eppendorf Centrifuge 5810 R). The plate was then run through thermal cycling on the Gene Amp PCR Systems 9700 PCR machine. The thermal cycles for the reaction are shown in table 2.3. After synthesis, the cDNA was stored at -20 °C until qPCR analysis. (NIFES 2009, 279 RT-reaction)

Table 2.3 *Reverse Transcriptase reaction, thermal cycling*

Step	Incubation	RT	Reverse Transcription Inactivation	End
Temperature (ºC)	25	48	95	4
Time(minutes)	10	60	5	∞
Volume (µl)	50 or 30			

2.6.5 Quantitative Real-Time PCR

Principle: Gene expression levels in the different tissues are determined by quantitative real-time polymerase chain reaction (qPCR). Sequence-specific primers bind to the cDNA made in the RT-reaction, amplifying the gene of interest. The amplification follows three steps:

1. Denaturation of DNA at 95°C: High temperature melts double-stranded DNA (dsDNA) into single-stranded DNA (ssDNA), without destroying it.
2. Annealing at 60°C: The primers of the gene of interest binds to complementary ssDNA.
3. Extension at 72°C: The primers bound to complementary ssDNA are extended, making a copy of the gene of interest.

The amplification is exponential, meaning that the number of cDNA copies is multiplied by two for each thermal cycle. This amplification can be followed by fluorescence, due to DNA-binding dye added to the reaction. The more a gene is expressed in the tissue, the faster it will accumulate in a qPCR reaction. The dye used in this reaction is SYBR GREEN, which binds to all double-stranded DNA (dsDNA) in a PCR reaction. Upon binding to dsDNA, SYBR GREEN emits a strong fluorescent signal. The point when the fluorescence from the dsDNA-SYBR GREEN complex is significantly greater than the background fluorescence is called the threshold level. This measures the amount of PCR product when the reaction is still in the exponential phase and it is only at the exponential phase it is possible to determine the starting amount of the cDNA. The fractional number of PCR cycles required to reach the threshold level is proportionate to the starting amount of cDNA in the sample. This value is called the cycle threshold (C_T) value. (Ginzinger 2002) An example of a qPCR reaction is illustrated in figure 2.2.

The sequences of the primers used can be found in Appendix II.

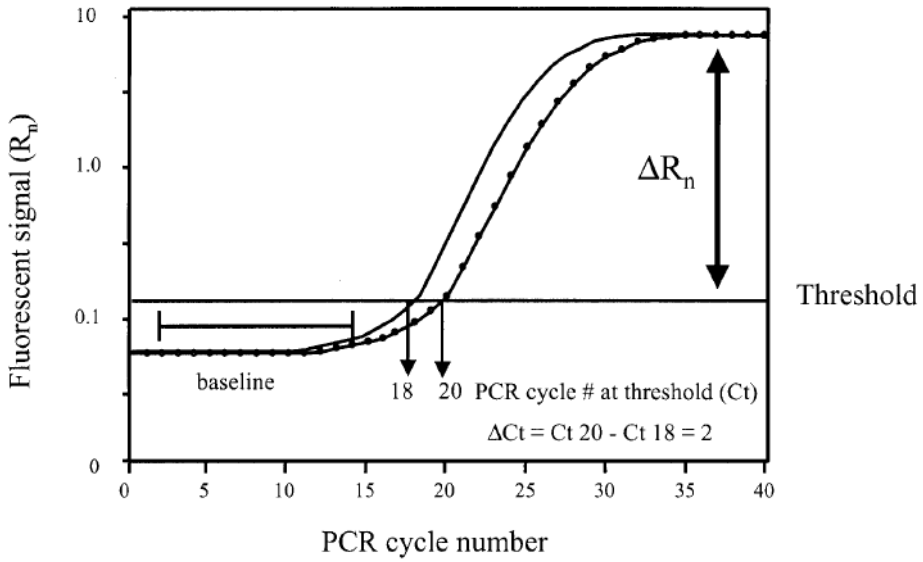

Figure 2.2 *Amplification plot of a hypothetical quantitative real-time PCR reaction. The amplification plot is the plot of the fluorescent signal vs PCR cycle numbers. The signal from the dsDNA-SYBR GREEN complex is accumulating during the baseline phase, but it is beneath the detection limit of the instrument. The signal measured during the baseline PCR cycles is used to plot the threshold level. The threshold level is calculated as 10 x the standard deviation of the average baseline fluorescent signal. A fluorescent signal above the threshold level is used to define the C_T value for the sample. The C_T is the fractional number of PCR cycles required to reach the threshold level. The C_T values for different samples are then compared to calculate the relative abundance of starting cDNA for each sample. The C_T values for this plot is 18 for the solid line and 20 for the dotted line. There is a difference of two cycles between these samples, which due to the exponential amplification of the PCR reaction means that there was four times as much cDNA in the sample represented by the solid line compared to the sample represented by the dotted line. (Ginzinger 2002)*

The gene expression levels were normalized to the relative expression of housekeeping genes. Housekeeping genes are expressed at relatively stable levels and are required for basic cellular functions, and should not be affected by experimental treatment. β-actin, TATA box binding protein (TBP) and calnexin were tested as housekeeping genes. After evaluation by geNorm, TBP was selected as the best normalizing gene (described below).

Procedure: Reaction mix was made of the reagents listed in table 2.4. This mix is sufficient for measuring one gene in four cDNA plates or four genes in one cDNA plate. 18 µl of the reaction mix along with 2 µl cDNA was transferred to each well in a 384-well reaction plate, using BioMek 3000 Laboratory Automation Workstation (Beckman Coulter, USA). That added up to a total of 20 µl reagent mix in each well.

Table 2.4: *SYBR GREEN reaction mixture for a 384-well reaction plate.*

Reagent	Volume (µl)
ddH_2O	290
Primer forward (100µM)	5
Primer reverse (100µM)	5
SYBR GREEN Master Mix	500

qPCR amplification of the target genes was performed on Light Cycler 480 Real-Time PCR System (Roche, Norway). First, there was an initial step of denaturation at 95 °C for 5 minutes, followed by 45 thermal cycles. These thermal cycles were each of 10 seconds of denaturation at 95 °C, 20 seconds of annealing at 60 °C, and 30 seconds of extension at 72 °C. The reaction is listed in table 2.5. (NIFES 2005, 280 RealTime PCR)

Table 2.5: *The SYBR GREEN program on Light Cycler 480*

Step	Preincubating	Amplification	Melting point analysis	Cooling
Temperature (ºC)	95	95 - 60 - 72	95 - 65 - 97	40
Time	5m	10s - 20s - 30s	5s - 1m -	10s
Number of cycles	1	45	1	1
Volume (µl)		20		

All samples were run in duplicates, whereas the standard curve was run in triplicates. The LightCyclers software program (LightCycler 480 Software release 1.5.0 SP4) draws graphs of the amplification curves. The curves of two duplicates or three triplicates were checked to verify that they matched. The program calculates the C_T value, efficiency value and error, based on the standard curve. An efficiency value of 2 is optimal, but between 1.8 and 2.2 is acceptable. An error value less than 0.04 was accepted in this study.

2.6.6 Calculating the relative gene expression in geNorm

Principle: geNorm is a software program used to calculate relative gene expression based on the C_T-values from the qPCR and normalize the expression relative to the expression of housekeeping genes. Housekeeping genes are transcribed into proteins that are necessary for basic cellular functions and are not expected to change by feeding the animals different diets. The housekeeping genes are used to calculate a normalization factor, which normalizes the expression of the target gene C_T-values. This excludes variables that could have an effect of the cDNA synthesis, such as differences in starting material or enzymatic reaction rates.

Procedure: The C_T-values of the all genes are first transferred to an Excel-sheet which gives the highest C_T-value a quantity of 1. The other C_T-values are given quantities lower than one, based on their C_T-value relative to the highest C_T-value. All quantities of the housekeeping genes are then copied into the geNorm program. This program calculates which of the housekeeping genes are better for normalization, or it uses a combination of several housekeeping genes. This gives a normalization factor for each tissue sample. TBP proved to be the best housekeeping gene. This has also been used in previous studies (Madsen et al 2008). The relative gene expression is the end result of the RNA extraction and is used to calculate statistics and draw graphs. The relative gene expression for each gene in each tissue sample is calculated in by the formula:

Relative gene expression = Quantity of the gene/ Normalization factor of the sample

2.7 HISTOLOGY

In order to examine obesity development and morphological structures of the adipose tissue, histological methods were used to examine the tissue under a microscope. Tissues were fixated in formaldehyde, dehydrated by ethanol, cleared by xylene and embedded in paraffin. The tissue in the paraffin block was cut into slides and stained by hematoxilin and eosin. The cells were now visible in a microscope.

2.7.1 Fixation and dehydration

Principle: Fixation in formaldehyde is used to protect the tissue against bacteria and enzymatic degradation. This preserves the structure of the tissue for later examination.

Procedure: After termination of the mice, the different tissues were fixed in 4% formaldehyde. After 24 hours, the tissues were washed with a 0.1 M phosphate buffer adjusted to pH 7.4. The phosphate buffer was then replaced by 50% ethanol and placed in a mixing machine (HS 501 D, JANKE & KUNKEL, IKA ® Labortechnik, Germany) for 1 hour. The ethanol was replaced and the process repeated three times. Finally, the 50% ethanol was replaced by 70% ethanol and stored at 4 °C. (NIFES 2009, 28 – UTTAK AV PRØVER TIL HISTOLOGI-ANALYSER)

2.7.2 Dehydration and clearing

Principle: The tissues are to be embedded in paraffin, but paraffin is not soluble in water. The water from the tissues is removed by placing them in different baths of ethanol with concentrations increasing from 70% to 100% ethanol. Then the tissues are made transparent by xylene and placed in liquid paraffin.

Procedure: Tissue samples of eWAT were placed in different solutions of ethanol, xylene and paraffin. When the ethanol was replaced by xylene, the tissues were kept in a fume hood. The tissues remained in xylene until they became transparent, before they were transferred into cassettes and placed in liquid paraffin. The procedure was performed twice, on two different sets of samples, with some variations in the protocol steps. The procedures are listed in tables 2.6 and 2.7. (NIFES 2010, Retningslinjer for bruk av histologilaboratoriet)

Table 2.6 *First attempt at dehydration of the tissues*

Step	Solution	Time
1	70% ethanol	30 minutes
2	96% ethanol	1-2 hours
3	96% ethanol	over night
4	100% ethanol	30 minutes
5	100% ethanol	until end of day
6	100% ethanol	over night
7	100% ethanol + a drop of eosin	1 hour
8	50/50 xylene and 100% ethanol	30 minutes
9	xylene	1-5 minutes
10	liquid paraffin	3 hours
11	liquid paraffin	3 hours
12	solid paraffin	over night

Table 2.7 *Second attempt at dehydration of the tissues*

Step	Solution	Time
1	75% ethanol	30 minutes
2	96% ethanol	75 minutes
3	96% ethanol	75 minutes
4	100% ethanol	60 minutes
5	100% ethanol	60 minutes
6	xylene	60 minutes
7	xylene	60 minutes
8	liquid paraffin	overnight
9	liquid paraffin	3 hours

2.7.3 Paraffin embedding and sectioning

Principle: To obtain sections of tissues thin enough to be studied in the microscope, tissues are embedded in paraffin. Cold paraffin blocks are then cut into 4 μm slides, containing cells in their original structure from that particular part of the tissue. The tissue sections are then transferred to glass slides.

Procedure: The tissue samples in their respective cassettes were transferred into a paraffin bath on the EC 350 Paraffin Embedding Center (Microm International, Waldorf, Germany). Each sample was placed in a steel tray which was partly filled with liquid paraffin. The bottom part of the cassette was placed on top of the steel tray and it was completely filled with liquid paraffin. The paraffin was hardened at 4 °C for at least 24 hours, until sectioning. Sectioning was performed on a manual microtome (Leica RM2165, Germany). 4 μm sections of the paraffin embedded tissue was cut off and transferred to a bowl of 50/50 ddH_2O and methanol. This bowl held a temperature of approximately 45 °C, due to its placement on a heater (Slide Warmer SW85, Adamas Instrumenten BV, Netherlands). The warm water and methanol made the sections stretch out before they were transferred to glass slides. The slides were left to dry in room temperature and then placed in a box for subsequent staining. (NIFES 2010, Retningslinjer for bruk av histologilaboratoriet)

2.7.4 Staining of the tissue with hematoxylin and eosin

Principle: The tissues are stained in order to examine the cells under a microscope. Hematoxylin colors the nuclei of the cells dark blue, eosin colors the cytoplasm pink. This makes it possible to differentiate cell types and determine cell size. The tissues are first rehydrated with water before staining. After staining with both colorants, the tissues are dehydrated with ethanol and xylene before they are sealed with mounting medium under and a thin glass slide.

Procedure: The tissue slides were put into racks which were placed in a number of glass baths. These glass baths were filled with the liquids listed in table 2.8. The time the rack spent in each bath is also listed in table 2.8. After the staining process, the slides were mounted with the xylene-based Entellan mounting medium (Merck, Germany) and a thin glass slide was placed on top. Weighs were used to spread the mounting medium evenly over the tissue section. (NIFES 2010, Retningslinjer for bruk av histologilaboratoriet)

Table 2.8 *Dying paraffin sections with hematoxylin and eosin*

Step	Solution	Time
1	Xylene	5 min
2	Xylene	5 min
3	100% ethanol	5 min
4	100% ethanol	5 min
5	96% ethanol	5 min
6	96% ethanol	5 min
7	70% ethanol	5 min
8	50% ethanol	5 min
9	ddH2O	5 min
10	Hematoxylin	3 min
11	warm tap water (45°C)	5 min
12	ddH2O	Rinse
13	96% ethanol	10 dips
14	Eosin	30 sec
15	96% ethanol	Rinse
16	96% ethanol	5 min
17	96% ethanol	5 min
18	100% ethanol	5 min
19	100% ethanol	5 min
20	Xylene	5 min
21	Xylene	5 min
Mount with Entellan		

2.7.5 Microscopy

The slides of adipose tissue were visually examined on a binocular microscope, (Olympus BX 51, System microscope, Japan). The slides were viewed at 100X and 400X magnifications. Pictures were taken using a Nikon DS-Fi1 camera (Nikon Corporation, Japan). The pictures were displayed by the software program NIS Elements F 3.0 (Nikon Corporation, Japan).

2.8 PLASMA ANALYSES

Plasma was analyzed for insulin levels, glucose, non-esterified fatty acids (NEFAs), triacylglycerols (TAGs), glycerol, D-3-hydroxybutyrate, alanine aminotransferase (ALT) and lactate dehydrogenase (LDH).

2.8.1 Insulin levels in plasma by ELISA-kit

Principle: Insulin is the primary hormone responsible for control of the glucose metabolism. Insulin levels are raised in mice suffering from Type 2 diabetes and obesity. The Insulin (Mouse) UltraSensitive ELISA-kit (DRG Instruments gmbH, Germany) was used to measure insulin levels in the plasma of each mouse. ELISA is the abbreviation for solid phase enzyme-linked immunosorbent assay. 96 wells are coated with a monoclonal antibody directed towards an antigenic area on the insulin molecule. The plasma samples are placed in the wells with enzyme conjugate, which is an anti-insulin antibody bound to biotin. This binds to the insulin in the sample. During the second step, streptavidin peroxidase enzyme complex binds to the biotin in the first conjugate. The amount of this complex, which is measured in its intensity of color developed by the reaction with 3,3'-5,5'-tetramethylbenzidine, is proportional to the concentration of insulin in the sample. The enzymatic reactions are proportional to incubation time and temperature, therefore it is important that all samples are treated equally and the test is run through all steps without delay.

Procedure: The kit was brought to room temperature before use. Standards and samples were run in duplicates. 25 µl of standard 0 from the kit was added to each of the 96 wells. 5 µl of standard 0 and 3-7 was added to each of the standard wells. 5 µl sample plasma was added to each sample well. 50 µl enzyme conjugate was dispensed into each well. This was thoroughly mixed, without foaming the liquids, on a shaker at 800 x g for 2 hours at room temperature. After incubation, the plate was rinsed 6 times with an automatic plate washer (Skan Washer 300 version B, Skatron Instruments, Lier, Norway) and the liquid was briskly discarded out of the wells onto absorbent paper. 200 µl of TMB solution from the kit was added to each well before incubation for 30 minutes. Then 50 µl of Stop solution from the kit was added to each well. The plate was shaken for 10 seconds at 800 x g and then immediately read by a microtiter plate reader (iEMS Reader MF, Labsystems Oy, Helsinki, Finland). The absorbance was measured at 450 nm and 620 nm. (User manual, Insulin (Mouse) UltraSensitive ELISA, DRG Diagnostics)

2.8.2 MAXMAT analysis

Plasma levels of glucose, NEFAs, TAGs, glycerol, D-3-Hydroxybutyrat, ALT and LDH were measured on an automatic multi-purpose analyzer (MAXMAT) by laboratory technician Jacob Wessels at NIFES.

2.8.3 Lipids in muscle and liver by thin layer chromatography

Analysis of cholesterol levels of muscle tissue and amount of total lipids in liver was measured by laboratory technician Jan Idar Hjelle at NIFES. This was done by thin layer chromatography (TLC) on a silica gel. (NIFES 2008, 375 – Fettsyresammensetning av totalfettsyrer i ulike lipidklasser)

2.9 SOFTWARE USED FOR STATISTICAL ANALYSIS

Statistical analysis was performed to find any significant differences between groups. All results are presented as the mean +/- standard error (SEM) of the mean for each group. The SEM gives an indication of how close the sample mean is likely to be to the mean of a whole population. The SEM is calculated from the standard deviation, divided by the square root of the number of animals:

$$SEM = \frac{Standard\ deviation}{\sqrt{n}}$$

All information on samples, analysis and results were stored on Labware LIMS.

The geNorm algorithm was used to assess the stability of the housekeeping genes.

Microsoft Excel was used to calculate means, standard deviations and standard error of the mean.

Statistica was used to test the results for significant differences between groups. The Sugar groups and GI groups were tested separately, both included the Chow control group. Levene's test was performed to test the equality of variances in each group. If the samples did not have equal variance, the values were log transformed and tested again. Data which did not have equal variance were tested by the Kruskal-Wallis non-parametric test for significant differences. Normally distributed data were tested with one-way analysis of variance and Fisher's exact test. P-values less than 0.05 were considered as significant difference.

All graphs were made on GraphPad Prism 5.

3. RESULTS – SUGAR GROUPS

The aim of this study was to investigate whether the anti obesity effect of fish oil is attenuated by sucrose. Also, we wanted to investigate whether the possible obesogenic effects derived from the glucose moiety in the sucrose molecule, the fructose moiety, or both.

The mice were *pair-fed* high fat diets containing fish oil + sucrose, fish oil + glucose or fish oil + fructose. Standard low fat chow diet was given to the control group. The compositions of the diets can be seen in table 2.1, page 40 of Materials and methods. From now on the different diet groups will be labeled chow, sucrose, glucose and fructose. Any significant differences will be marked by different letters on the graphs.

This study was performed parallel to the study of different starches in combination with fish oil. The results of that study are described at page 71-85, section 4.

3.1 FOOD INTAKE, BODY WEIGHT DEVELOPMENT AND FEED EFFICENCY

The mice were fed the experimental diets for 9 weeks. The chow group was given food *ad libitum*, whereas the other groups were restricted in their food intake. The chow feed contained lesser calories per gram than the other feeds, so these mice ate more food measured in grams than the other groups (not shown). The accumulated calories ingested, the weight gain and the energy efficiency is shown in Figure 3.1A-C. The body weight development is shown in figure 3.1D.

All *pair-fed* groups ate of course the same amount of calories, and luck would have it that the chow group also ate the same as the other groups, when adjusted for calories (Fig 3.1A). After 9 weeks of feeding, the mice where weighed before termination. The total weight gain in grams is shown in figure 3.1B. Mice on fish oil diets gained less weight than mice on chow diet and the difference is statistically significant for the fructose group. The energy efficiency is shown in figure 3.1C. All mice on fish oil diets showed a tendency towards lower weight gain compared to the chow group. Mice with fructose as their main carbohydrate source gained significantly less weight per calorie ingested than mice on chow and glucose diet. The mice were weighed twice a week. The body weight development is shown in figure 3.1D.

There was a drop in the weight development some days before termination due to changes in the mice's environment, but it does not seem to have affected the end result.

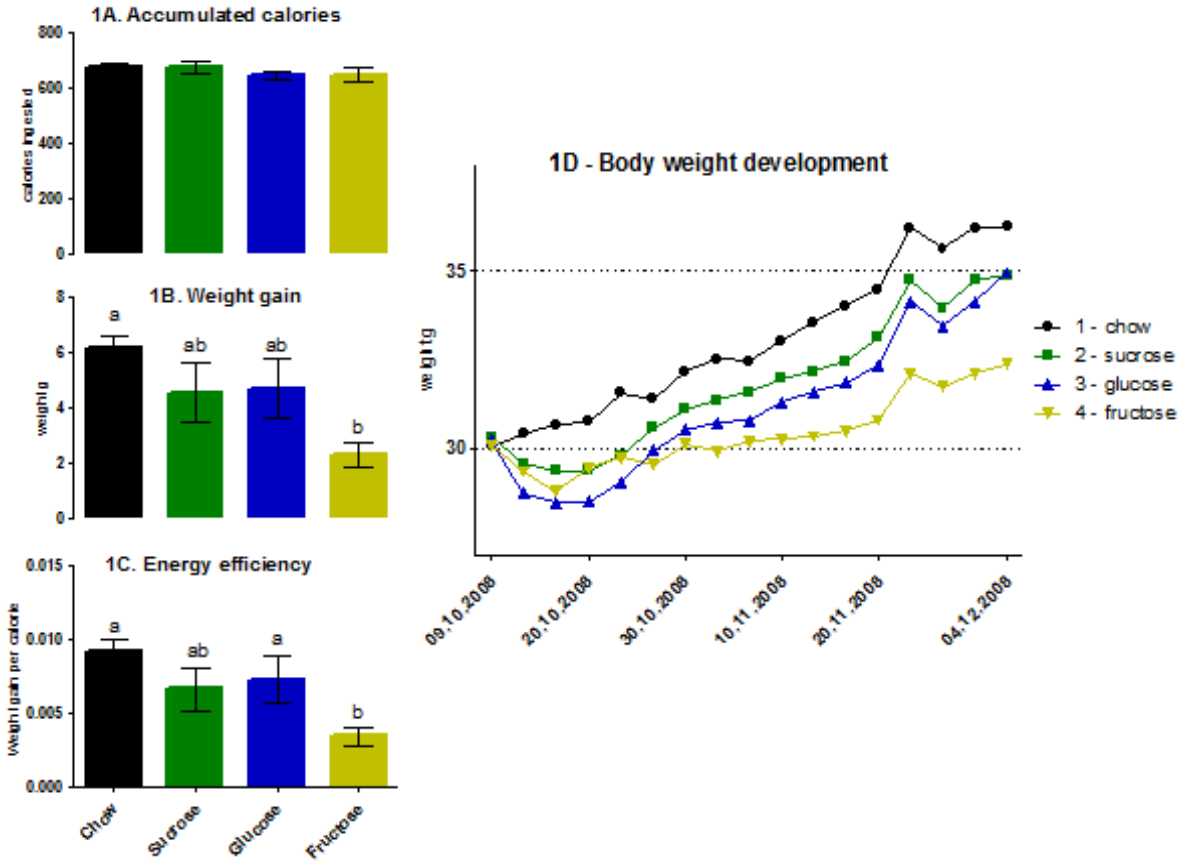

***Figure 3.1**: Feed intake and body weight development of the C57BL/6J mice. Total calories ingested (A), total weight gain from start to end of the experiment (B), weight gain (g) per calorie ingested (C) and Body weight development during the experiment. Groups marked by different letters are significantly different.*

3.2 ORGAN WEIGHTS

Figure 3.2A shows the end mean body weights of the groups. After termination, organ weights were recorded. We selected the retroperitoneal adipose tissue (rWAT, Fig 3.2B), epididymal adipose tissue (eWAT, Fig 3.2C), inguinal adipose tissue (iWAT, Fig 3.2D), intrascapular brown adipose tissue (iBAT, Fig 3.2E), tibialis muscle (Fig 3.2F) and liver (Fig 3.2G).

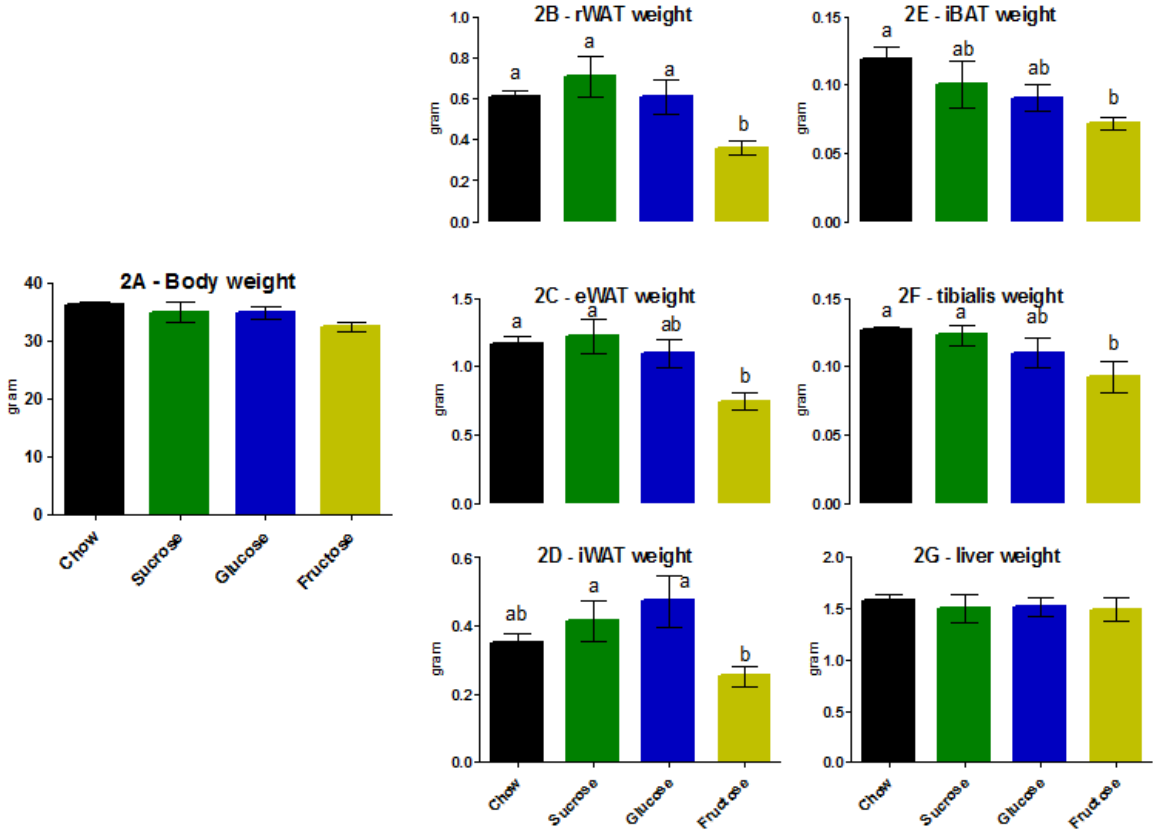

***Figure 3.2**: Total body weight (A), rWAT weight (B), eWAT weight (C), iWAT weight (D), iBAT weight (E), tibialis weight (F) and liver weight (G). All weights are displayed in grams. Groups marked by different letters are significantly different.*

Although the weight gain varied significantly (Fig 3.1B), the total body weights at the end of the experiment did not (Fig 3.2A). Still, the organ weights varied, especially within the adipose tissue depots. The sucrose group showed a tendency towards having more visceral fat, and the glucose group had slightly more subcutaneous fat. Whereas white adipose tissue mainly stores energy, brown adipose tissue is also capable of burning energy. The chow group had the largest depots of brown fat, which is considered a healthier type of fat capable of turning stored fat into heat to regulate body temperature (Gesta et al 2007). It is to be noted that the chow group, who ended up as slightly heavier than the other groups, did not have the largest white adipose tissue depots. The smaller mice in the fructose group continuously had the smallest adipose tissue depots.

Retroperitoneal white adipose tissue (rWAT) weights are shown in figure 3.2B. This is a visceral fat depot and the sucrose group had the largest amounts of it, even though the chow group had gained somewhat more weight during the experiment (Fig 3.1B). The difference

was only statistically significant for the fructose group, which had the smallest amounts of rWAT. The sucrose group also had slightly more epididymal white adipose tissue (eWAT) (Fig 3.2C), which is also a visceral fat depot. The fructose group had significantly smaller eWAT depots compared to sucrose and chow groups. Inguinal white adipose tissue (iWAT) is a subcutaneous fat depot. Here, the glucose group had the largest amounts, second only to the sucrose group (Fig 3.2D). Both had significantly larger iWAT depots compared to the fructose group, whereas the chow group fell somewhere in the middle.

Intrascapular brown adipose tissue (iBAT) depots were larger in the chow fed mice. They were significantly larger compared to the fructose fed mice (Fig 3.2E). The trend seems to be that the mice who gained the most weight had the largest amounts of iBAT. This trend is also seen in the comparisons of the tibialis weights (Fig 3.2F), which is a muscle located at the hind leg of the mouse. Although not significantly smaller in body weight, the mice fed fructose had significantly smaller tibialis compared to the chow fed mice. Liver weights were not significantly different between groups (Fig 3.2G).

3.3 HEPATIC GENE EXPRESSION

A great number of genes were measured in the liver to elucidate potential differences in metabolisms between groups. The liver is capable of both lipid synthesis and breakdown, as well as glucose and amino acid metabolism. All genes measured were normalized to the housekeeping gene TBP.

Lipogenic gene expression

The relative expression levels of lipogenic genes are shown in figure 3.3. Lipogenic genes are genes coding for proteins associated with the *de novo* synthesis of fatty acids. They are expressed when food is at a surplus and the body has the opportunity to store excess calories. We measured the relative expressions of *Srebp1c*, *Acc1*, *Acc2*, *Scd1*, *Fas* and *Dgat*. The function and regulation of these genes are described at page 21-25 of the Introduction.

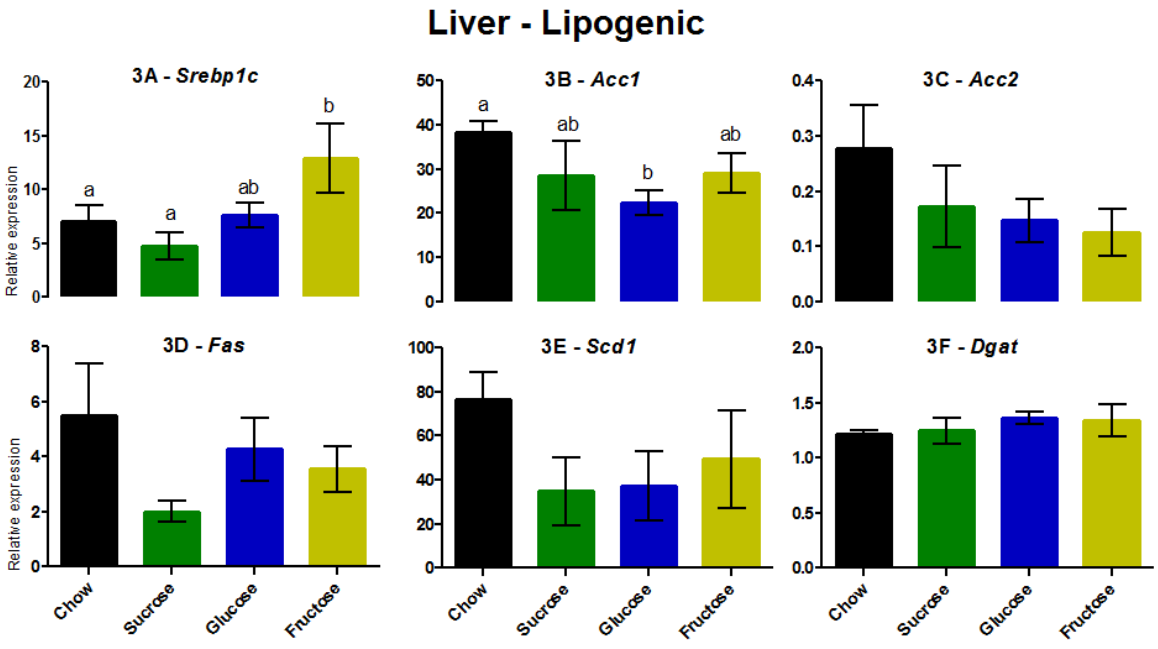

***Figure 3.3**: The relative expression levels of hepatic Srebp1c (A), Acc1 (B), Acc2 (C), Scd1 (D), Fas (E) and Dgat (F) mRNA. Groups marked by different letters are significantly different.*

The expression of the transcription factor *Srebp1c* was significantly higher in the fructose group, compared to the chow and glucose group (Fig 3.3A). Fructose consumption has been shown to lead to overexpression of *Srebp1c*, although the link between fructose and *Srebp1c* is less prominent in C57BL/6J mice (Nagata et al 2004). Therefore it is surprising to find that the fructose group had the highest level of *Srebp1c*, since insulin caused by sucrose consumption is also known to increase *Srebp1c* expression rates (Osborne 2000). The effect of PUFAs did not seem to protect the sugar-fed mice against high *Srebp1c* expression rates, since none of the groups given fish oil have significantly lower expression levels compared to the chow group. The glucose group had the lowest level of *Acc1* mRNA, significantly lower than the chow group (Fig 3.3B). *Acc1* is partly controlled by the transcription factor *Srebp1c* (Kim 1997), but there seems to be no correlation between the expressions of these two genes. Other factors, such as posttranslational modifications of SREBP-1c, must be affecting the expression of lipogenic genes. A low-fat, carbohydrate-rich diet can up-regulate the expression of both *Acc*s and *Fas* (Ishii et al 2004). The trend is that the chow group has the highest expression rates of *Acc1*, *Acc2*, *Fas* and *Scd1* (Fig 3.3B-E). The difference does not reach statistical significance for all values, but it is previously shown that PUFAs are inhibitors of *Scd1* (Ntambi 1999) and *Fas* (Ren et al 1997). *Dgat* expression was not affected by the different diets (Fig 3.3F).

Genes increasing fatty acid breakdown

The relative expression levels of genes which increases fatty acid breakdown are shown in figure 3.4. These genes code for enzymes involved in breaking down fatty acids to satisfy energy demands. We measured the expression levels of *Pparα*, *Pparδ*, *Aco*, *Cpt1a*, *Cpt2* and *Hmgcs2*. The function and regulation of these genes are described at page 25-28 of the Introduction.

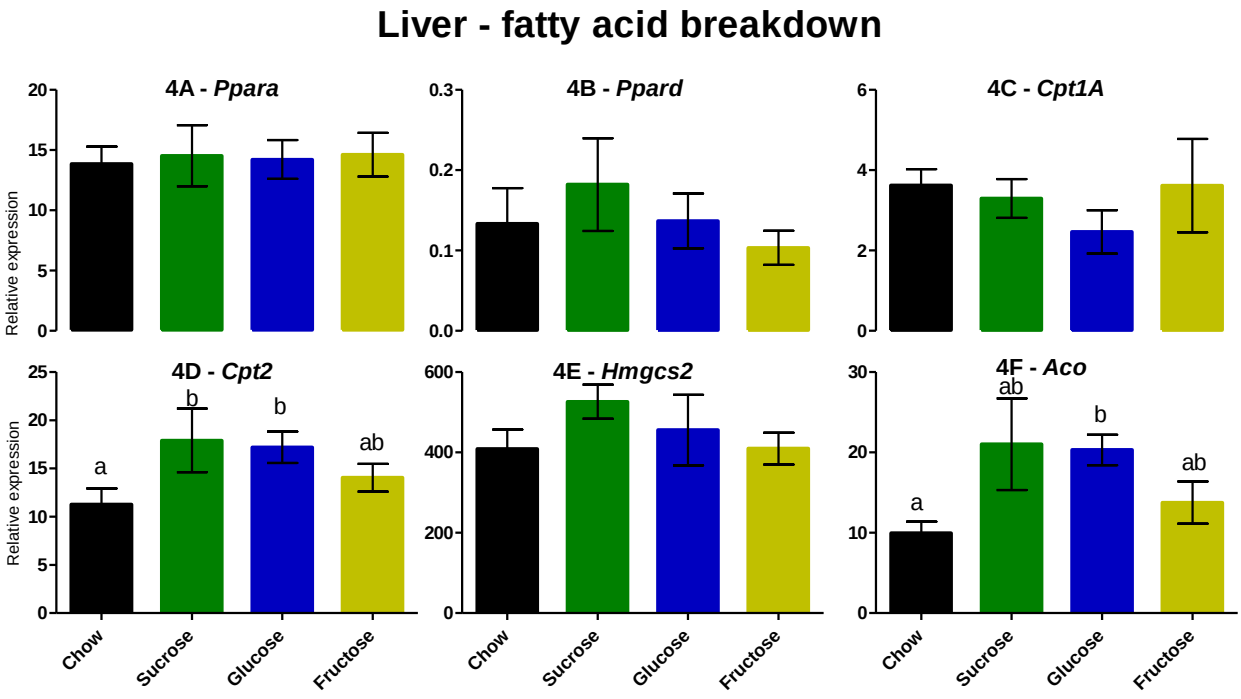

***Figure 3.4**: Relative expression levels of the genes Pparα (A), Pparδ (B), Cpt1a (C), Cpt2 (D), Hmgcs2 (E) and Aco (F) in liver. Groups marked by different letters are significantly different.*

There were no significant differences in the expressions of *Pparα*, *Pparδ*, *Cpt1a* or *Hmgcs2* (Fig 3.4A, B, C and E). *Cpt2*-expressions in sucrose and glucose-groups were significantly higher than the *Cpt2* levels in chow-group (Fig 3.4D), but as described in the introduction, this is not a rate-limiting enzyme. The *Aco* gene, coding for the peroxisomal enzyme Acyl-CoA oxidase, was significantly up-regulated in the glucose-group, compared to the chow-group (Fig 3.4F). It also seems to be up-regulated in the sugar and fructose-groups, although the standard error is high.

Gluconeogenesis

The relative expression levels of genes involved in gluconeogenesis are shown in figure 3.5. The function and regulation of these genes are described at page 28 of the Introduction. Gluconeogenesis is the making of new glucose during fasting. Patients with Type 2 diabetes have elevated blood glucose levels during fasting, due to high gluconeogenesis. PCK1 is the rate-limiting enzyme during gluconeogenesis and PGC-1α is a coactivator of PCK1.

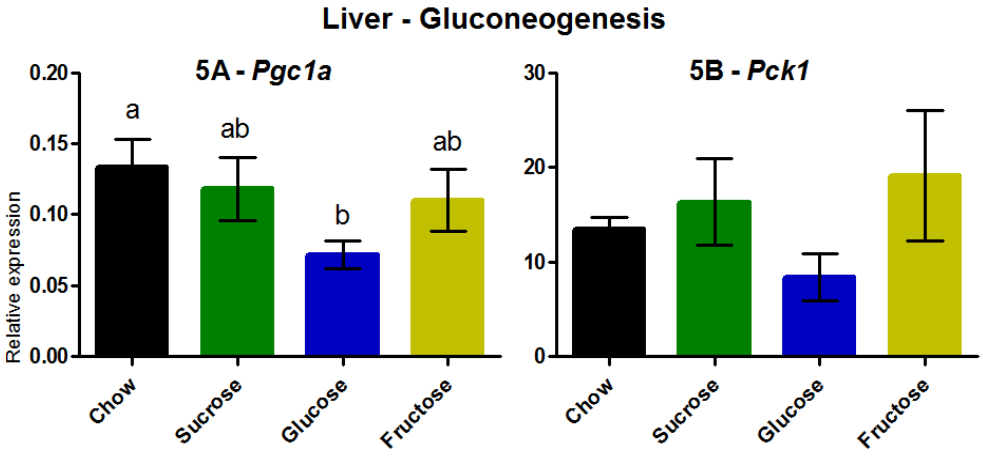

***Figure 3.5**: Relative expressions of the gluconeogenetic enzymes Pgc1α (A) and Pck1 (B) in liver. Groups marked by different letters are significantly different.*

As seen in figure 3.5, mice given fish oil and sugars did not have elevated levels of *Pgc1α* compared to the chow group (Fig 3.5A). Mice given glucose even had significantly lower levels of *Pgc1α* compared to the chow group. The levels of *Pck1* showed no significant differences, although some of the mice in the fructose group had elevated levels of this mRNA (Fig 3.5B).

Amino acid degradation

The relative expression levels of genes involved in amino acid degradation are shown in figure 3.6. Amino acids can be turned into glucose molecules when there is a shortage of glucose. Glucose is required as energy for the brain and red blood cells. We measured the expressions of *Agxt*, *Got*, *Gpt1* and *Cps1*. The enzyme products of these genes are described at page 29 of the Introduction.

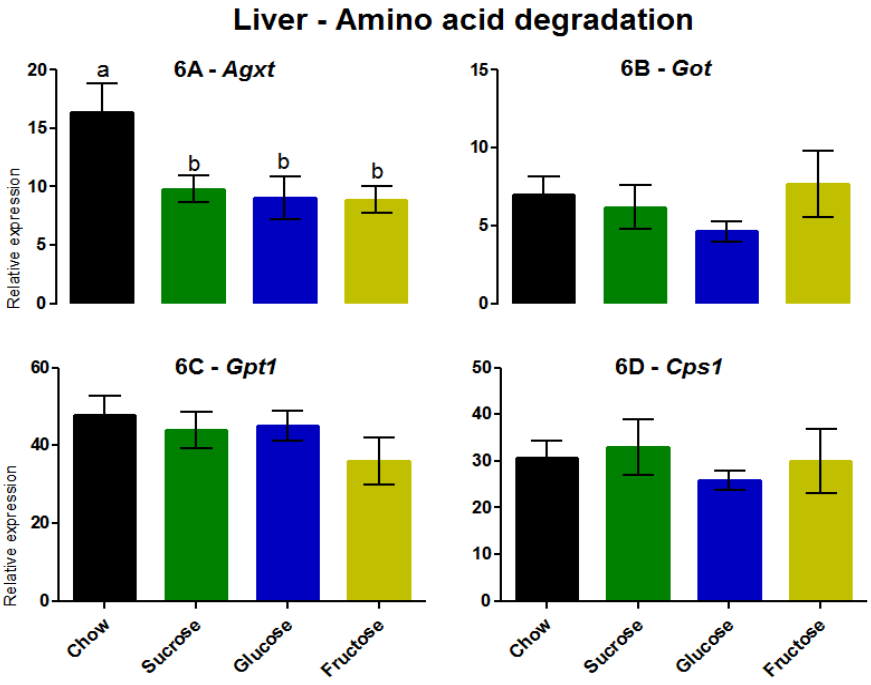

***Figure 3.6**: The relative expressions of mRNA coding for hepatic enzymes involved in amino acid degradation. Agxt (A), Got (B), Gpt1 (C) and Cps1 (D) were measured. Groups marked by different letters are significantly different.*

Only *Agxt* showed significant differences (Fig 3.6A). It seems that amino acid degradation is more or less the same for mitochondrial enzymes, whereas the peroxisomal enzyme *Agxt* is up-regulated in the chow group compared to all fish oil groups.

Cyclic AMP signaling

The relative expression levels of genes involved cyclic AMP (cAMP) signaling are shown in figure 3.7. cAMP is an intracellular second messenger which induces gluconeogenesis in the liver. CREM and the cAMP-dependent protein kinase (PKA) isoforms RIα and RIIβ are enzymes in the cAMP signaling pathway. PDE4c is an enzyme which degrades cAMP. Low level of *Pde4c* is linked to an anti-inflammatory state. These genes are described at page 30-31 of the Introduction.

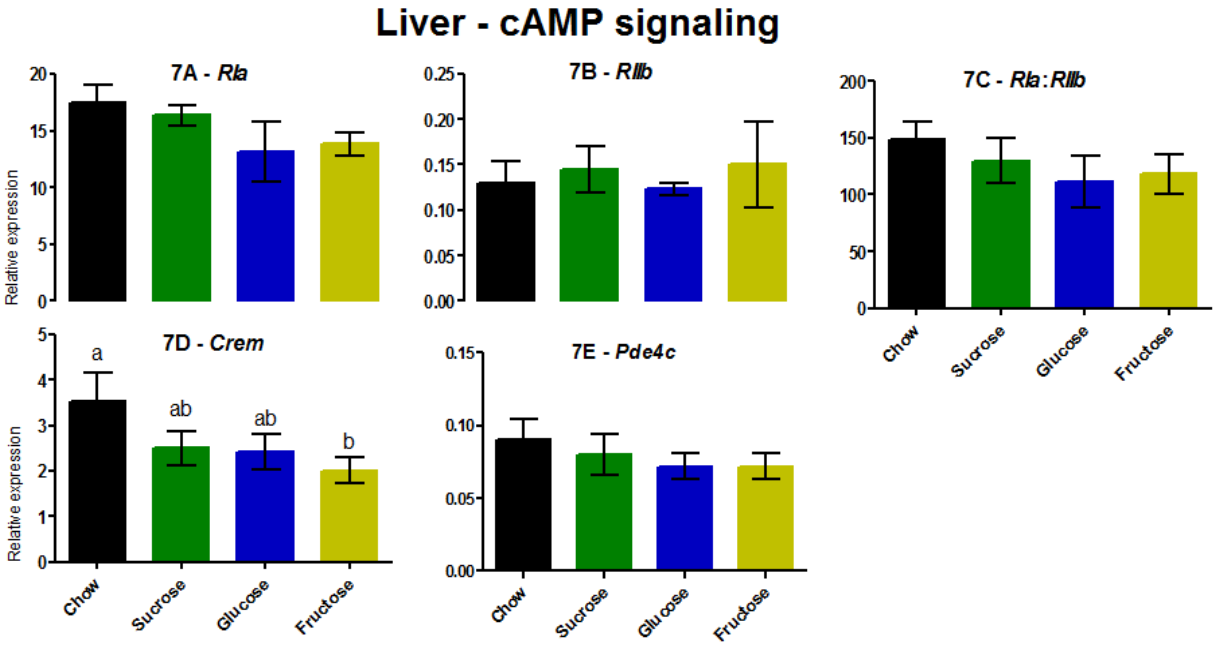

***Figure 3.7**: cAMP signaling. The relative expressions of RIα (A), RIIβ (B), Crem (D) and Pde4c (E). Figure 7C shows the RIα: RIIβ-ratio. Groups marked by different letters are significantly different.*

As seen from the graph, there were no significant differences in the *RIα* and *RIIβ* expression levels (Fig 3.7A and B). The *RIα: RIIβ* ratios were a little lower for the fish oil groups compared to the chow group, but differences were not statistically significant (Fig 3.7C). The level of *Crem* was significantly lower in the fructose group, compared to the chow group (Fig 3.7D). The levels of *Crem* in sucrose and glucose group were also lower, but the values did not reach statistical significance. The levels of *Pde4c* were not very different, but there might be a trend towards a slight reduction in the fish oil groups (Fig 3.7E).

3.4 GENE EXPRESSIONS IN WHITE ADIPOSE TISSUE

Expressions of genes involved in adipogenesis, inflammation and genes that give white adipocytes a brown-like phenotype were measured in white adipose tissue. All genes measured were normalized to the housekeeping gene TBP.

Adipogenesis

The relative mRNA expressions of the lipogenic transcription factors PPARγ2 and SREBP-1c were measured, along with the expressions of the lipogenic enzyme FAS (Fig 3.8). These enzymes are described at page 21-25 of the Introduction. Two different fat depots were

analyzed, eWAT and iWAT. eWAT is a visceral fat depot, whereas iWAT is a subcutaneous fat depot.

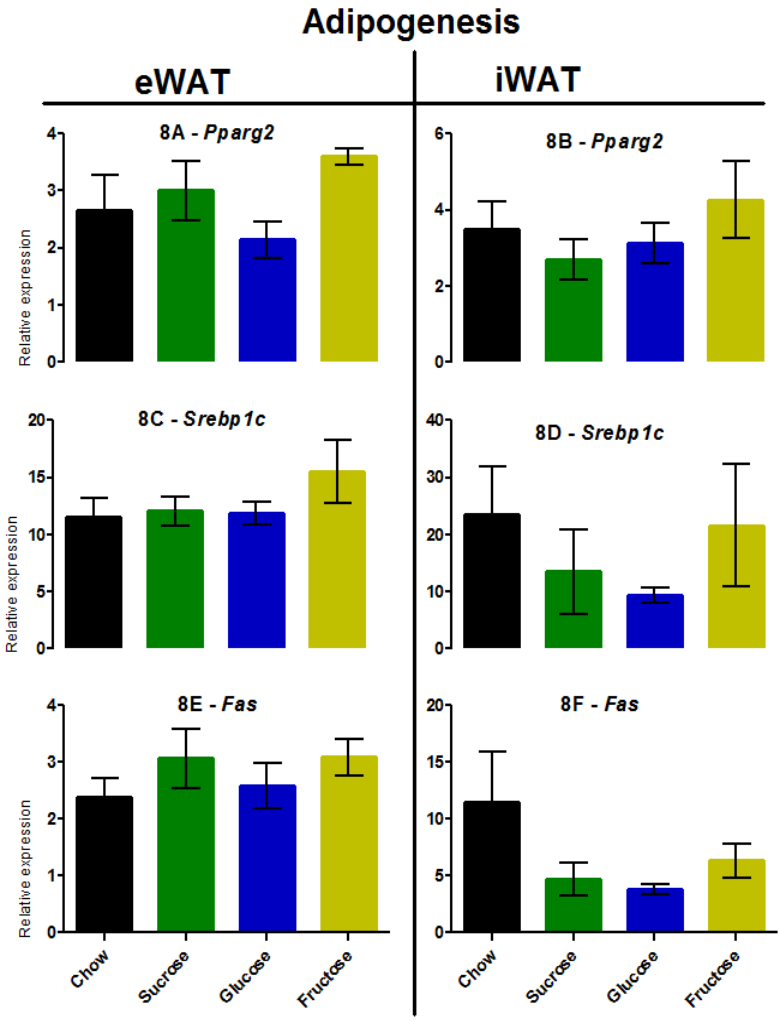

***Figure 3.8**: Relative expressions of adipogenic genes in white adipose tissue: Pparγ2 (A and B), Srebp1c (C and D) and Fas (E and F). Measurements from epididymal fat to the left and inguinal fat to the right.*

Differences in the levels of *Pparγ2*, *Srebp1c* and *Fas* did not reach significant differences (Fig 3.8A-F). The levels in eWAT were about the same between groups, whereas the levels in iWAT were more diverged. The standard errors were too high to claim anything with certainty, but the trend seems to be that the lipogenic genes in iWAT are expressed at higher levels in the chow and fructose group. The mRNA expression levels of the transcription factor PPARγ2 and SREBP-1c is not necessary the best indicator for the level of active PPARγ2 and SREBP-1c enzymes in the cells, as both enzymes have to be activated posttranslationally before functioning as transcription factors.

Inflammation markers

The expression levels of the inflammation markers *Ccl2*, *Cd68*, *Emr1* and *Serpine1* were measured in both epididymal and inguinal white adipose tissue. These genes are involved in macrophage accumulation and are described at page 31-34 of the Introduction. The results of *Serpine1* are not shown due to high standard errors of the mean. The rest of the results are shown in figure 3.9.

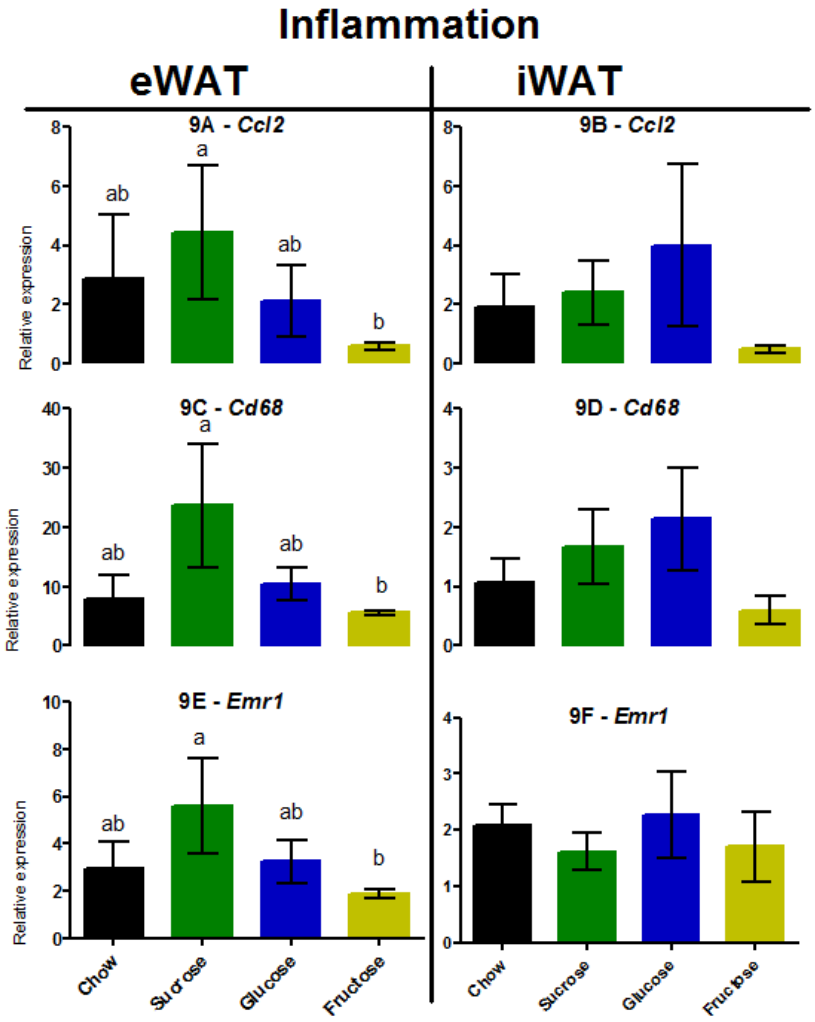

***Figure 3.9**: Relative expression levels of inflammatory genes in white adipose tissue: Ccl2 (A and B), Cd68 (C and D) and Emr1 (E and F). Measurements from epididymal fat to the left and inguinal fat to the right. Groups marked by different letters are significantly different.*

As seen from the figure, the expression levels in the visceral epididymal fat exhibits a clear trend for the three genes measured. Visceral fat is known to exhibit more inflammatory markers compared to subcutaneous fat (Ouchi et al 2011). The expression levels of inflammatory markers in epididymal WAT were higher in the sucrose group for all genes

measured. The differences reach statistical significance compared to fructose group for *Ccl2*, *Cd68* and *Emr1*. The differences were not significant for *Serpine1*, but the trend of the sucrose group to have the highest level is still there (not shown). It must be noted that the mRNA levels are measured as concentration levels, and sucrose group had the highest amounts of visceral fat, which dramatically increases the burden of inflammation compared to the fructose group. The fructose group had lower concentrations of inflammatory markers and also smaller visceral adipose tissues, so the total burden of inflammation is probably distinctly lower in this group.

The results for the subcutaneous inguinal WAT do not show any significant differences, and there is less consistency between expression levels of the different inflammation markers. There is a trend towards glucose having higher levels of inflammatory markers. This makes sense considering that this group had the largest iWAT depots (Fig 3.2D). There is a correlation between large adipose mass and high inflammation, although the causal relationship between these two factors are not fully understood.

Brown-like phenotype of WAT

We measured the expression levels of *Pgc1α* and *Ucp1* in both epididymal and inguinal fat depots. Unfortunately, the results from *Ucp1* showed high variance within groups, indicating that something had gone wrong with this the measurement of this gene. The results of *Ucp1* levels are therefore not shown, but the expression level of *Pgc1α* is found in figure 3.10. The function of PGC-1α in adipose tissue can be found at page 35 of the Introduction.

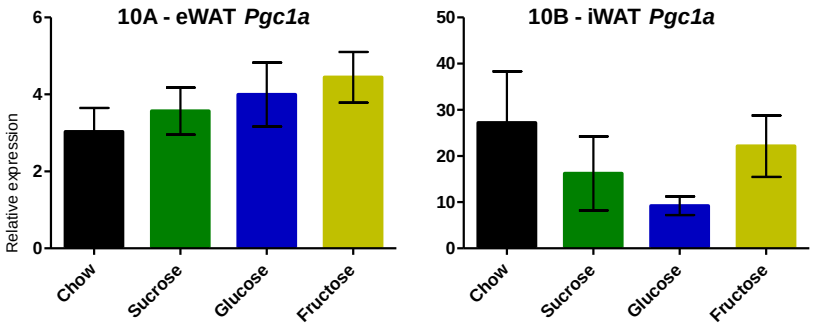

***Figure 3.10**: The relative expression levels of Pgc1α in epididymal (A) and inguinal (B) fat.*

No significant differences were reached, but there seems to be a trend towards fish oil groups having higher levels of *Pgc1α* in visceral fat. This might be considered as a positive effect of

fish oil, since visceral fat is regarded as the more unhealthy type of fat. Increasing the brown-like phenotypes in visceral fat could improve the metabolic status of this adipose tissue. Within the fish oil groups, fructose has the highest level of *Pgc1α* in eWAT and sucrose group has the lowest.

In contrast, the fish oil groups seem to have lower values of *Pgc1α* in subcutaneous fat compared to chow group.

3.5 GENE EXPRESSION LEVELS IN BROWN ADIPOSE TISSUE

In intrascapular brown adipose tissue, *Pgc1α*, *Dio2* and *Ucp1* were measured to examine differences in adipocyte phenotypes. Unfortunately, for reasons described above, *Ucp1* results are not shown. The expression levels of *Cox2* were determined as a measurement of mitochondrial function. The expressions of the lipogenic genes *Srebp1c* and *Rip140* were also measured in BAT. The enzyme products of these genes are described at page 34-36 of the Introduction. All genes measured were normalized to the housekeeping gene TBP. The results are displayed in figure 3.11.

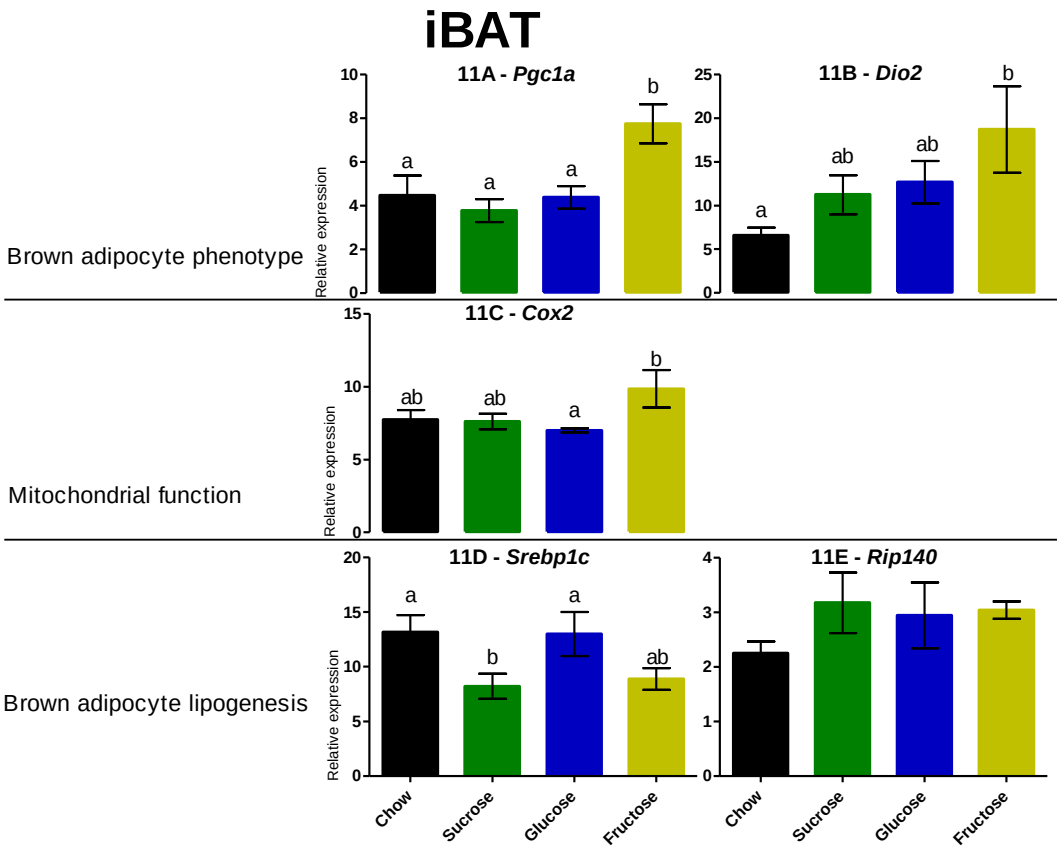

***Figure 3.11**: The expression levels of genes involved in adipocyte phenotype, mitochondrial function and lipogenesis in BAT. Pgc1α (A), Dio2 (B), Cox2 (C), Srebp1c (D) and Rip140 (E). Groups marked by different letters are significantly different.*

As seen from the figure, the fructose group had significantly higher expression levels of the BAT-specific genes *Pgc1α* (Fig 3.11A) and *Dio2* (Fig 3.11B). This indicates that the fructose group has a higher capacity of turning fat into heat, which would explain why these mice are leaner than the other groups. They also have higher expression levels of *Cox2* (Fig 3.11C), which is consistent with the hypothesis of the fructose mice having higher capacity of burning fat.

The expression of lipogenic genes is less consistent. Fructose group have lower expression levels of *Srebp1c* compared to chow and glucose group, but the difference does not reach statistical significance. Surprisingly, sucrose group had the lowest levels of *Srebp1c*. The results from *Rip140* expression levels indicate a slight increase in the fish oil groups compared to chow group. This is not consistent with the fact that chow and sucrose group had the highest body weights and the largest fat depots. These results combined with the results from lipogenic expression levels in liver and white adipose tissue indicates that the expression levels of lipogenic genes are not rate-limiting for the capacity of accumulating fat. Activation and repression of translation of mRNA into proteins or posttranslational modulation of enzyme activity could have higher impact on the cells lipid-storing capacity.

3.6 LIPID CONTENT IN LIVER AND MUSCLE

Lipid content was measured in both liver and the tibialis muscle. Note that the results show the content of the whole organ, not the concentration per weight unit. Liver weights were about the same for all groups, whereas muscle weights were highest in chow group and lowest in fructose group (see Fig 3.2, F and G).

The amounts of total lipid in liver (Fig 3.12A) did not differ between groups. In contrast, triacylglycerol contents were significantly lower in glucose and fructose group compared to chow group (Fig 3.12B). Also sucrose group exhibits somewhat lower values, making it a trend that the fish oil groups have the lowest contents of triacylglycerol (TAG). The amounts of phospholipids were higher in the groups given fish oil, and the difference was significant for the sucrose and glucose groups compared to chow group (Fig 3.12C). Phospholipids are

primarily components of cellular membranes, and the higher levels of phospholipids in the liver of the fish oil groups merely indicate a higher number of cells of smaller size in these groups. This explain why the total lipid content was similar between groups, even though TAG content was reduced in the fish oil groups. Cholesterol contents were about the same for all groups (Fig 3.12D).

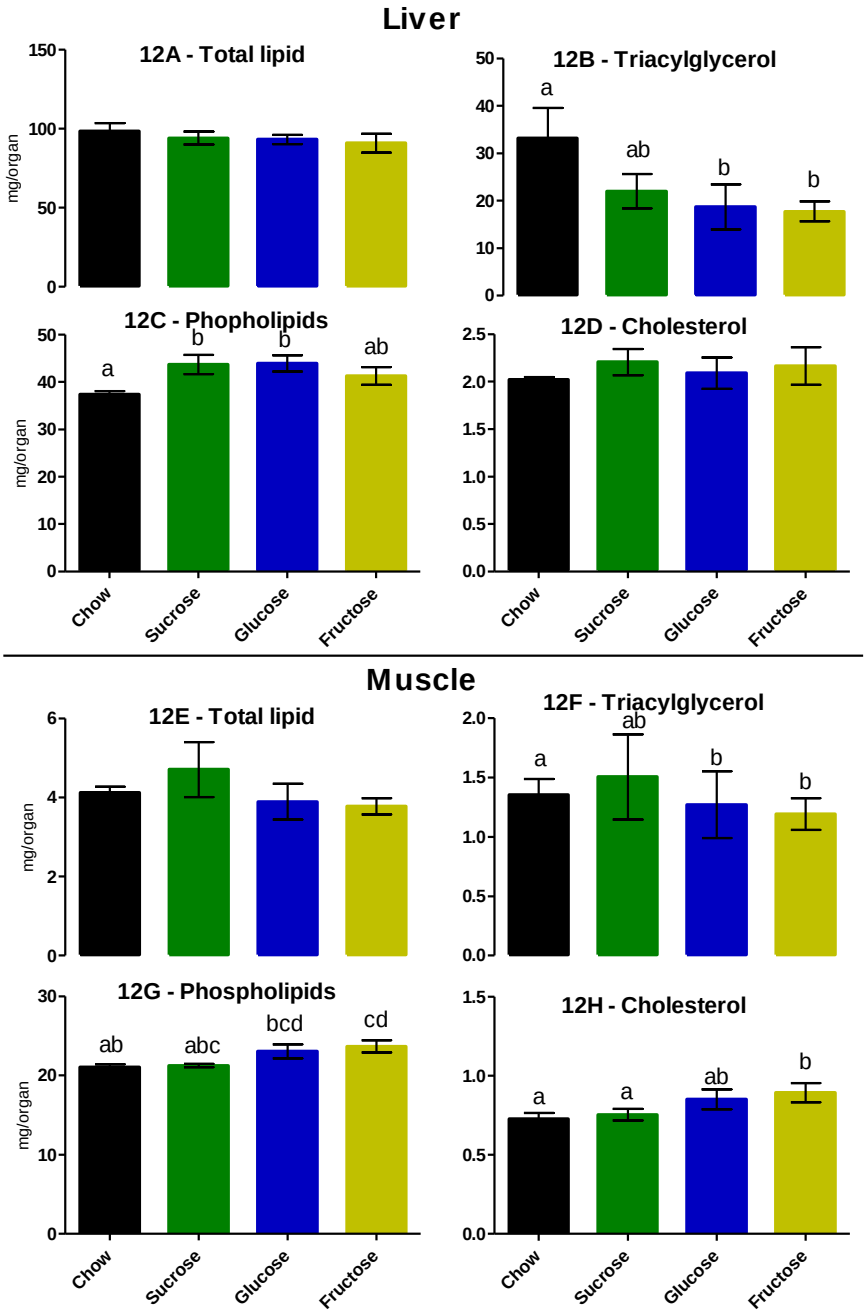

***Figure 3.12**: Lipid content in liver (A-D) and muscle (E-H). The amounts of total lipids (A and E), triacylglycerol (B and F), phospholipids (C and G) and cholesterol (D and H) were measured. Groups marked by different letters are significantly different.*

Amounts of total lipid in the tibialis muscle were highest in the sucrose group, although the difference did not reach statistical significance (Fig 3.12E). Triacylglycerol contents were significantly reduced in glucose and fructose group, compared to chow group (Fig 3.12F), which is consistent with the results seen in hepatic triacylglycerol content (Fig 3.12B). Amounts of phospholipids in muscle are higher in the fish oil groups compared to chow group (Fig 3.12F). This is also consistent with the results of phospholipid content in liver (Fig 3.12B). The phospholipid content in muscle is significantly higher for the fructose group compared to chow group (Fig 3.12G). Cholesterol contents are somewhat higher in fish oil groups compared to chow group and the difference is significant for the fructose group (Fig 3.12H).

3.7 PLASMA PARAMETERS

All plasma parameters were measured from fed mice. Plasma insulin levels were not expected to differ much in the fed state, and indeed the results were not significantly different (not shown). The results of the plasma glucose, glycerol, triglyceride, alanine transaminase, lactate dehydrogenase and D3 hydroxybutyrate are shown in figure 3.12.

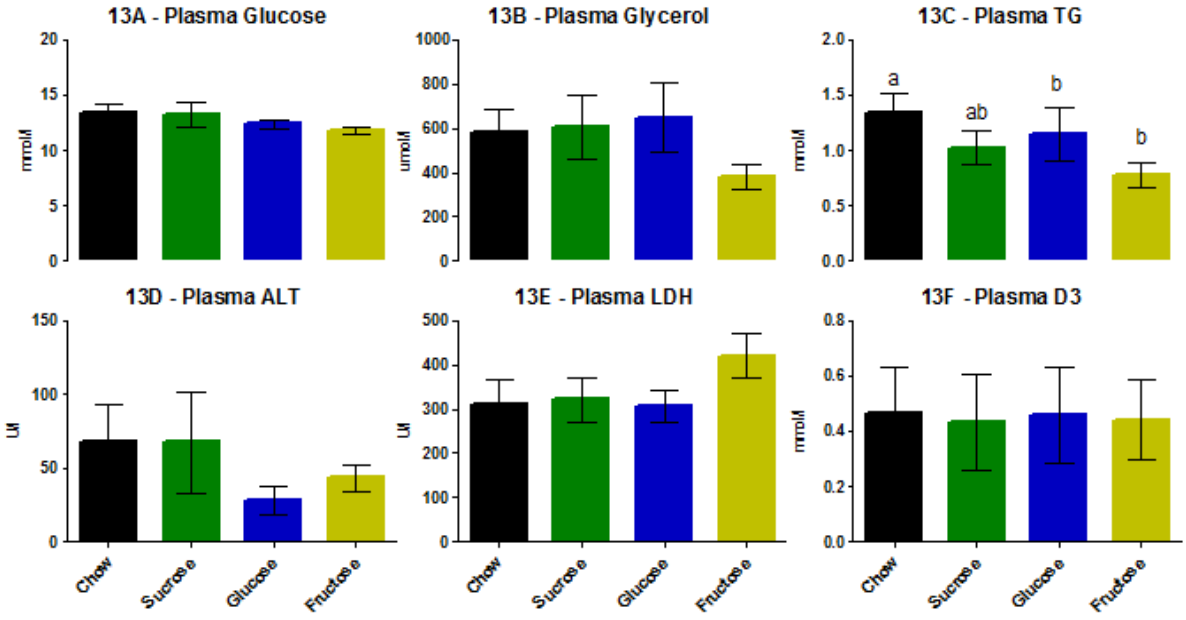

***Figure 3.13**: Plasma levels of glucose (A), glycerol (B), triglyceride (C), alanine transaminase (D), lactate dehydrogenase (E) and D3 hydroxybutyrate (F). Groups marked by different letters are significantly different.*

Plasma glucose (Fig 3.13A) did not show any significant differences, as is expected in the fed state. In the fasted state, elevated plasma glucose is also a sign of Type 2 diabetes. Differences in plasma glycerol levels (Fig 3.13B) were not significantly different, but it indicates that the fructose group has the lowest levels.

Elevated plasma triglyceride level is a sign of insulin resistance. Fructose group had the lowest levels of plasma triglyceride, significantly lower than chow group (Fig 3.13C). This is consistent with the chow group being the fattest and the fructose group being the leanest. Elevated levels of alanine transaminase (ALT) are a sign of liver damage. The differences did not reach significant differences, but it seems glucose and fructose group have lower values compared to chow and sucrose group (Fig 3.13D).

Lactate dehydrogenase (LDH) is an enzyme which converts pyruvate into lactate to produce energy, without the expenditure of oxygen. Elevated level of LDH is a sign of tissue breakdown. No significant differences were reached, but the fructose group clearly has the highest levels (Fig 3.13E).

D3 hydroxybutyrate is a ketone body which can be used as a source of energy when glucose is in short supply. There were no differences in the levels of D3 hydroxybutyrate between groups (Fig 3.13F).

3.8 HISTOLOGY

Histological examinations were done to visualize the morphologies of the adipose tissues. Unfortunately, the tissues did not survive the storage time while I was away during maternity leave. Histology was performed twice with the variations describes in Materials and methods, but all tissues had degraded. A section of the disrupted tissue can be seen in Appendix III.

4. RESULTS – STARCH GROUPS

The aim of this study was to investigate whether the GI index of the food in combination with fish oil would affect the mice in any way.

This study consists of two experimental groups in addition to the control group. One group was fed food containing the low GI starch amylose. The other group was fed food containing the high GI starch amylopectin. The control group ate standard mice chow and is the same control group used in the parallel study of sugars and fish oil. The diet composition is shown at page 40 of Materials and methods. The concept of the GI index is explained at page 16-17 of the Introduction. A meal-tolerance test of low and high GI diets comparable to ours, performed on C57BL/6J mice, is illustrated in Appendix IV.

The two experimental groups were *pair-fed*, so that all mice received the same amount of calories. They were also pair fed with the sugar groups in the parallel study, to make it possible to compare any of the five experimental diets. From now on the different diet groups in this study will be labeled chow, low GI and high GI. Any significant differences will be marked by different letters on the graphs. All genes measured were normalized to the housekeeping gene TBP.

4.1 FOOD INTAKE, BODY WEIGHT DEVELOPMENT AND FEED EFFICENCY

The mice were fed the experimental diets for 9 weeks. The chow group was given food *ad libitum*, whereas the other groups were restricted in their food intake. The chow feed contained lesser calories per gram than the other feeds, so these mice ate more food measured in grams than the other groups (not shown). The accumulated calories ingested, the weight gain and the energy efficiency is shown in Figure 4.1A-C. The body weight development is shown in figure 4.1D.

The *pair-fed* experimental groups ate roughly the same amount of calories. The chow group ingested less calories compared to the low GI group (Fig 4.1A). After 9 weeks of feeding, the mice where weighed before termination. The total weight gain in grams is shown in figure 4.1B. Mice on fish oil diets gained less weight than mice on chow diet, but the difference is statistically significant only for the low GI group. The energy efficiency is shown in figure

4.1C. Both groups on fish oil diets had to eat more calories to gain weight compared to the chow group, but the difference is only significant for the low GI group. There is clearly a difference between low and high GI diets in respect to weight gain and calorie efficiency, but the differences between the two groups are not large enough to reach significant levels.

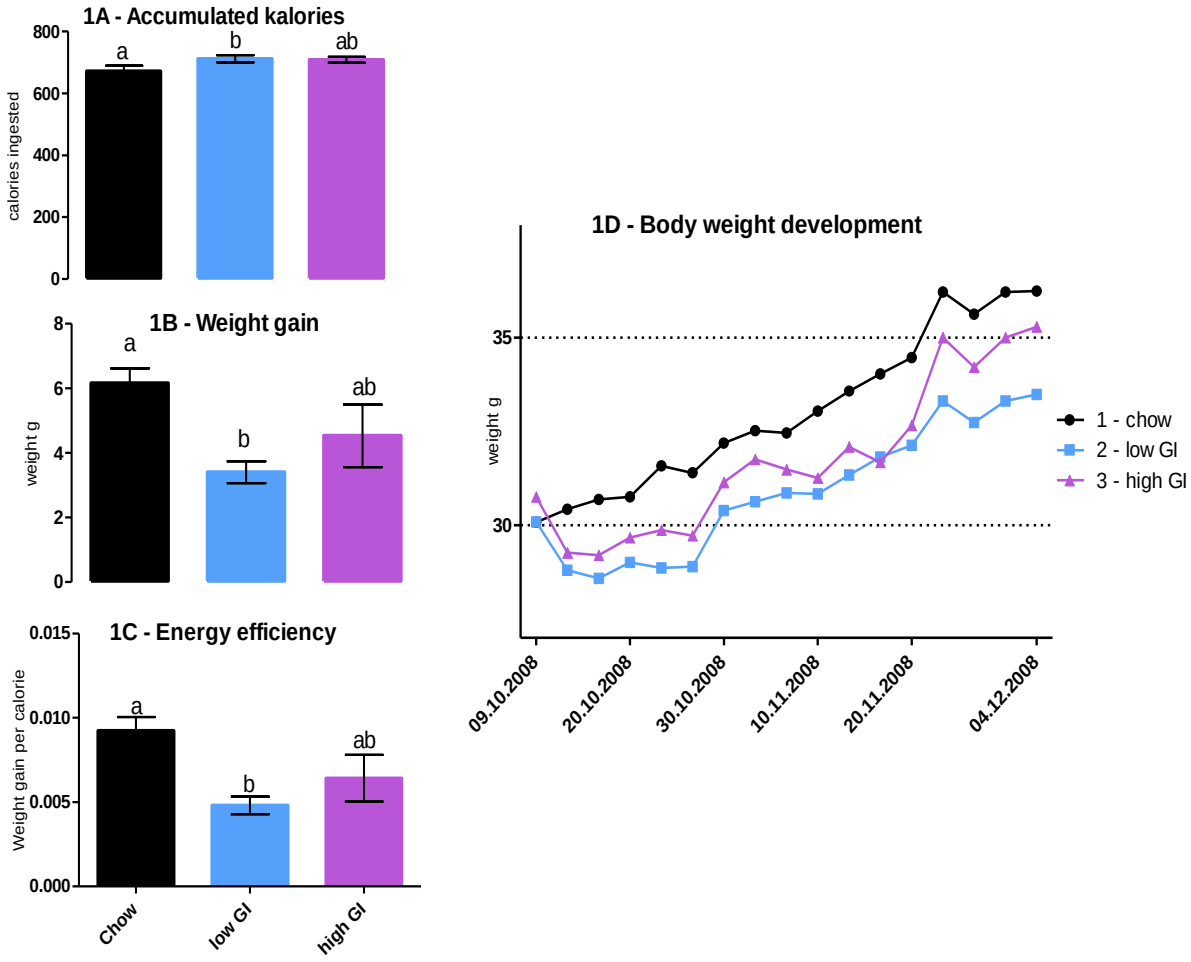

***Figure 4.1**: Feed intake and body weight development of the C57BL/6J mice. Total calories ingested (A), total weight gain from start to end of the experiment (B), weight gain (g) per calorie ingested (C) and body weight development during the experiment. Groups marked by different letters are significantly different.*

The mice were weighed twice a week. The body weight development is shown in figure 4.1D. There was a drop in the weight development some days before termination due to changes in the mice's environment, but it does not seem to have affected the end result. As seen from the graph, the low-calorie chow group who ate fewer calories, gained the most weight. The low GI diet group, who ate the most calories, ended up as the lightest group.

4.2 ORGAN WEIGHTS

Figure 4.2A shows the end mean body weights of the groups. After termination, organ weights were recorded. We harvested the retroperitoneal adipose tissue (Fig 4.2B), epididymal adipose tissue (Fig 4.2C), inguinal adipose tissue (Fig 4.2D), intrascapular brown adipose tissue (Fig 4.2E), tibialis muscle (Fig 4.2F) and liver (Fig 4.2G).

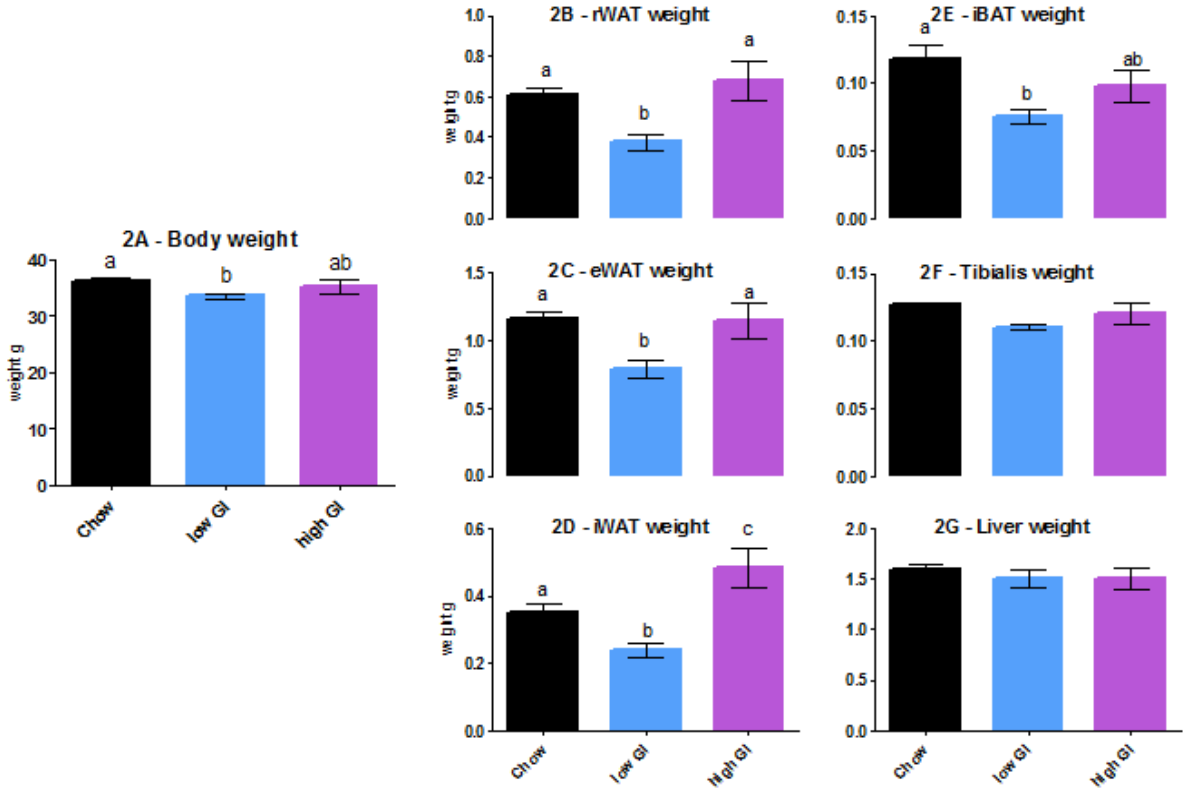

***Figure 4.2**: Total body weight (A), rWAT weight (B), eWAT weight (C), iWAT weight (D), iBAT weight (E), tibialis weight (F) and liver weight (G). All weights are displayed in grams. Groups marked by different letters are significantly different.*

In this experiment, total body weight was significantly lower for the low GI group compared to chow group (Fig 4.2A). This difference did not reach significant levels for the high GI group, nor in any of the groups who ate sugars (Fig 3.2A). Adipose tissues were continuously smaller in the low GI groups (Fig 4.2B-E). The subcutaneous fat depot inguinal WAT (iWAT) varied the most, low GI had significantly less iWAT compared to chow group, and high GI group had significantly more iWAT compared to chow group (Fig 4.2D). The difference in intrascapular brown adipose tissue (iBAT) was less protrudent, low GI group had significantly less iBAT compared to the chow group, but the difference was not significant compared to the high GI group (Fig 4.2E). Weight of the muscle (Fig 4.2F) and

liver (Fig 4.2G) organs did not show any significant differences, although the lighter mice in the low GI group had somewhat smaller tibialis muscles.

4.3 HEPATIC GENE EXPRESSION

The same genes were measured in the starch groups as in the sugar groups.

Lipogenic gene expression

The relative expression levels of lipogenic genes are shown in figure 4.3. We measured the relative expressions of *Srebp1c*, *Acc1*, *Acc2*, *Scd1*, *Fas* and *Dgat*. The function and regulation of these genes are described at page 21-25 of the Introduction.

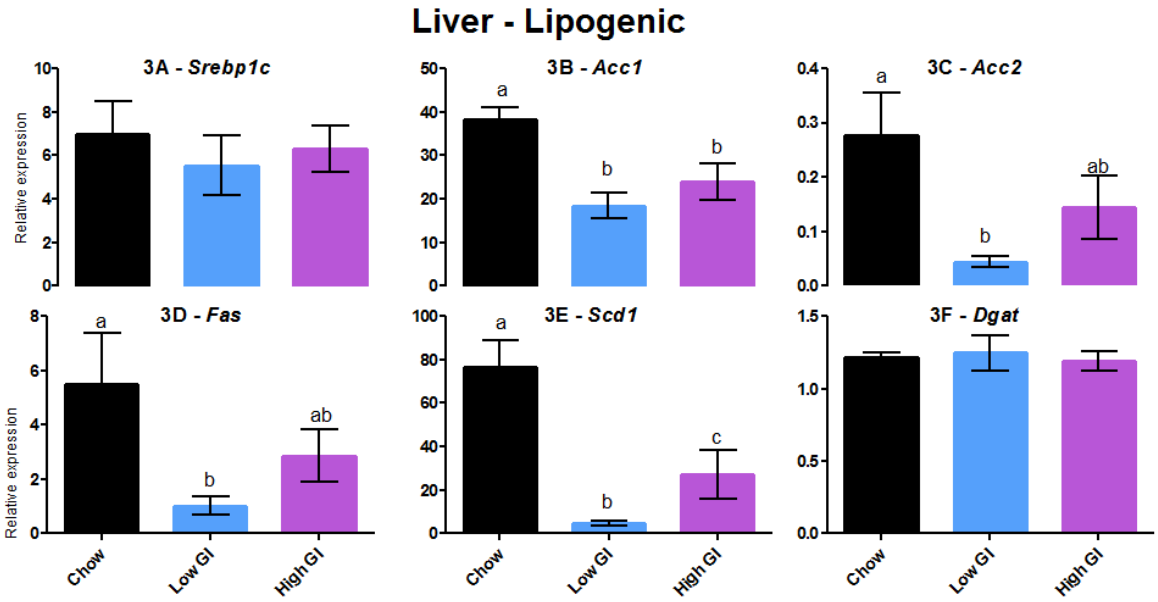

***Figure 4.3**: Relative expression levels of hepatic Srebp1c (A), Acc1 (B), Acc2 (C), Scd1 (D), Fas (E) and Dgat (F) mRNA. Groups marked by different letters are significantly different.*

The groups who were given fish oil showed a tendency towards lower expression levels of the lipogenic transcription factor *Srebp1c* compared to the chow group (Fig 4.3A), although the results were not significantly different. The chow group has significantly higher expression levels of the lipogenic enzymes *Acc1*, *Acc2*, *Fas* and *Scd1* (Fig 4.3B-E), which are influenced by the SREBP-1c transcription factor. Both fish oil groups have a tendency towards lower expression levels of these genes, but the low GI group continuously has even lower expression rates compared to high GI group. The difference was biggest for the *Scd1*

expressions, where the low GI group had significantly reduced *Scd1* levels compared to high GI group (Fig 4.3E). This shows that the type of carbohydrate ingested affects the ability of PUFAs in fish oil to decrease lipogenesis. Like in the parallel study of sugar diets, expression levels of *Dgat* did not vary between groups (Fig 4.3F).

Genes increasing fatty acid breakdown

The relative expression levels of the genes which increases fatty acid breakdown are shown in figure 4.4. We measured the expression levels of *Pparα*, *Pparδ*, *Aco*, *Cpt1a*, *Cpt2* and *Hmgcs2*. The function and regulation of these genes are described at page 25-28 of the Introduction.

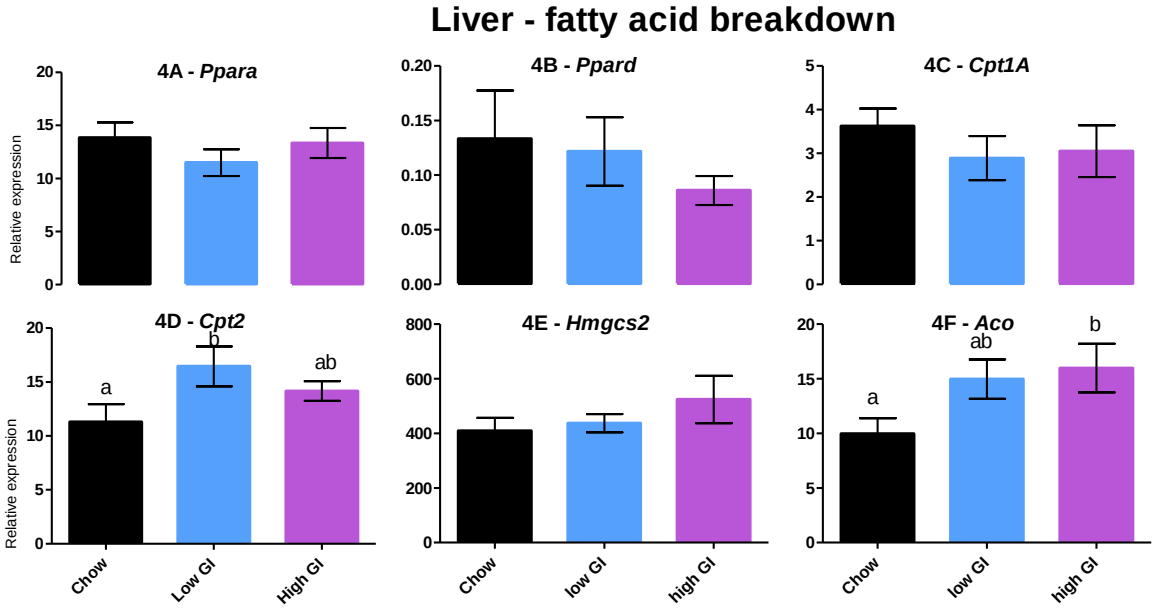

***Figure 4.4**: Relative expression levels of the genes Pparα (A), Pparδ (B), Cpt1a (C), Cpt2 (D), Hmgcs2 (E) and Aco (F) in liver. Groups marked by different letters are significantly different.*

There were no significant differences in the expressions of *Pparα*, *Pparδ*, *Cpt1a* or *Hmgcs2* (Fig 4.4 A, B, C and E). This is in correlation with the results from the parallel study of mice given different sugars in combination with fish oil (Fig 3.4). *Cpt2*-expressions were higher in the fish oil groups compared to the low-fat chow group, and the difference was significant for the low GI group (Fig 4.4D). *Aco* expression levels were also higher in fish oil groups, but here the difference was significant only for the high GI group (Fig 4.4F).

Gluconeogenesis

The relative expression levels of genes involved in gluconeogenesis are shown in figure 4.5. We measured the expression levels of *Pgc1α* and *Pck1*. These genes are described at page 28 of the Introduction.

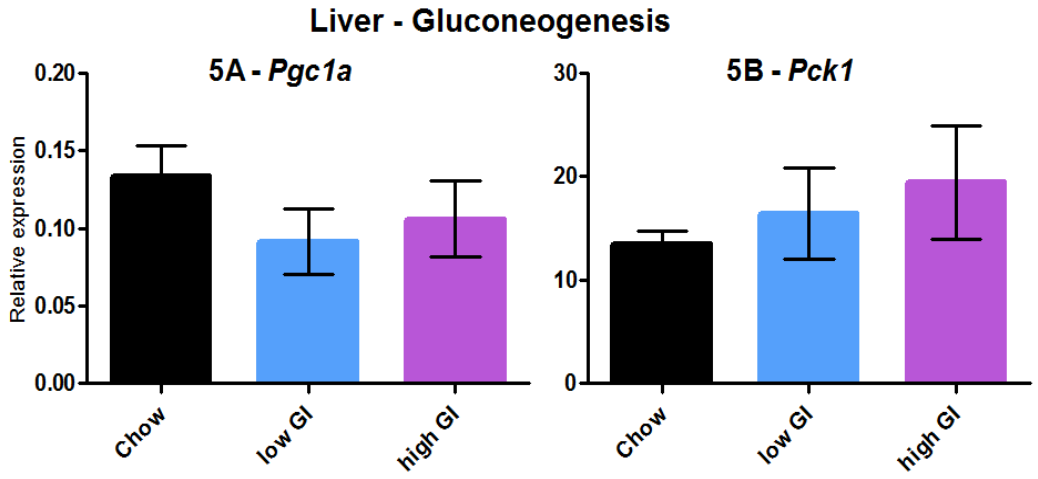

***Figure 4.5**: Relative expressions of the gluconeogenetic enzymes Pgc1α (A) and Pck1 (B) in liver. Groups marked by different letters are significantly different.*

Like in the study of the sugar diets, mice given fish oil had somewhat reduced expression levels of *Pgc1α*, although the difference did not reach statistical significance (Fig 4.5A and B). The fish oil groups did however have somewhat elevated levels of *Pck1*, but standard errors were high.

Amino acid degradation

The relative expression levels of genes involved in amino acid degradation are shown in figure 4.6. We measured to expressions of *Agxt*, *Got*, *Gpt1* and *Cps1*. The enzyme products of these genes are described at page 29 of the Introduction.

Like in the study of the sugar diets, only *Agxt* showed significant differences (Fig 4.6A). *Agxt* expression levels are reduced in both fish oil groups, but the difference is only significant for the low GI group. The expression levels of *Got, Gpt1 and Cps1* also show a tendency towards lower values in the fish oil group, although the differences do not reach statistical significance (Fig 4.6 B-D).

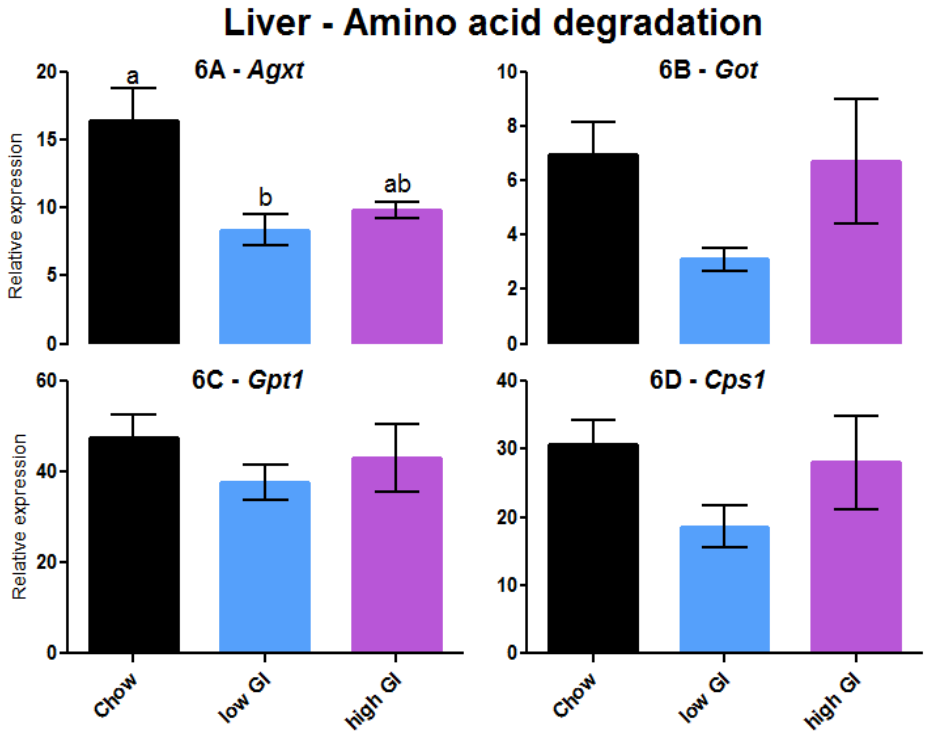

***Figure 4.6**: The relative expressions of mRNA coding for hepatic enzymes involved in amino acid degradation. Agxt (A), Got (B), Gpt1 (C) and Cps1 (D) were measured. Groups marked by different letters are significantly different.*

Cyclic AMP signaling

The relative expression levels of genes involved cyclic AMP (cAMP) signaling are shown in figure 4.7. We measured the expression levels of *RIα, RIIβ, Crem* and *Pde4c*. These genes are described at page 30-31 of the Introduction.

As seen in the study of sugar diets, there were no significant differences in the *RIα* and *RIIβ* expression levels, although *RIα* seems to be somewhat reduced in the low GI diet group (Fig 4.7A and B). The *RIα: RIIβ* ratios were also a little lower in the fish oil groups compared to chow group (Fig 4.7C). The levels of *Crem* were significantly reduced in the fish oil groups compared to the chow group (Fig 4.7D). The levels of *Pde4c* were not significantly different, although there was a slight reduction in the fish oil groups (Fig 4.7E). This trend was also seen in the fish oil groups from the sugar diet study (Fig 3.7E).

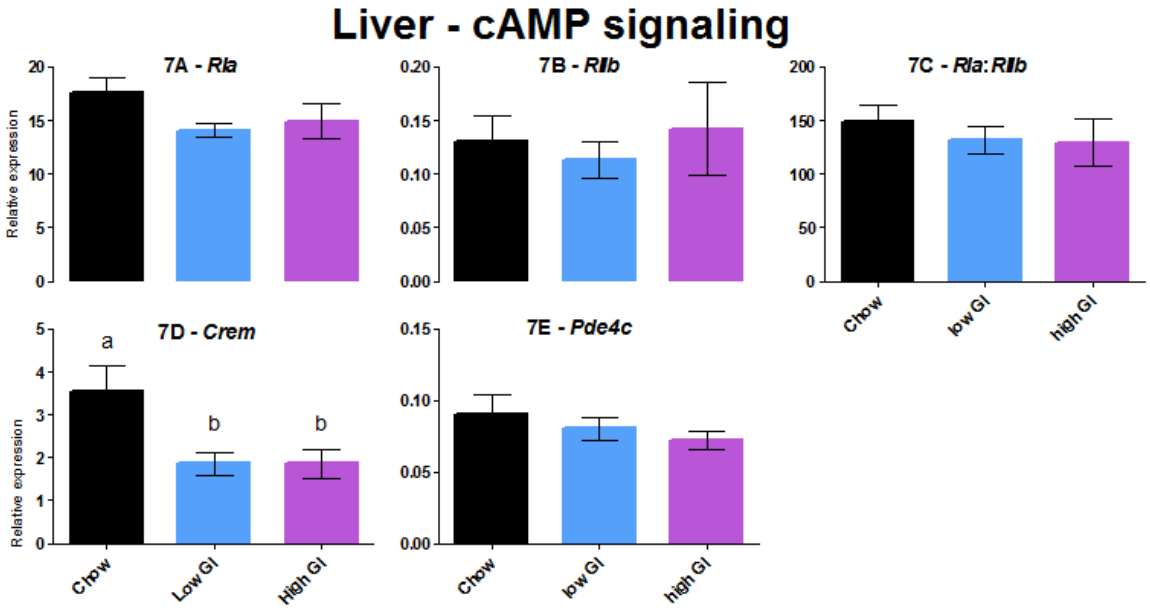

***Figure 4.7**: cAMP signaling. The relative expressions of RIα (A), RIIβ (B), Crem (D) and Pde4c (E). Figure 7C shows the RIα: RIIβ-ratio. Groups marked by different letters are significantly different.*

4.4 GENE EXPRESSIONS IN WHITE ADIPOSE TISSUE

Expressions of genes involved in adipogenesis, inflammation and genes that give white adipocytes a brown-like phenotype were measured in white adipose tissue. The same genes were measured in this experiment as in the sugar diets experiment.

Adipogenesis

The relative expressions of *Pparγ2*, *Srebp1c* and *Fas* were measured in eWAT and iWAT (Fig 4.8). These genes are described at page 21-25 of the Introduction.

As in the experiment with the sugar diets, differences in the levels of *Pparγ2*, *Srebp1c* and *Fas* did not reach significant differences (Fig 4.8A-F). The levels in eWAT were a bit higher in the fish oil groups, and the levels in iWAT were a bit lower in the fish oil groups. The same pattern for the iWAT expression levels of lipogenic genes are seen in the fish oil groups of the sugar study (Fig 3.8).

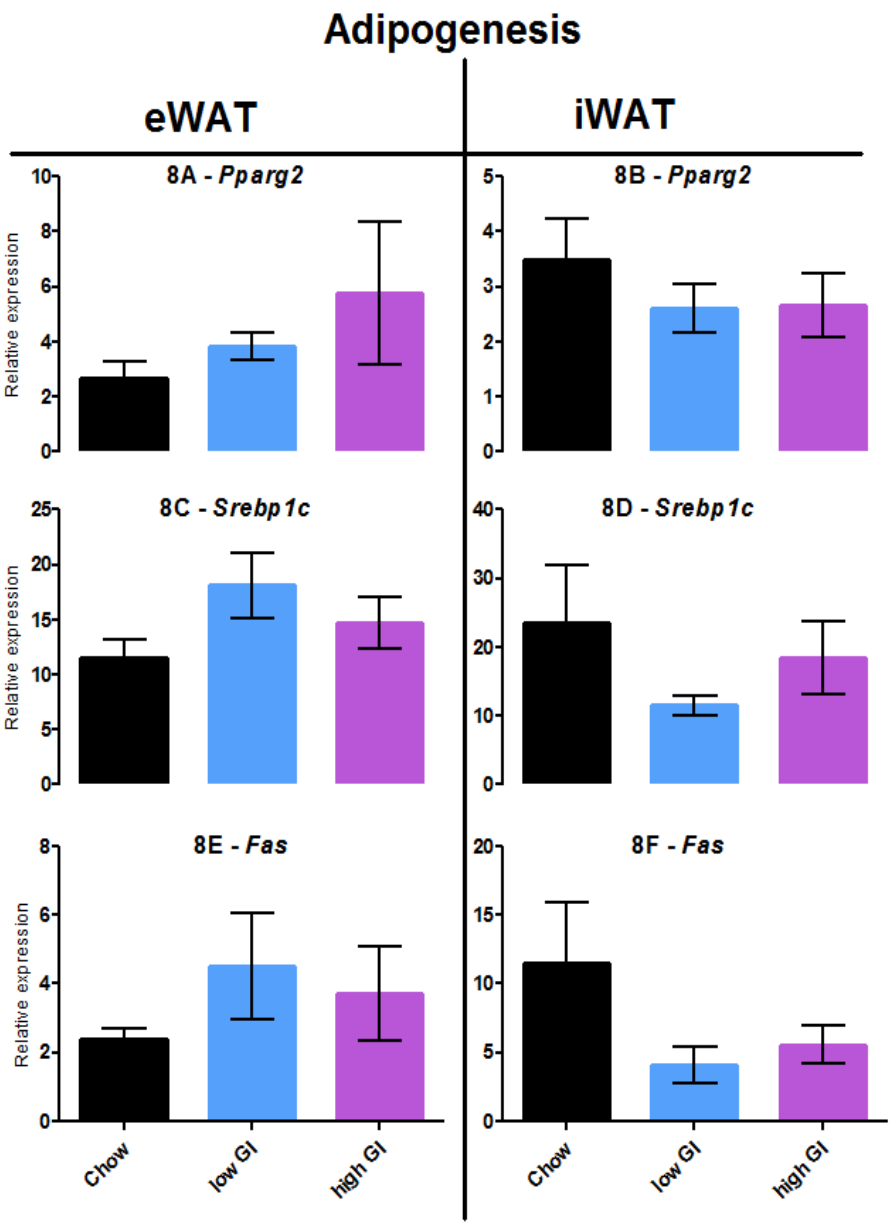

***Figure 4.8**: Relative expressions of adipogenic genes in white adipose tissue: Pparγ2 (A and B), Srebp1c (C and D) and Fas (E and F). Measurements from epididymal fat to the left and inguinal fat to the right.*

Inflammation markers

The expression levels of the inflammation markers *Ccl2*, *Cd68*, *Emr1* and *Serpine1* were measured in eWAT and iWAT. Results from *Serpine1* are not shown due to high standard errors of the mean. These genes are described at page 31-34 of the Introduction. The results are shown in figure 4.9.

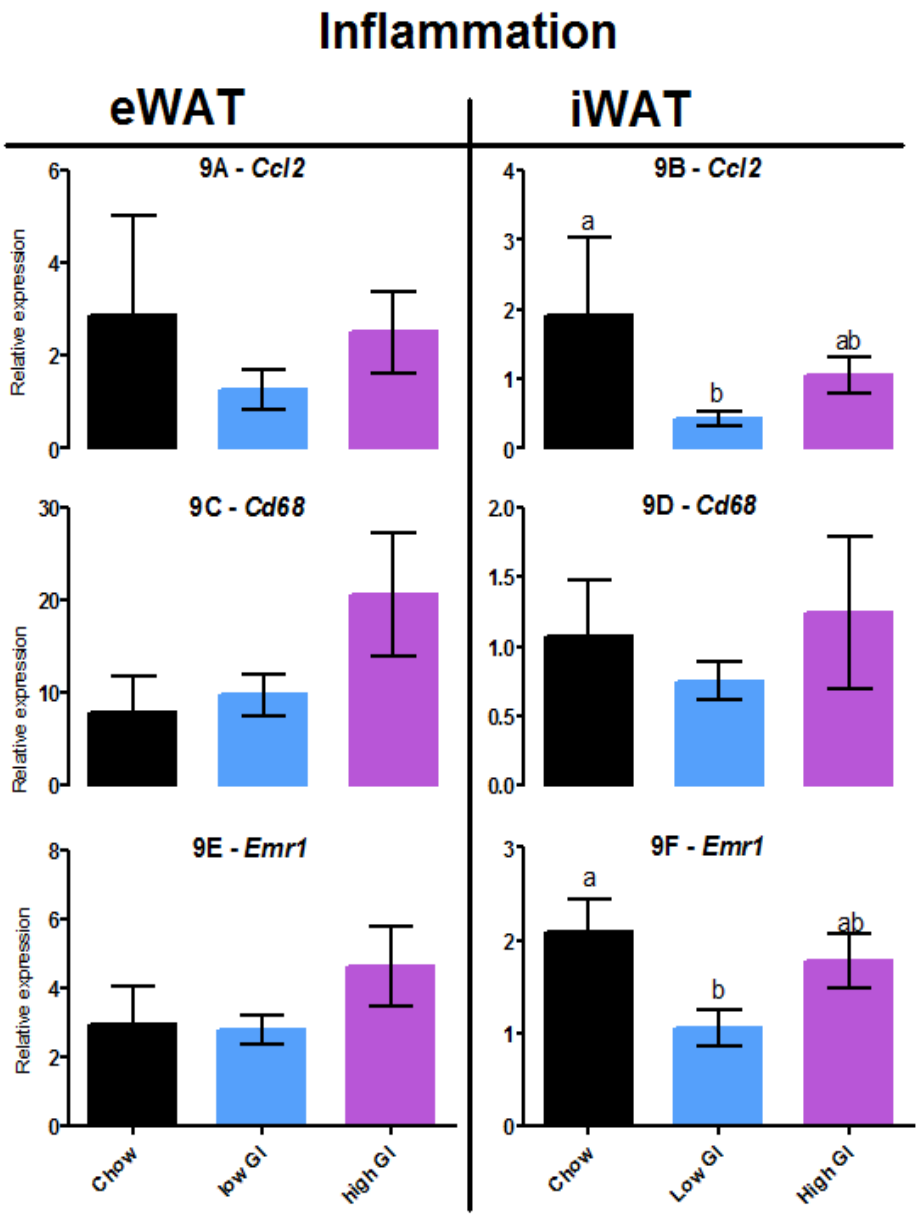

***Figure 4.9**: Relative expression levels of inflammatory genes in white adipose tissue: Ccl2 (A and B), Cd68 (C and D) and Emr1 (E and F). Measurements from epididymal fat to the left and inguinal fat to the right. Groups marked by different letters are significantly different.*

Expression levels in eWAT showed no statistical significant differences (Fig 4.9 A, C and E). The low GI group had lower expressions of for *Ccl2*, *Cd68* and *Emr1* compared to the high GI group.

The expressions of the inflammatory genes in iWAT were lower in the low GI group (Fig 4.9 B, D and F), and the difference was significant for *Ccl2* and *Emr1*, compared to the chow group (Fig 4.9 B and F).

Brown-like phenotype of WAT

We measured the expression levels of *Pgc1α* and *Ucp1* in eWAT and iWAT. For reasons described at page 65, results from *Ucp1* measurement are not shown, but the expression level of *Pgc1α* is found in figure 4.10. The function of PGC-1α in adipose tissue can be found at page 35 of the Introduction.

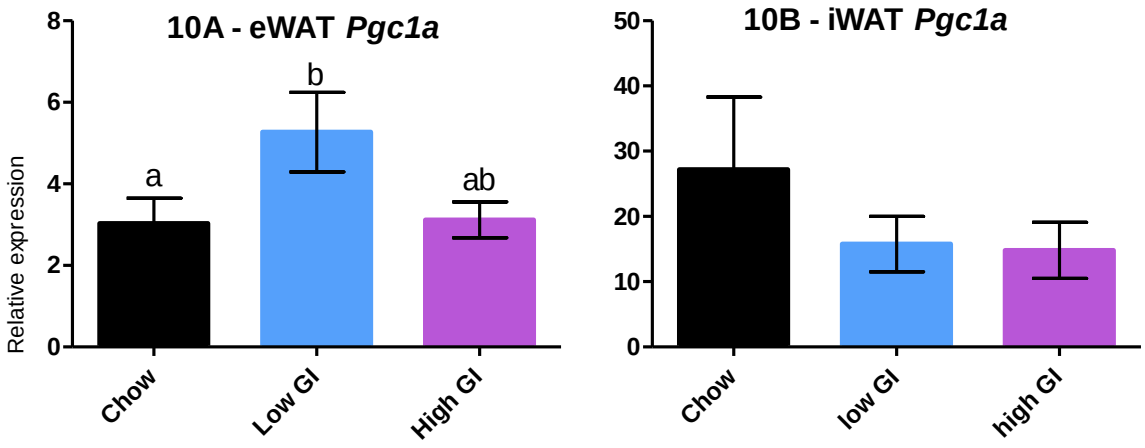

***Figure 4.10**: The relative expression levels of Pgc1α in epididymal (A) and inguinal (B) fat.*

The low GI group has significantly elevated expression levels of *Pgc1α* in visceral fat compared to the chow group (Fig 4.10A). Levels of *Pgc1α* in subcutaneous fat do not reach statistical significant differences, but the levels are somewhat reduced on both fish oil groups (Fig 4.10B). These results are consistent with the results found in the sugar diets study (Fig 3.10).

3.5 GENE EXPRESSION LEVELS IN BROWN ADIPOSE TISSUE

In intrascapular brown adipose tissue (iBAT), *Pgc1α*, *Dio2* and *Ucp1* were measured to examine differences in adipocyte phenotypes. Unfortunately, for reasons described above, *Ucp1* results are not shown. The expression levels of *Cox2* were determined as a measurement of mitochondrial function. The expressions of the lipogenic genes *Srebp1c* and *Rip140* were also measured in iBAT. The enzyme products of these genes are described at page 34-36 of the Introduction. The results are displayed in figure 4.11.

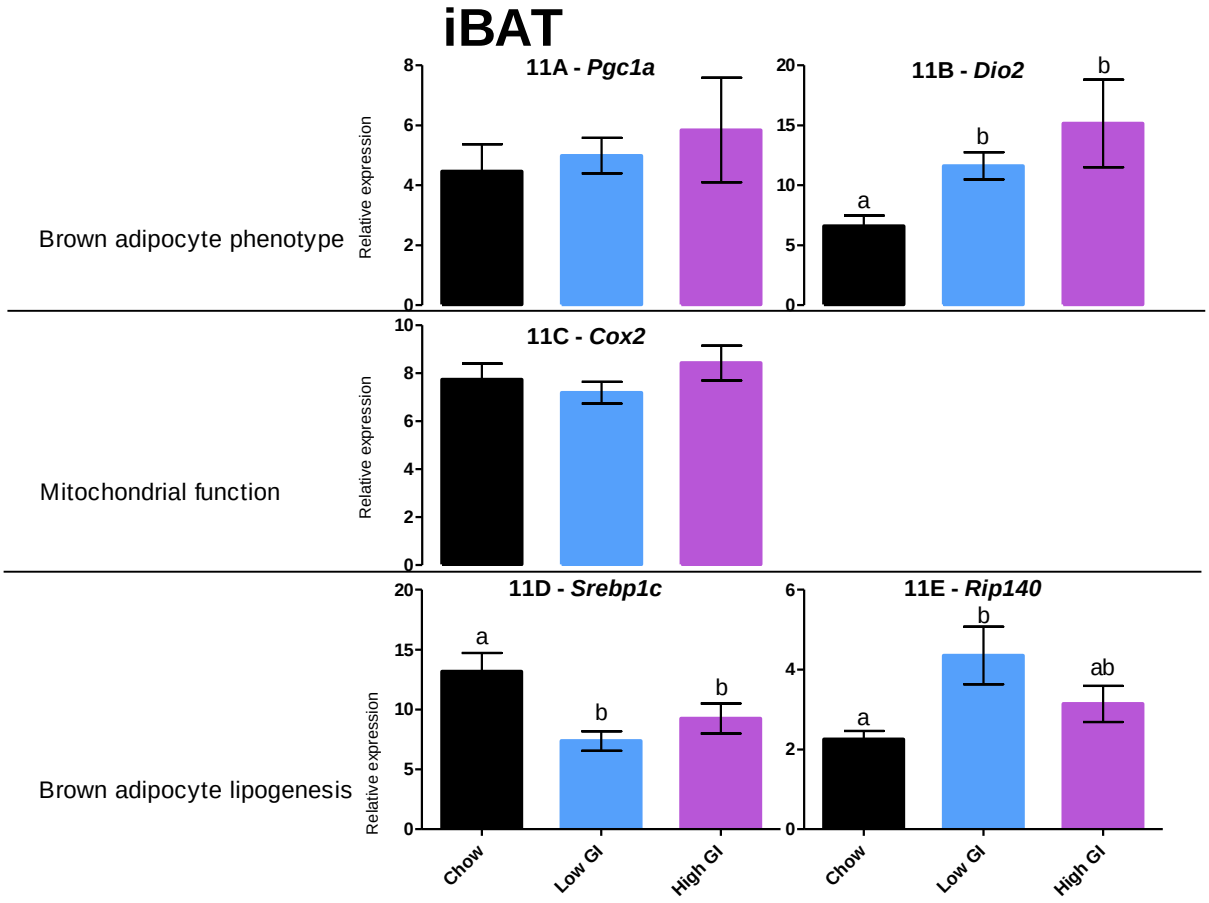

***Figure 4.11**: The expression levels of genes involved in adipocyte phenotype, mitochondrial function and lipogenesis in BAT. Pgc1α (A), Dio2 (B), Cox2 (C), Srebp1c (D) and Rip140 (E). Groups marked by different letters are significantly different.*

Fish oil groups showed a trend towards higher expression levels of the Bat-specific genes *Pgc1α* (Fig 3.11A) and *Dio2* (Fig 3.11B) compared to the chow group. The difference was significant for *Dio2* (Fig 3.11B). This might indicate that the fish oil groups had a higher capacity of turning fat into heat, which would explain why they are leaner while they still ate more calories than the chow group. Interestingly, the heavier high GI group had slightly higher levels of these genes compared to the low GI group. The fish oil groups did not, however, have higher levels of *Cox2* compared to the chow group (Fig 4.11C).

The expression levels of lipogenic genes are, as seen in the sugar diets study, less consistent. Both fish oil groups had significantly reduced levels of *Srebp1c* compared to chow group (Fig 4.11D), but the expression levels of *Rip140* were lower in the chow group. This is also consistent with the results found in the sugar diets study.

4.6 LIPID CONTENT IN LIVER AND MUSCLE

Lipid content was measured in both liver and the tibialis muscle. Note that the results show the content of the whole organ, not the concentration per weight unit. Liver weights were about the same for all groups, whereas muscle weights were somewhat lower in the low GI group (see Fig 4.2, F and G).

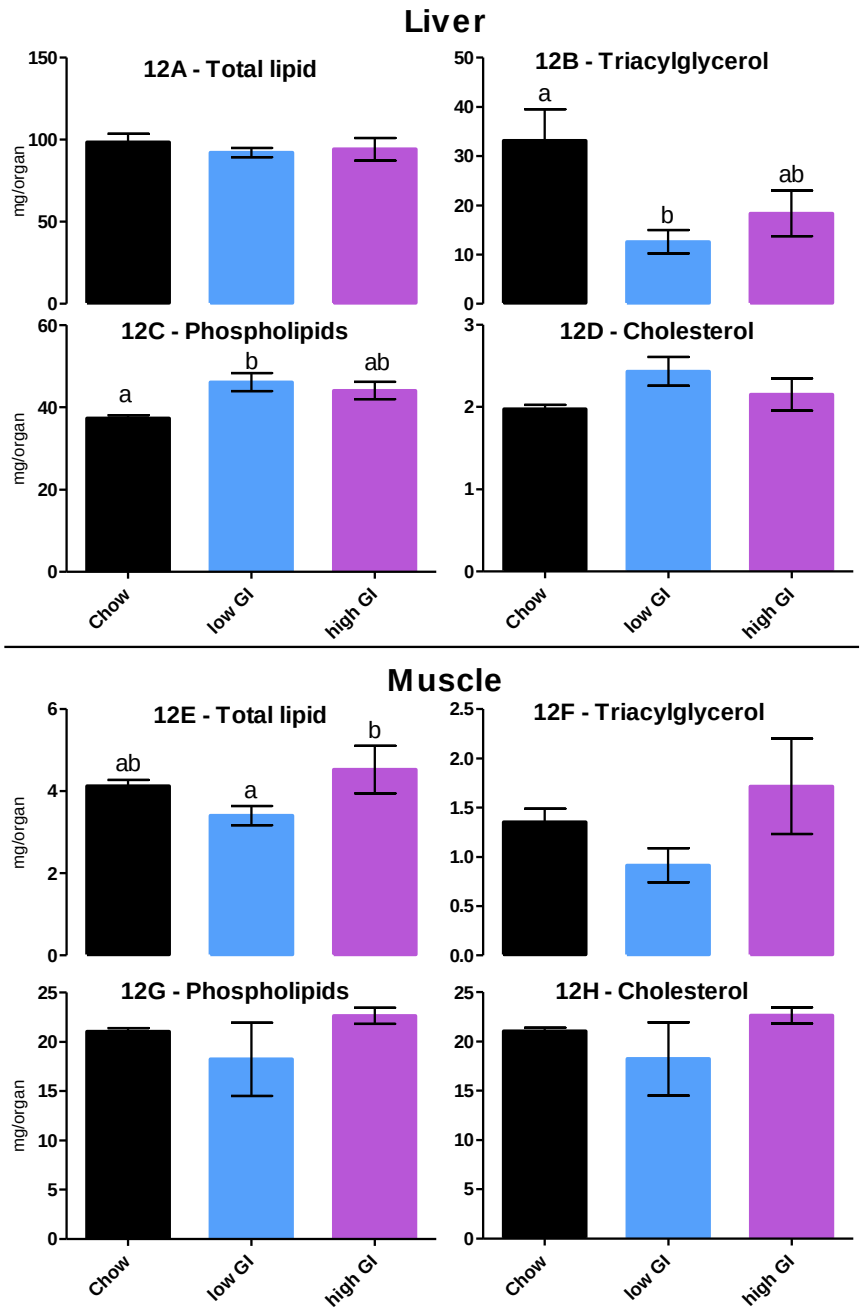

***Figure 4.12**: Lipid content in liver (A-D) and muscle (E-H). The amounts of total lipids (A and E), triacylglycerol (B and F), phospholipids (C and G) and cholesterol (D and H) were measured. Groups marked by different letters are significantly different.*

The amounts of total lipid in liver (Fig 4.12A) did not differ between groups. In contrast, liver triacylglycerol contents were lower in both fish oil groups compared to chow group, and the difference reach statistical significance for the low GI group (Fig 4.12B). This trend was also seen in the sugar diets study (Fig 3.12B). The amounts of phospholipids were higher in the fish oil groups compared to the low-fat chow group, and the difference was significant for the low GI group (Fig 4.12C). Cholesterol contents were somewhat higher in the low GI group, but the difference was not statistically significant (Fig 4.12D).

Lipid contents in the tibialis muscle were consistently higher in the high GI group (Fig 4.12 E-H). Total lipid contents were higher in both fish oil groups compared to chow group, and the difference reached statistical significance for the high GI group (Fig 4.12E). Triacylglycerol contents were somewhat lower in the low GI group, but the difference was not significant (Fig 4.12F). Amounts of phospholipids in muscle did not show high variations between groups, but the low GI group had somewhat lower phospholipid contents compared to high GI group (Fig 4.12G). Cholesterol contents followed the same pattern (Fig 4.12H).

4.7 PLASMA PARAMETERS

All plasma parameters were measured from fed mice. Plasma insulin levels were not expected to differ much in the fed state, and indeed the results were not significantly different (not shown). The results of the plasma glucose, glycerol, triglyceride, alanine transaminase (ALT), lactate dehydrogenase (LDH) and D3 hydroxybutyrate are shown in figure 4.13.

Plasma glucose did not show any significant differences, as is expected in the fed state, but the low GI group has slightly reduced levels compared to the other groups (Fig 4.13A). Plasma glycerol was lower in the fish oil groups compared to the chow group, but the difference did not reach statistical significance (Fig 4.13B). Plasma triglyceride levels are significantly reduced in the fish oil groups compared to the chow group (Fig 4.13C). The values of plasma ALT varied within groups, but it seems that the low GI group has the lower values compared to the other groups (Fig 4.13D). High levels of ALT may be a symptom of liver failure. Differences in plasma LDH did not vary between groups (Fig 4.13E). The levels of the ketone body D3 hydroxybutyrate did not reach significant differences, but was slightly elevated in the low GI group (Fig 4.13F).

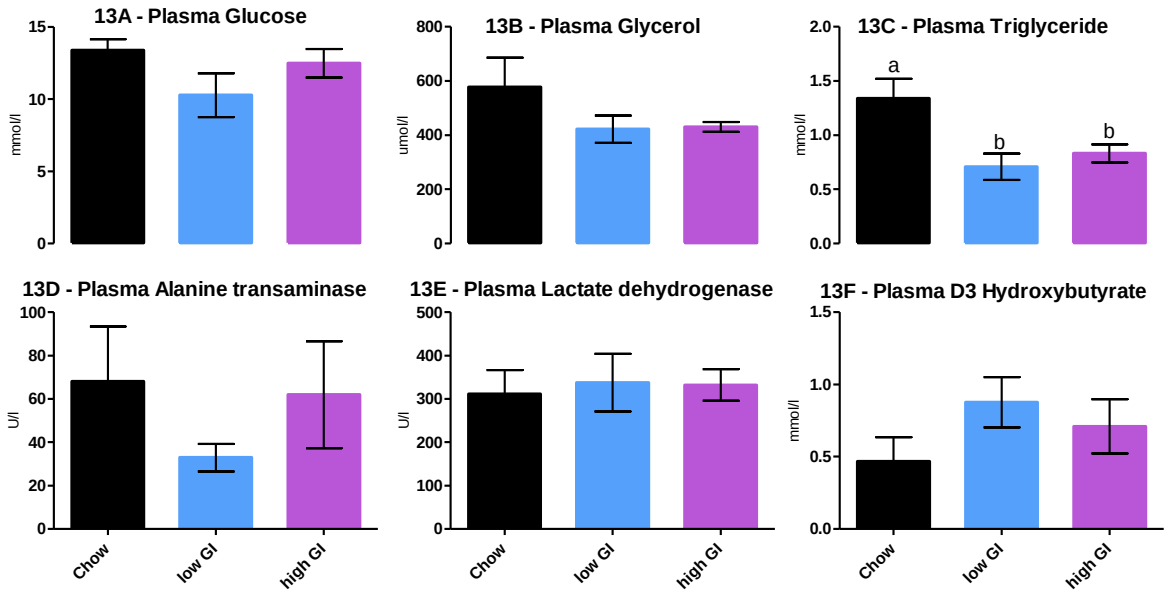

***Figure 4.13**: Plasma levels of glucose (A), glycerol (B), triglyceride (C), alanine transaminase (D), lactate dehydrogenase (E) and D3 hydroxybutyrate (F). Groups marked by different letters are significantly different.*

4.8 HISTOLOGY

Histological examinations were done to visualize the morphologies of the adipose tissues. Unfortunately, the tissues did not survive the storage while I was away during maternity leave. Histology was performed twice, but all tissues had degraded.

5. DISCUSSION

Previous studies have demonstrated the anti-obesogenic effects of fish oil in obesity-promoting diets (Arai et al 2009, Belzung et al 1993, Flachs et al 2005). The present studies were performed to elucidate whether the anti-obesogenic effect of fish oil is influenced by types of carbohydrates in the background diet. The experimental diets contained the same amounts fat, protein and carbohydrates. The types of fat and protein were equal, whereas the type of carbohydrate varied. The animals in the experimental groups were all *pair-fed*. We wanted to investigate potential differences in body weight, adipose tissue weights, lipogenesis, fatty acid breakdown, gluconeogenesis, amino acid degradation, brown-like phenotypes in adipose tissues, inflammation, accumulation of fatty acids in liver, muscle and plasma, and plasma other parameters.

5.1 ANIMAL MODEL AND DIETS

36 male C57BL/6J mice were given 6 different diets. The C57BL/6J (black six) mouse model was chosen because it is widely used in obesity studies, which makes it possible to compare results with previously performed studies. The black six mice easily develop diet-induced obesity and metabolic traits seen in obese humans over a relatively short period of time. It also lacks the ability to induce thermogenesis when exposed to high-caloric diets, a trait that is seen in obesity-resistant mice (Collins et al 2004).

One of the diets was standard chow diet, high in carbohydrates and low in fat. The other diets were high fat diets containing primarily fish oil, but also a small of amount soy bean oil, which provides n-6 fatty acids, also required for growth. The experimental diets contained high sucrose, high glucose, high fructose, high amylose or high amylopectin, as listed in table 2.1, page 40.

5.2 BODY WEIGHT DEVELOPMENT AND FEED EFFICIENCY

Of all the groups, the group given standard chow diet gained the most weight, despite the fact that they did not eat more calories than other groups. The amount of energy is lower in the low fat feed than in the experimental diets, but as the chow fed mice consumed more feed, the

energy intake was comparable. It should be noted that the amount of eWAT in the chow group, which was more than average 1g, indicates that the low fat fed mice were obese. This shows that fish oil to some extent protects against obesity, regardless of the type of carbohydrate ingested. Of the different fish oil groups, the mice given glucose as their main carbohydrate gained the most weight, closely followed by the sucrose group, whereas the fructose group remained relatively lean, indicating that the obesogenic effect of sucrose stems from the glucose molecule. It is to be noted that the mean weight gain of the glucose and sucrose groups were very close (4.7 g and 4.6 g). When digested, sucrose is split into one molecule of glucose and one molecule of fructose, so these results clearly show that while fructose in this study does not have an obesogenic effect, it doesn't protect against obesity either. Mice receiving the high GI starch became as obese as the sucrose fed mice, whereas the low GI group remained relatively lean.

5.3 ADIPOSE TISSUE DEVELOPMENT

As previously mentioned, visceral adipose tissue is regarded as more unhealthy and increases the risk of developing Type 2 diabetes and metabolic syndrome, compared to subcutaneous adipose depots. The sucrose group developed the most visceral fat mass (eWAT and rWAT combined) of all groups, closely followed by high GI group (Fig 3.2A+B and 4.2 A+B). The percentage of visceral fat mass of total body weight is illustrated in figure 5.1. The chow mice, although heavier, had less visceral adipose tissue mass compared to mice given sucrose and high GI starch. This might indicate that even though the chow mice were bigger and most likely were fatter, they probably had a more healthy body composition of more subcutaneous fat mass compared to visceral fat mass. On the other end of the scale, the fructose and low GI fed mice developed the least adipose tissue mass and also had smaller visceral adipose depots compared to total body weight.

The distribution of subcutaneous fat is not illustrated, since we only dissected one depot of this fat and this might not be representative for the total subcutaneous fat mass. As mentioned in the Introduction, subcutaneous fat is distributed under the skin, all over the body. For future studies, I suggest an in vivo MRI scan of the animals to visualize the total body fat content.

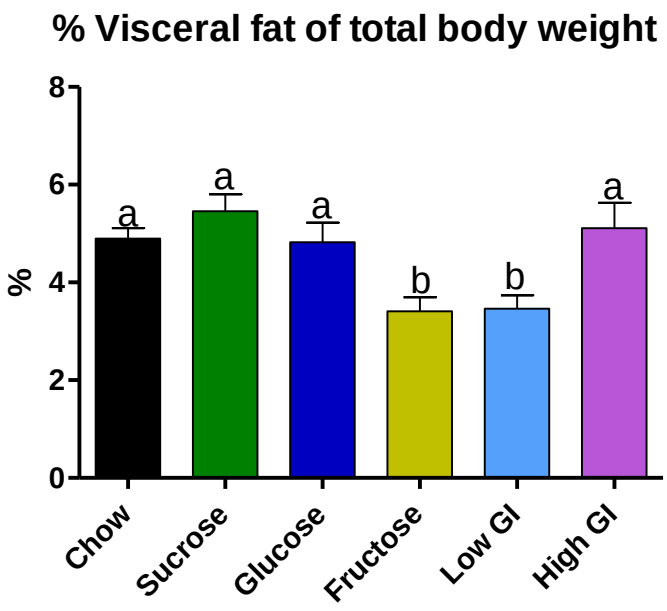

Figure 5.1: *Visceral fat (eWAT + rWAT combined) weight of total body weight, in percent. The different amounts and different distributions of body fat clearly show that the carbohydrates in the diet affect the anti-obesogenic effect of fish oil.*

5.4 ENERGY EFFICIENCY

Both fructose and low GI group had significantly reduced energy efficiencies compared to the chow group, despite the fact that the fructose group ate the same amount of calories and the low GI group even ate more. The mice were kept in equal cages under equal conditions, but it is theoretically possible that the fructose and low GI mice were more physically active compared to other groups. Any differences in activity levels were not detectable by normal observation during the feeding trial. It is more likely that the differences in energy efficiency are in fact due to the carbohydrate components of the diets. This is also supported by the differences found in expressions of genes involved in metabolism and brown-like phenotypes of adipocytes. Other studies have also found differences in feed efficiency of *pair-fed* mice (Madsen et al 2008).

5.5 GENE EXPRESSION LEVELS IN LIVER

PUFAs are demonstrated to reduce hepatic levels of the lipogenic transcription factor *Srebp1c* (Xu et al 2001). Liver *Srebp1c* was not downregulated in our fish oil groups, but the fish oil groups seemed to be protected against elevated levels of the lipogenic genes *Acc1*, *Acc2*, *Fas*

and *Scd1* (Figs 3.3 and 4.3). This may be due to the fact that the SREBP-1c enzyme has to be activated before functioning as a transcription factor (Horton et al 2002). High level of *Srebp1c* mRNA is not a guarantee for high levels of active SREBP-1c enzyme, since the enzyme is regulated by posttranslational modifications. As seen from the expression levels of *Acc1*, *Acc2*, *Fas* and *Scd1*, SREBP-1c is probably more active in the chow group, but not in the fish oil groups. PUFAs found in fish oil are demonstrated to disrupt the inactive precursor proteins of SREBP-1c before they reach the nucleus (Yahagi et al 1999). This reduces the expressions of lipogenic genes in the liver (Osborne 2000).

The expression levels of the genes involved in fatty acid breakdown could not explain why the fish oil mice were leaner compared to the mice who ate chow feed. The expression levels of *Cpt2* were upregulated in the fish oil groups (Figs 3.4 and 4.4). This is probably not of physiological relevance, because CPT2 is not a rate-limiting enzyme (Eaton 2002). The rest of the genes coding for mitochondrial enzymes, *Pparα*, *Pparδ, Cpt1a* and *Hmgcs2*, did not show any significant differences. PPARα and PPARδ are transcription factors which have to be activated posttranslationally (Chawla et al 2001), so the slight reduction of these genes seen in some of the fish oil groups is alone not enough to support a theory of increased fatty acid breakdown. On the other hand, the mRNA levels of the peroxisomal enzyme ACO were higher in all fish oil groups compared to the chow group. This might not be a anti-obesity effect of the fish oil, since this enzyme specifically oxidized long-chained PUFAs, as found in fish oil (Duplus and Forest 2002). *Aco* levels are higher in the sucrose, glucose and high GI groups compared to the fructose and low GI groups. This is probably due to the size of the adipose tissue mass, and not caused by a beneficial effect of sucrose, glucose and high GI starch. The large adipose tissue mass found in these groups means that there are more long-chained fatty acids available for oxidation, and therefore *Aco* is upregulated.

Hyperglycemia is a symptom of insulin resistance and development of Type 2 diabetes (Hajer et al 2008). The hyperglycemia seen in obese patients is partly due to increased hepatic gluconeogenesis. Obese mice are previously demonstrated to have elevated levels of hepatic *Pgc1α* and *Pck1*, which are involved in gluconeogenesis (Yoon et al 2001). All the fish oil groups did have reduced expressions of *Pgc1α*, even though three of the groups were obese (Figs 3.5 and 4.5). PGC-1α activity is regulated by phosphorylation and deacetylations (Lin et al 2005), so although the result is interesting, we cannot claim that our fish oil mice are protected from increased gluconeogenesis without supporting findings from *Pck1* expressions, which was not reduced in the fish oil groups.

Upregulation of *Agxt, Got, Gpt1* and *Cps1*, which are involved in amino acid degradation, is not a good thing for the obese mouse. All our mice ate the same amount of proteins, so high amino acid degradation could imply that the mice have increased rates of gluconeogenesis. All our fish oil groups showed a tendency towards reduced expressions of *Agxt, Got, Gpt1* and *Cps1* compared to the chow group (Figs 3.6 and 4.6). This might indicate that the mice given fish oil were protected against amino acid-derived hyperglycemia.

Of genes involved in cAMP signaling, only *Crem* showed significant differences (Figs 3.7 and 4.7). *Crem* was significantly reduced in all the fish oil groups, save the sucrose group where the difference did not reach significant levels. CREM is a transcription factor that can be translated into both an activator or a repressor of CRE-genes (Inada et al 1999), making the mRNA levels of this gene impossible to interpret. The results clearly show that this gene is affected by the fish oil, and I suggest that the activity level of this protein should be measured in future studies.

5.6 GENE EXPRESSION IN WHITE ADIPOSE TISSUE

The transcription factors *Pparγ2* and *Srebp1c*, involved in adipogenesis, were somewhat downregulated in the subcutaneous fat pad of fish oil mice (Figs 3.8 and 4.8). The *Fas* gene was even more profoundly downregulated. This was not seen in the visceral fat pad, where these genes were expressed at comparable or higher levels compared to the chow group. This may indicate that the PUFAs in fish oil protect these mice against adipogenesis in subcutaneous, but not visceral fat. Considering the fact that the fructose group has higher levels of lipogenic genes compared to other fish oil groups, it is likely that the regulations of these genes are affected by the diet, not by the degree of obesity.

The n-3 fatty acids EPA and DHA are associated with reduced levels of inflammatory macrophages, which reduced the burden of inflammation (Oh et al 2010). The inflammation markers in visceral fat were upregulated in the sucrose group compared to all other groups. Of the sugar groups, fructose continuously had the lowest expression levels of inflammatory markers, but the difference was not significant compared to the chow group (Fig 3.9). Of the starch groups, the low GI group had somewhat lower expression levels compared to the high GI group (Fig 4.9). When comparing the sucrose group and the high GI group, the inflammation markers are higher in the sugar group (not shown). In the subcutaneous fat pad,

the sugar groups showed no consistent trend towards higher or lower levels of inflammation markers compared to the chow group. The starch groups, on the other hand, had lower levels of *Ccl2* and *Emr1*. The levels were lower in the low GI group compared to the high GI group. To sum it up, inflammation is probably lower in the fructose and low GI group, compared to the chow group. PUFAs did not protect against inflammation in sugar, glucose and high GI group. We cannot at this point say whether this is related to the types of carbohydrates ingested or the level of obesity of the animals.

Pgc1α is upregulated in epididymal fat of all fish oil groups compared to the chow group, but it is downregulated in the inguinal fat. Since the fish oil groups were lighter compared to the chow group, the upregulation in the visceral epididymal fat pad is probably of physiological importance. One could postulate that the upregulation of *Pgc1α* in visceral adipose tissue may have positive health effects, since *Pgc1α* increases β-oxidation and heat production (Lin et al 2005). Increasing fatty acid breakdown in the epididymal fat pad might limit the size of this unhealthy tissue. In consistency with this theory, the chow group had the highest percentage of visceral fat depots compared to total WAT (not shown).

5.7 GENE EXPRESSION IN BROWN ADIPOSE TISSUE

PGC-1α is a transcriptional coactivator for *Ucp1* (Lin et al 2005), and Dio2 prolongs the longevity of the UCP-1 protein (Bianco et al 2002). Increased expressions of these genes in brown adipose tissue are indicators of increased capacity of burning fat. *Dio2* was indeed upregulated in all fish oil groups, compared to the chow group. The levels of *Pgc1α* was only elevated in the fructose group, but as mentioned earlier, PGC-1α activity is modified posttranslationally, meaning that *Pgc1α* mRNA levels are not always a good measurement of PGC-1α enzyme activity.

The lipogenic transcription factor *Srebp1c* is downregulated in brown adipose tissue of all fish oil groups, excluding the glucose group. This is in consistence with earlier studies (Kim et al 1999). Also, *Rip140*, which is a repressor of fatty acid oxidation, is upregulated in the fish oil groups.

5.8 TRIGLYCERIDE CONTENT IN LIVER, MUSCLE AND PLASMA

Elevated levels of triglycerides (TGs) are a sign of insulin resistance and the possible development of hepatic steatosis. It is caused by increased release of fatty acids from the adipose tissues, which is seen in obese patients (Ferre and Foufelle 2010, Hajer et al 2008). The total hepatic lipid content did not differ between groups, but the TG contents were reduced in all fish oil groups. The TG contents of the tibialis muscle were reduced in glucose, fructose and low GI group, but raised in the sucrose and high GI group. In plasma, TG was reduced in all fish oil groups. This means that fish oil protects from TG accumulation regardless of the carbohydrate ingested, but more so when the mice eats low GI food.

The higher levels of phospholipids seen in the fish oil groups are not of pathological relevance. Phospholipids are primarily found in cellular membranes, and a high level of these fatty acids merely indicates that the livers of the fish oil groups contains an increased number of smaller cells compared to the chow group.

The combined results from the liver, muscle and plasma analysis showed that none of the mice suffered from liver damage.

6. CONCLUSIONS

Fish oil to some extent protects the mice against weight gain, regardless of the type of carbohydrate in the diet. However, these studies clearly show that when administered with sucrose, glucose or high GI carbohydrates, fish oil does not protect against obesity. These mice grew less obese compared to the chow group, but they were still obese. This is of great concern, given that consumption of these carbohydrates remain high, even though WHO have recommended to decrease consumption of sugar (WHO 2011) and stated that populations with high sugar intake are at risk of developing obesity and other chronic diseases (WHO 2003).

The fructose and low GI carbohydrate fed mice remained relatively lean during the trial. The mice fed fructose demonstrate that fructose is not obesogenic, but the weight gain of the sucrose group clearly shows that the fructose moiety of the sucrose molecule does not protect against obesity either. Also, this diet is not suitable for human consumption. The amount of fructose added to the diet given is not comparable to the amount of fructose found in human diets. Fructose ingested from fruit and honey is accompanied by approximately the same amounts of glucose (Tappy and Le 2010), making it impossible to follow the diet given to the fructose group, unless one eats copious amounts of commercially fabricated fructose sugar. That might not be a good idea, since the health benefits from eating fructose are controversial. Although mice stay lean on a fructose diet, rats fed fructose quickly develop insulin resistance and become obese (Hwang et al 1987, Tran et al 2009). In humans, studies have linked fructose to dyslipidemia (Le et al 2009), raise fasting TG and LDL levels (Schaefer et al 2009), decreased insulin sensitivity and increased visceral adiposity (Stanhope et al 2009). This might indicate that the fructose metabolism of humans is more similar to the fructose metabolism of rats, not mice. There are, however, no evidence indicating that eating fructose in moderate amounts in the form of fruits and honey is unsafe (Tappy and Le 2010).

The lower obesogenic effect of fructose is probably because fructose does not raise insulin levels like glucose does. If one wishes to obtain the same weight responses as seen in the fructose group, it would be more sensible to try the low carbohydrate diet, which has a less dramatic impact on blood insulin and glucose levels compared to high GI carbohydrates (Pawlak et al 2004). A glucose meal-tolerance test of low and high GI carbohydrates given to C57BL/6 mice is illustrated in Appendix IV.

In this study we saw that eating high GI carbohydrates like sucrose, glucose and amylopectin to some extent disrupts the ameliorating effect of fish oil on the development of obesity. This means that one cannot rely on omega-3 supplements for weight management. Taking omega-3 supplements and eating fish are good dietary habits in many respects, but it does not legitimize binging in high GI foods. The good news is that our low GI group exhibited far better responses compared to the high GI carbohydrate groups. The low GI diet of our study is not free of high GI components. As listed in table 2.1, page 40, it also contains some sucrose and amylopectin. This means that one does not have to follow an ascetic diet to benefit from the anti-obesogenic effects of fish oil, small improvements are likely to be seen by moderate dietary improvements.

For future studies, it would be interesting to investigate the effects of a diet high in fish oil and low GI carbohydrate on humans. To my knowledge, there are to date no studies linking low GI diets to obesity or any health problems in humans, and there are several studies linking fish oil to positive health effects. A recent study also indicates that the amino acids present in fish can reduce adipose tissue mass (Liaset et al 2009). I suggest an intervention study with a diet rich in fish, vegetables and whole grains, including omega-3 supplements, where the patients register intake of sweets, cakes, potato chips and soda beverages. After the study, e.g. 12 months, changes in adipose tissue mass would be recorded and compared to the amount of high GI carbohydrates and total calories ingested.

This diet rich in fish and vegetables would also be applauded be many parents worldwide, who are struggling to encourage their children to finish their dinners.

7. REFERENCES

Abete I, Astrup A, Martinez JA, Thorsdottir I, Zulet MA (2010). Obesity and the metabolic syndrome: role of different dietary macronutrient distribution patterns and specific nutritional components on weight loss and maintenance. *Nutr Rev* **68:** 214-231.

Abu-Elheiga L, Almarza-Ortega DB, Baldini A, Wakil SJ (1997). Human acetyl-CoA carboxylase 2. Molecular cloning, characterization, chromosomal mapping, and evidence for two isoforms. *J Biol Chem* **272:** 10669-10677.

Alaynick WA (2008). Nuclear receptors, mitochondria and lipid metabolism. *Mitochondrion* **8:** 329-337.

Arai T, Kim HJ, Chiba H, Matsumoto A (2009). Anti-obesity effect of fish oil and fish oil-fenofibrate combination in female KK mice. *J Atheroscler Thromb* **16:** 674-683.

Aston LM (2006). Glycaemic index and metabolic disease risk. *Proc Nutr Soc* **65:** 125-134.

Aston LM, Stokes CS, Jebb SA (2008). No effect of a diet with a reduced glycaemic index on satiety, energy intake and body weight in overweight and obese women. *Int J Obes (Lond)* **32:** 160-165.

Atkinson FS, Foster-Powell K, Brand-Miller JC (2008). International tables of glycemic index and glycemic load values: 2008. *Diabetes Care* **31:** 2281-2283.

Barak Y, Liao D, He W, Ong ES, Nelson MC, Olefsky JM *et al* (2002). Effects of peroxisome proliferator-activated receptor delta on placentation, adiposity, and colorectal cancer. *Proc Natl Acad Sci U S A* **99:** 303-308.

Belzung F, Raclot T, Groscolas R (1993). Fish oil n-3 fatty acids selectively limit the hypertrophy of abdominal fat depots in growing rats fed high-fat diets. *Am J Physiol* **264:** R1111-1118.

Bianco AC, Salvatore D, Gereben B, Berry MJ, Larsen PR (2002). Biochemistry, cellular and molecular biology, and physiological roles of the iodothyronine selenodeiodinases. *Endocr Rev* **23:** 38-89.

Bray GA, Nielsen SJ, Popkin BM (2004). Consumption of high-fructose corn syrup in beverages may play a role in the epidemic of obesity. *Am J Clin Nutr* **79:** 537-543.

Buckley JD, Howe PR (2009). Anti-obesity effects of long-chain omega-3 polyunsaturated fatty acids. *Obes Rev* **10:** 648-659.

Castle JC, Hara Y, Raymond CK, Garrett-Engele P, Ohwaki K, Kan Z *et al* (2009). ACC2 is expressed at high levels in human white adipose and has an isoform with a novel N-terminus [corrected]. *PLoS One* **4:** e4369.

Chawla A, Repa JJ, Evans RM, Mangelsdorf DJ (2001). Nuclear receptors and lipid physiology: opening the X-files. *Science* **294:** 1866-1870.

Christian M, Kiskinis E, Debevec D, Leonardsson G, White R, Parker MG (2005). RIP140-targeted repression of gene expression in adipocytes. *Mol Cell Biol* **25:** 9383-9391.

Collins S, Martin TL, Surwit RS, Robidoux J (2004). Genetic vulnerability to diet-induced obesity in the C57BL/6J mouse: physiological and molecular characteristics. *Physiol Behav* **81:** 243-248.

Cummings DE, Brandon EP, Planas JV, Motamed K, Idzerda RL, McKnight GS (1996). Genetically lean mice result from targeted disruption of the RII beta subunit of protein kinase A. *Nature* **382:** 622-626.

Cummings JH, Englyst HN (1995). Gastrointestinal effects of food carbohydrate. *Am J Clin Nutr* **61:** 938S-945S.

de Groot RP, Ballou LM, Sassone-Corsi P (1994). Positive regulation of the cAMP-responsive activator CREM by the p70 S6 kinase: an alternative route to mitogen-induced gene expression. *Cell* **79:** 81-91.

Duplus E, Forest C (2002). Is there a single mechanism for fatty acid regulation of gene transcription? *Biochem Pharmacol* **64:** 893-901.

Eaton S (2002). Control of mitochondrial beta-oxidation flux. *Prog Lipid Res* **41:** 197-239.

Elmadfa I, Meyer A, Nowak V, Hasenegger V, Putz P, Verstraeten R *et al* (2009). European Nutrition and Health Report 2009. *Forum Nutr* **62:** 1-405.

Felig P (1973). The glucose-alanine cycle. *Metabolism* **22:** 179-207.

Ferre P, Foufelle F (2010). Hepatic steatosis: a role for de novo lipogenesis and the transcription factor SREBP-1c. *Diabetes Obes Metab* **12 Suppl 2:** 83-92.

FHI (2011). Overvekt og fedme hos voksne - faktaark. In: fedme Oo (ed). *Faktaark om overvekt voksne*: Folkehelseinstituttet.

Finkelstein EA, Fiebelkorn IC, Wang G (2003). National medical spending attributable to overweight and obesity: how much, and who's paying? *Health Aff (Millwood)* **Suppl Web Exclusives:** W3-219-226.

Flachs P, Horakova O, Brauner P, Rossmeisl M, Pecina P, Franssen-van Hal N *et al* (2005). Polyunsaturated fatty acids of marine origin upregulate mitochondrial biogenesis and induce beta-oxidation in white fat. *Diabetologia* **48:** 2365-2375.

Gesta S, Tseng YH, Kahn CR (2007). Developmental origin of fat: tracking obesity to its source. *Cell* **131:** 242-256.

Ginzinger DG (2002). Gene quantification using real-time quantitative PCR: an emerging technology hits the mainstream. *Exp Hematol* **30:** 503-512.

Giralt A, Hondares E, Villena JA, Ribas F, Diaz-Delfin J, Giralt M *et al* (2011). PGC-1{alpha} controls the transcription of the SIRT3 gene, an essential component of the thermogenic brown adipocyte phenotype. *J Biol Chem*.

Hajer GR, van Haeften TW, Visseren FL (2008). Adipose tissue dysfunction in obesity, diabetes, and vascular diseases. *Eur Heart J* **29:** 2959-2971.

Harris WS (1997). n-3 fatty acids and serum lipoproteins: human studies. *Am J Clin Nutr* **65:** 1645S-1654S.

Hegardt FG (1999). Mitochondrial 3-hydroxy-3-methylglutaryl-CoA synthase: a control enzyme in ketogenesis. *Biochem J* **338 (Pt 3):** 569-582.

Helsedirektoratet (2008). Overvekt. In: Ernæring (ed). *Mat og helse*. Helsedirektoratet.

Herzig S, Long F, Jhala US, Hedrick S, Quinn R, Bauer A *et al* (2001). CREB regulates hepatic gluconeogenesis through the coactivator PGC-1. *Nature* **413:** 179-183.

Holness CL, da Silva RP, Fawcett J, Gordon S, Simmons DL (1993). Macrosialin, a mouse macrophage-restricted glycoprotein, is a member of the lamp/lgp family. *J Biol Chem* **268:** 9661-9666.

Horton JD, Bashmakov Y, Shimomura I, Shimano H (1998). Regulation of sterol regulatory element binding proteins in livers of fasted and refed mice. *Proc Natl Acad Sci U S A* **95:** 5987-5992.

Horton JD, Goldstein JL, Brown MS (2002). SREBPs: activators of the complete program of cholesterol and fatty acid synthesis in the liver. *J Clin Invest* **109:** 1125-1131.

Hostetler HA, Petrescu AD, Kier AB, Schroeder F (2005). Peroxisome proliferator-activated receptor alpha interacts with high affinity and is conformationally responsive to endogenous ligands. *J Biol Chem* **280:** 18667-18682.

Houslay MD, Adams DR (2003). PDE4 cAMP phosphodiesterases: modular enzymes that orchestrate signalling cross-talk, desensitization and compartmentalization. *Biochem J* **370:** 1-18.

Hwang IS, Ho H, Hoffman BB, Reaven GM (1987). Fructose-induced insulin resistance and hypertension in rats. *Hypertension* **10:** 512-516.

Inada A, Someya Y, Yamada Y, Ihara Y, Kubota A, Ban N *et al* (1999). The cyclic AMP response element modulator family regulates the insulin gene transcription by interacting with transcription factor IID. *J Biol Chem* **274:** 21095-21103.

Ishii S, Iizuka K, Miller BC, Uyeda K (2004). Carbohydrate response element binding protein directly promotes lipogenic enzyme gene transcription. *Proc Natl Acad Sci U S A* **101:** 15597-15602.

Jadhao SB, Yang RZ, Lin Q, Hu H, Anania FA, Shuldiner AR *et al* (2004). Murine alanine aminotransferase: cDNA cloning, functional expression, and differential gene regulation in mouse fatty liver. *Hepatology* **39:** 1297-1302.

Jucker BM, Cline GW, Barucci N, Shulman GI (1999). Differential effects of safflower oil versus fish oil feeding on insulin-stimulated glycogen synthesis, glycolysis, and pyruvate dehydrogenase flux in skeletal muscle: a 13C nuclear magnetic resonance study. *Diabetes* **48:** 134-140.

Jump DB, Botolin D, Wang Y, Xu J, Christian B, Demeure O (2005). Fatty acid regulation of hepatic gene transcription. *J Nutr* **135:** 2503-2506.

Kawai M, Rosen CJ (2010). PPARgamma: a circadian transcription factor in adipogenesis and osteogenesis. *Nat Rev Endocrinol* **6:** 629-636.

Kim HJ, Takahashi M, Ezaki O (1999). Fish oil feeding decreases mature sterol regulatory element-binding protein 1 (SREBP-1) by down-regulation of SREBP-1c mRNA in mouse liver. A possible mechanism for down-regulation of lipogenic enzyme mRNAs. *J Biol Chem* **274:** 25892-25898.

Kim KH (1997). Regulation of mammalian acetyl-coenzyme A carboxylase. *Annu Rev Nutr* **17:** 77-99.

Kurushima H, Ramprasad M, Kondratenko N, Foster DM, Quehenberger O, Steinberg D (2000). Surface expression and rapid internalization of macrosialin (mouse CD68) on elicited mouse peritoneal macrophages. *J Leukoc Biol* **67:** 104-108.

Lara-Esqueda A, Aguilar-Salinas CA, Velazquez-Monroy O, Gomez-Perez FJ, Rosas-Peralta M, Mehta R *et al* (2004). The body mass index is a less-sensitive tool for detecting cases with obesity-associated co-morbidities in short stature subjects. *Int J Obes Relat Metab Disord* **28:** 1443-1450.

Le KA, Ith M, Kreis R, Faeh D, Bortolotti M, Tran C *et al* (2009). Fructose overconsumption causes dyslipidemia and ectopic lipid deposition in healthy subjects with and without a family history of type 2 diabetes. *Am J Clin Nutr* **89:** 1760-1765.

Lehner R, Kuksis A (1996). Biosynthesis of triacylglycerols. *Prog Lipid Res* **35:** 169-201.

Liang G, Yang J, Horton JD, Hammer RE, Goldstein JL, Brown MS (2002). Diminished hepatic response to fasting/refeeding and liver X receptor agonists in mice with selective deficiency of sterol regulatory element-binding protein-1c. *J Biol Chem* **277:** 9520-9528.

Liaset B, Madsen L, Hao Q, Criales G, Mellgren G, Marschall HU *et al* (2009). Fish protein hydrolysate elevates plasma bile acids and reduces visceral adipose tissue mass in rats. *Biochim Biophys Acta* **1791:** 254-262.

Lin J, Handschin C, Spiegelman BM (2005). Metabolic control through the PGC-1 family of transcription coactivators. *Cell Metab* **1:** 361-370.

Lombardo YB, Chicco AG (2006). Effects of dietary polyunsaturated n-3 fatty acids on dyslipidemia and insulin resistance in rodents and humans. A review. *J Nutr Biochem* **17:** 1-13.

Madsen L, Pedersen LM, Liaset B, Ma T, Petersen RK, van den Berg S *et al* (2008). cAMP-dependent signaling regulates the adipogenic effect of n-6 polyunsaturated fatty acids. *J Biol Chem* **283:** 7196-7205.

Madsen L, Kristiansen K (2010). The importance of dietary modulation of cAMP and insulin signaling in adipose tissue and the development of obesity. *Ann N Y Acad Sci* **1190:** 1-14.

Marik PE, Varon J (2009). Omega-3 dietary supplements and the risk of cardiovascular events: a systematic review. *Clin Cardiol* **32:** 365-372.

Mauvoisin D, Mounier C (2011). Hormonal and nutritional regulation of SCD1 gene expression. *Biochimie* **93:** 78-86.

McGarry JD, Mannaerts GP, Foster DW (1977). A possible role for malonyl-CoA in the regulation of hepatic fatty acid oxidation and ketogenesis. *J Clin Invest* **60:** 265-270.

McKnight AJ, Macfarlane AJ, Dri P, Turley L, Willis AC, Gordon S (1996). Molecular cloning of F4/80, a murine macrophage-restricted cell surface glycoprotein with homology to the G-protein-linked transmembrane 7 hormone receptor family. *J Biol Chem* **271:** 486-489.

Mick DU, Fox TD, Rehling P (2011). Inventory control: cytochrome c oxidase assembly regulates mitochondrial translation. *Nat Rev Mol Cell Biol* **12:** 14-20.

Miyazaki M, Sampath H, Liu X, Flowers MT, Chu K, Dobrzyn A *et al* (2009). Stearoyl-CoA desaturase-1 deficiency attenuates obesity and insulin resistance in leptin-resistant obese mice. *Biochem Biophys Res Commun* **380:** 818-822.

Montminy M (1997). Transcriptional regulation by cyclic AMP. *Annu Rev Biochem* **66:** 807-822.

Nagata R, Nishio Y, Sekine O, Nagai Y, Maeno Y, Ugi S *et al* (2004). Single nucleotide polymorphism (-468 Gly to A) at the promoter region of SREBP-1c associates with genetic defect of fructose-induced hepatic lipogenesis [corrected]. *J Biol Chem* **279:** 29031-29042.

Napal L, Marrero PF, Haro D (2005). An intronic peroxisome proliferator-activated receptor-binding sequence mediates fatty acid induction of the human carnitine palmitoyltransferase 1A. *J Mol Biol* **354:** 751-759.

Noguchi T, Okuno E, Takada Y, Minatogawa Y, Okai K, Kido R (1978). Characteristics of hepatic alanine-glyoxylate aminotransferase in different mammalian species. *Biochem J* **169:** 113-122.

Ntambi JM (1999). Regulation of stearoyl-CoA desaturase by polyunsaturated fatty acids and cholesterol. *J Lipid Res* **40:** 1549-1558.

Oh DY, Talukdar S, Bae EJ, Imamura T, Morinaga H, Fan W *et al* (2010). GPR120 is an omega-3 fatty acid receptor mediating potent anti-inflammatory and insulin-sensitizing effects. *Cell* **142:** 687-698.

Osborne TF (2000). Sterol regulatory element-binding proteins (SREBPs): key regulators of nutritional homeostasis and insulin action. *J Biol Chem* **275:** 32379-32382.

Ouchi N, Parker JL, Lugus JJ, Walsh K (2011). Adipokines in inflammation and metabolic disease. *Nat Rev Immunol* **11:** 85-97.

Park EA, Mynatt RL, Cook GA, Kashfi K (1995). Insulin regulates enzyme activity, malonyl-CoA sensitivity and mRNA abundance of hepatic carnitine palmitoyltransferase-I. *Biochem J* **310 (Pt 3):** 853-858.

Park SH, Gammon SR, Knippers JD, Paulsen SR, Rubink DS, Winder WW (2002). Phosphorylation-activity relationships of AMPK and acetyl-CoA carboxylase in muscle. *J Appl Physiol* **92:** 2475-2482.

Pawlak DB, Kushner JA, Ludwig DS (2004). Effects of dietary glycaemic index on adiposity, glucose homoeostasis, and plasma lipids in animals. *Lancet* **364:** 778-785.

Petersen KF, Shulman GI (2002). Pathogenesis of skeletal muscle insulin resistance in type 2 diabetes mellitus. *Am J Cardiol* **90:** 11G-18G.

Poll-The BT, Roels F, Ogier H, Scotto J, Vamecq J, Schutgens RB *et al* (1988). A new peroxisomal disorder with enlarged peroxisomes and a specific deficiency of acyl-CoA oxidase (pseudo-neonatal adrenoleukodystrophy). *Am J Hum Genet* **42:** 422-434.

Rakhshandehroo M, Knoch B, Muller M, Kersten S (2010). Peroxisome proliferator-activated receptor alpha target genes. *PPAR Res* **2010**.

Ren B, Thelen AP, Peters JM, Gonzalez FJ, Jump DB (1997). Polyunsaturated fatty acid suppression of hepatic fatty acid synthase and S14 gene expression does not require peroxisome proliferator-activated receptor alpha. *J Biol Chem* **272:** 26827-26832.

Riserus U, Willett WC, Hu FB (2009). Dietary fats and prevention of type 2 diabetes. *Progress in Lipid Research* **48:** 44-51.

Rosen ED, MacDougald OA (2006). Adipocyte differentiation from the inside out. *Nat Rev Mol Cell Biol* **7:** 885-896.

Rufer AC, Thoma R, Hennig M (2009). Structural insight into function and regulation of carnitine palmitoyltransferase. *Cell Mol Life Sci* **66:** 2489-2501.

Sato Y, Ito T, Udaka N, Kanisawa M, Noguchi Y, Cushman SW *et al* (1996). Immunohistochemical localization of facilitated-diffusion glucose transporters in rat pancreatic islets. *Tissue Cell* **28:** 637-643.

Schaefer EJ, Gleason JA, Dansinger ML (2009). Dietary fructose and glucose differentially affect lipid and glucose homeostasis. *J Nutr* **139:** 1257S-1262S.

Schmitz G, Ecker J (2008). The opposing effects of n-3 and n-6 fatty acids. *Prog Lipid Res* **47:** 147-155.

Shambaugh GE, 3rd (1978). Urea biosynthesis II. Normal and abnormal regulation. *Am J Clin Nutr* **31:** 126-133.

Song DH, Wolfe MM (2007). Glucose-dependent insulinotropic polypeptide and its role in obesity. *Curr Opin Endocrinol Diabetes Obes* **14:** 46-51.

Stanhope KL, Schwarz JM, Keim NL, Griffen SC, Bremer AA, Graham JL *et al* (2009). Consuming fructose-sweetened, not glucose-sweetened, beverages increases visceral adiposity and lipids and decreases insulin sensitivity in overweight/obese humans. *J Clin Invest* **119:** 1322-1334.

Storlien LH, Kraegen EW, Chisholm DJ, Ford GL, Bruce DG, Pascoe WS (1987). Fish oil prevents insulin resistance induced by high-fat feeding in rats. *Science* **237:** 885-888.

Tappy L, Le KA (2010). Metabolic effects of fructose and the worldwide increase in obesity. *Physiol Rev* **90:** 23-46.

Tiraby C, Tavernier G, Lefort C, Larrouy D, Bouillaud F, Ricquier D *et al* (2003). Acquirement of brown fat cell features by human white adipocytes. *J Biol Chem* **278:** 33370-33376.

Tran LT, Yuen VG, McNeill JH (2009). The fructose-fed rat: a review on the mechanisms of fructose-induced insulin resistance and hypertension. *Mol Cell Biochem* **332:** 145-159.

Usfar AA, Lebenthal E, Atmarita, Achadi E, Soekirman, Hadi H (2010). Obesity as a poverty-related emerging nutrition problems: the case of Indonesia. *Obes Rev* **11:** 924-928.

van Baak MA, Astrup A (2009). Consumption of sugars and body weight. *Obes Rev* **10 Suppl 1:** 9-23.

van der Leij FR, Kram AM, Bartelds B, Roelofsen H, Smid GB, Takens J *et al* (1999). Cytological evidence that the C-terminus of carnitine palmitoyltransferase I is on the cytosolic face of the mitochondrial outer membrane. *Biochem J* **341 (Pt 3):** 777-784.

Vila-Brau A, De Sousa-Coelho AL, Mayordomo C, Haro D, Marrero PF (2011). Human HMGCS2 regulates mitochondrial fatty acid oxidation and FGF21 expression in HepG2 cell line. *J Biol Chem*.

Wakil SJ, Abu-Elheiga LA (2009). Fatty acid metabolism: target for metabolic syndrome. *J Lipid Res* **50 Suppl:** S138-143.

Wang YX, Lee CH, Tiep S, Yu RT, Ham J, Kang H *et al* (2003). Peroxisome-proliferator-activated receptor delta activates fat metabolism to prevent obesity. *Cell* **113:** 159-170.

Wei W, Wang X, Yang M, Smith LC, Dechow PC, Sonoda J *et al* (2010). PGC1beta mediates PPARgamma activation of osteoclastogenesis and rosiglitazone-induced bone loss. *Cell Metab* **11:** 503-516.

Wheeler ML, Pi-Sunyer FX (2008). Carbohydrate issues: type and amount. *J Am Diet Assoc* **108:** S34-39.

WHO (2003). Populations with high sugar consumption are at increased risk of chronic disease, South African researchers report. *Bulletin of the World Health Organization* World Health Organization.

WHO (2008). Action plan for the global strategy for the prevention and control of noncommunicable diseases World Health Organization.

WHO (2011). Obesity and overweight. In: centre M (ed). *Fact sheets*. World Health Organization.

Wolever TMS, Brand-Miller JC, Abernethy J, Astrup A, Atkinson F, Axelsen M *et al* (2008). Measuring the glycemic index of foods: interlaboratory study. *American Journal of Clinical Nutrition* **87:** 247s-257s.

Wood IS, Trayhurn P (2003). Glucose transporters (GLUT and SGLT): expanded families of sugar transport proteins. *Br J Nutr* **89:** 3-9.

Xu J, Nakamura MT, Cho HP, Clarke SD (1999). Sterol regulatory element binding protein-1 expression is suppressed by dietary polyunsaturated fatty acids. A mechanism for the coordinate suppression of lipogenic genes by polyunsaturated fats. *J Biol Chem* **274:** 23577-23583.

Xu J, Teran-Garcia M, Park JH, Nakamura MT, Clarke SD (2001). Polyunsaturated fatty acids suppress hepatic sterol regulatory element-binding protein-1 expression by accelerating transcript decay. *J Biol Chem* **276:** 9800-9807.

Yahagi N, Shimano H, Hasty AH, Amemiya-Kudo M, Okazaki H, Tamura Y *et al* (1999). A crucial role of sterol regulatory element-binding protein-1 in the regulation of lipogenic gene expression by polyunsaturated fatty acids. *J Biol Chem* **274:** 35840-35844.

Yen CL, Stone SJ, Koliwad S, Harris C, Farese RV, Jr. (2008). Thematic review series: glycerolipids. DGAT enzymes and triacylglycerol biosynthesis. *J Lipid Res* **49:** 2283-2301.

Yoon JC, Puigserver P, Chen G, Donovan J, Wu Z, Rhee J *et al* (2001). Control of hepatic gluconeogenesis through the transcriptional coactivator PGC-1. *Nature* **413:** 131-138.

APPENDIX I

***Table I.1**: Chemicals and reagents used in RNA extraction*

Product	**Vendor**
Trizol	Invitrogen art.no. 15596-026, USA
Chloroform	Merck, Germany
Isopropanol (2-propanol)	Arcus kjemi, Norway
Ethanol	Arcus kjemi, Norway
DEPC	Sigma art. No. F32490, USA
RNase free ddH_2O	MilliQ Gradient, Lab-tec, Norway
DNA free kit	Ambion art.no. 1906, USA

***Table I.2**: Chemicals and reagents used in RNA quality Bioanalyzer*

Product	Vendor
RNA 6000 Nano LabChip kit	Agilent Technologies art.nr 5065-4476, USA
RNA 6000 Ladder	Ambion art.nr 7152, USA
RNase free ddH_2O	MilliQ Gradient, Lab-tec, Norway

***Table I.3**: Chemicals and reagents used in RT-reaction*

Product	Vendor
TaqMan RT buffer 10X	**Applied Biosystems art.no N808 0234,** **TaqMan® Reverse Transcription Reagents, USA**
25 mM Magnesium Chlorid	
10 mM deoxyNTPs	
50 µM Oligo dT 16 primer	
RNase inhibitor (20 U/µl)	
Multiscribe reverse transcriptase (50 U/µl)	
RNase free ddH_2O	MilliQ Gradient, Lab-tec, Norway

***Table I.4**: Chemicals and reagents used in quantitative real-time PCR*

Product	**Vendor**
SYBR GREEN Master	Roche, Norway
Primer	Invitrogen Ltd, UK
RNase free ddH_2O	MilliQ Gradient, Lab-tec, Norway

***Table I.5:** Chemicals and reagents used in histology*

Product	**Vendor**
4% formaldehyde	Merck art.no 1.04003.1000, Germany
NaH_2PO_4 x H_2O	Merck art.no 1.06346.0500, Germany
$NaHPO_4$ x $2H_2O$	Merck art.no 1.06580.0500, Germany
Ethanol 100%	Arcus kjemi, Norway
RNase free ddH_2O	MilliQ Gradient, Lab-tec, Norway
Methanol	Merck art.no 1.06018.2500, Germany
Xylene	Prolabo, VWR, art.no 28973.328, USA
Haematoxylin	Chemi-teknik AS, Norway
Eosin Y	Chemi-teknik AS, Norway
Entellan, rapid mounting medium for microscopy	Merck art.no 1.07960.0500, Germany

***Table I.6**: Chemicals and reagents in Insulin Mouse Ultrasensitive ELISA kit, 96 wells*

Product		**Vendor**
Insulin Mouse Ultrasensitive ELISA kit:		DRG Instruments, GmbH, Germany
Standard 0	Lot no 17609	
Standard 1 (0.175 µg/l)	Lot no 17599	
Standard 2 (0.45 µg/l)	Lot no 17600	
Standard 3 (1.0 µg/l)	Lot no 17601	
Standard 4 (2.5 µg/l)	Lot no 17602	
Standard 5 (6.5 µg/l)	Lot no 17603	
Coated plate	Lot no 15771	
Enzyme conjugate 11X	Lot no 15878	
Enzyme Conjugate Buffer	Lot no 17606	
Wash Buffer 21 X	Lot no 17557	
TMB Substrate Solution	Lot no 15873	
Stop Solution 0.5 M H_2SO_4	Lot no 17561	

APPENDIX II

***Table II.1**: Primer sequences used in quantitative real-time PCR. Obtained from Invitrogen Ltd, UK.*

Housekeeping genes		
TBP	**5'→ 3'**	ACCCTTCACCAATGACTCCTATG
	3'→ 5'	ATGATGACTGCAGCAAATCGC
Calnexin	**5'→ 3'**	GCAGCGACCTATGATTGACAACC
	3'→ 5'	GCTCCAAACCAATAGCACTGAAAGG
β-actin	**5'→ 3'**	ATGGGTCAGAAGGACTCCTACG
	3'→ 5'	AGTGGTACGACCAGAGGCATAC
Tested genes		
Srebp1c	**5'→ 3'**	GGA GCC ATG GAT TGC ACA TT
	3'→ 5'	GCT TCC AGA GAG GAG GCC AG
Acc1	**5'→ 3'**	TGCTGCCCCATCCCCGGG
	3'→ 5'	TCGAACTCTCACTGACACG
Acc2	**5'→ 3'**	TTC CAG ATG CTA ATG GGT TG
	3'→ 5'	GCA GGT CCA GTT TCT TGT GTT
Scd1	**5'→ 3'**	GATGTTCCAGAGGAGGTACTACAAGC
	3'→ 5'	ATGAAGCACATCAGCAGGAGG
Fas	**5'→ 3'**	CTTCGCCAACTCTACCATGG
	3'→ 5'	TTCCACACCCATGAGCGAGT
Dgat	**5'→ 3'**	GGTGCCATCGTCTGCAAGA
	3'→ 5'	CCACCAGGATGCCATACTTGA
Pparα	**5'→ 3'**	CGTTTGTGGCTGGTCAAGTT
	3'→ 5'	AGAGAGGACAGATGGGGCTC
Pparδ	**5'→ 3'**	CAG AAG TGC CTG GCA CTC G
	3'→ 5'	TCC GTC CAA AGC GGA TAG C
Aco	**5'→ 3'**	GGGTCATGGAACTCATCTTCGA
	3'→ 5'	GAATGAACTCTTGGGTCTTGGG
Cpt1a	**5'→ 3'**	ACAAATTATGTGAGTGACTGG
	3'→ 5'	GATCCCAGAAGACGAATAGG
Cpt2	**5'→ 3'**	AGCCTGCCCAGGCTGCC
	3'→ 5'	AAACCAGGGGCCCTGAGATG
Hmgcs2	**5'→ 3'**	AGCCCAGCAGAGGTTTTCTACAA
	3'→ 5'	CATACGGGTCTGGCCCAAG
Agxt	**5'→ 3'**	AAAAAGAGATGCTTCAGATCATGGA
	3'→ 5'	CACATACTGGATGCCTTGCTTG
Got	**5'→ 3'**	TTTGTGTCTGAAGGCTTCGAGC

	3'→ 5'	TCTCATTGTAGAGCCCGAAGTTCT
Gpt1	**5'→ 3'**	AGGTCCTGGCCCTCTGTGTC
	3'→ 5'	CCTTCTCTTGGCATCCTCTGG
Cps1	**5'→ 3'**	AGGATGTCAAGGTGTTTGGCA
	3'→ 5'	CTCGCTTAACTAGCAGGCGG
Pgc1α	**5'→ 3'**	CATTTGATGCACTGACAGATGGA
	3'→ 5'	CCGTCAGGCATGGAGGAA
Pck1 (Pepck)	**5'→ 3'**	CCACACCATTGCAATTATGC
	3'→ 5'	CATATTTCTTCAGCTTGCGG
RIα	**5'→ 3'**	CCT ACG TTA GAA AGG TTA TTC C
	3'→ 5'	TAT CCC CTT CAT CAC CTT GC
RIIβ	**5'→ 3'**	GCG TGC CTC GGT CTG TGC
	3'→ 5'	GGA CAT CTG CTC TGG ATC C
Crem	**5'→ 3'**	AAGTCACATGGCTGCTGCC
	3'→ 5'	GCTCGGATCTGGTAAGTTGGC
Pde4c	**5'→ 3'**	GGAGACACTGCAGACTCGTCG
	3'→ 5'	CATGCGCTTGAACTTGTTGG
Pparγ2	**5'→ 3'**	ACAGCAAATCTCTGTTTTATGC
	3'→ 5'	TGCTGGAGAAATCAACTGTGG
Ccl2 (Mcp1)	**5'→ 3'**	GTGTTGGCTCAGCCAGATGC
	3'→ 5'	GCTTGGTGACAAAAACTA
Serpine1 (Pai1)	**5'→ 3'**	AGCGGGACCTAGAGCTGGTC
	3'→ 5'	CCAGTAAGTCATTGATCATACCTTTGGT
Cd68	**5'→ 3'**	CTTCCCACAGGCAGCACAG
	3'→ 5'	AATGATGAGAGGCAGCAAGAGG
Emr1 (F4/80)	**5'→ 3'**	CTTTGGCTATGGGCTCTCAGTC
	3'→ 5'	GCAAGGAGGACAGAGTTTATCGTG
Dio2	**5'→ 3'**	GCC CAG CAA ATG TAG AC
	3'→ 5'	TGG CAA TAA GGA GCT AGA A
Cox2	**5'→ 3'**	GACTGGGCCATGGAGTGG
	3'→ 5'	CACCTCTCCACCAATGACC
Ucp1	**5'→ 3'**	AGCCGGCTTAATGACTGGAG
	3'→ 5'	TCTGTAGGCTGCCCAATGAAC

APPENDIX III

Result of the histological procedures:

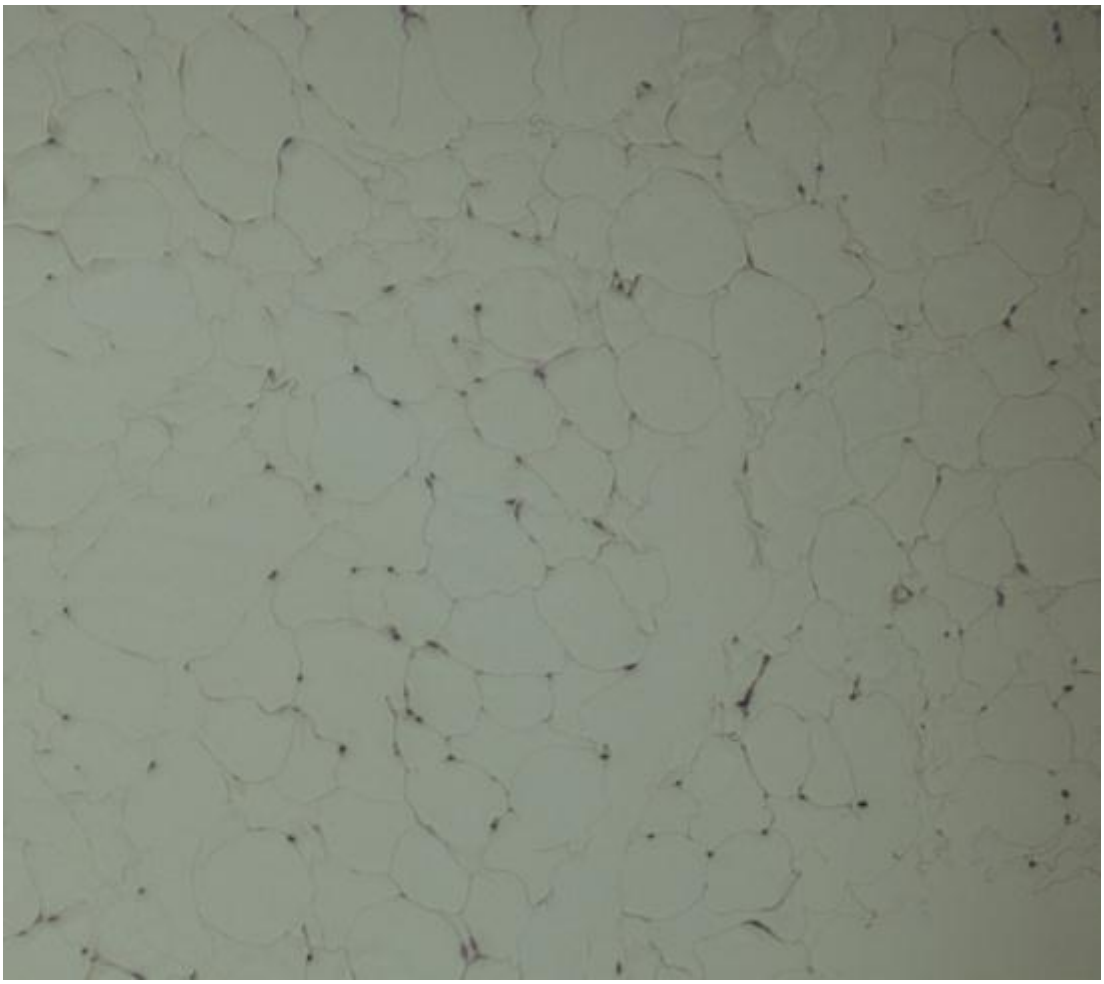

Figure A: *Disrupted adipose tissue. The depressing result of a lengthy histological method performed twice.*

APPENDIX IV

MTT-test of high and low GI starch:

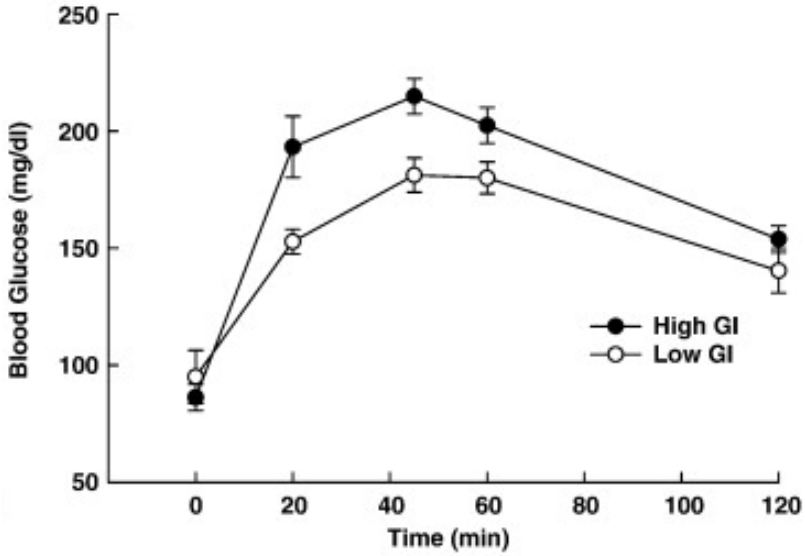

Figure B: *The result of a meal-tolerance-test (MTT), performed on C57BL/6 mice. The diet contained high fat and the same amount of carbohydrates. The high GI group received Amioca (amylopectin), the low GI group received Hi-Maize (high in amylose). Adapted from (Coate and Huggins 2010)*